博士学位論文

Nutritional studies on the endothelial cell function in lifestyle-related diseases

安澤　俊紀

Toshinori Yasuzawa

博士学位論文

Nutritional studies on the endothelial cell function in lifestyle-related diseases

2022年5月18日

安澤　俊紀

Table of contents

1. Preface....1
2. Antithrombotic effect of mozuku (*Cladosiphon okamuranus* Tokida, brown algae) in carotid artery thrombosis rat....5
    2.1. INTRODUCTION....5
    2.2. METHODS....6
    2.3. RESULTS....9
    2.4. DISCUSSION....15
3. The effect of inflammation and oxidative stress on albuminuria in obesity....18
    3.1. INTRODUCTION....18
    3.2. METHODS....18
    3.3. RESULTS....21
    3.4. DISCUSSION....26
4. The effect of eicosapentaenoic acid on endothelial to mesenchymal transition in diabetes....30
    4.1. INTRODUCTION....30
    4.2. METHODS....31
    4.3. RESULTS....38
    4.4. DISCUSSION....54
5. The effects of linagliptin on high glucose-induced podocyte apoptosis and glomerular insulin signaling in diabetic mouse....59
    5.1. INTRODUCTION....59
    5.2. METHODS....60

5.3. RESULTS 64

5.4. DISCUSSION 78

6. Summary and perspectives 83

7. Abbreviations 87

8. Acknowledgments 88

9. References 89

10. List of publications 113

1. Preface

Lifestyle changes have led to a rapid increase in the number of patients with lifestyle-related diseases, which has become a problem both in Japan and abroad. The leading causes of death in Japan are cancer, heart disease, and cerebrovascular disease, which are associated with lifestyle. The pathologies of obesity and diabetes are closely related to lifestyle and can lead to various complications. Therefore, it is expected that lifestyle-related diseases can be prevented or ameliorated through nutrition and food ingredients. In this study, I researched the food function in order to maintain the health and suppress the progression of lifestyle-related diseases.

Vascular endothelial cells (VEC) regulate blood coagulation, thrombolysis, vasoconstriction, vasodilation, vascular permeability, and angiogenesis. Dysfunction of VEC can cause hypertension, atherosclerosis, diabetes, renal failure, myocardial infarction, and cerebral infarction (1). Lifestyle changes are associated with vascular endothelial cell function. Chronic inflammation and oxidative stress cause endothelial cell dysfunction. It is reported that healthy diet reduces the risk of cardiovascular disease via improving the VEC's function (2). Further nutritional studies on VEC's function will promote prevention and treatment of lifestyle-related diseases.

VEC are involved in the regulation of blood flow via their antithrombogenicity. VEC play a role in anticoagulation and fibrinolysis in the antithrombogenicity. Heparan sulfate proteoglycan (HSPG) and thrombomodulin (TM) existing on endothelial cell surface are important for anticoagulation. HSPG inhibits coagulation cascade by binding with tissue factor pathway inhibitor or antithrombin III (3, 4). TM and thrombin complex activates protein C and inhibits coagulation cascade (3). VEC produce fibrinolytic properties such as tissue-type plasminogen activator (t-PA), urokinase-type plasminogen

activator (u-PA) and plasminogen activator inhibitor-1 (PAI-1). Plasminogen activator activates plasminogen to plasmin that has degradation activity of fibrin, which is a main component of thrombus (Fig. 1). Normally, fibrinolysis and coagulation have been balanced well. However, the dysfunctions of VEC caused by oxidative stress, hyperlipidemia, hyperglycemia, hypertension, or inflammation can result in thrombosis (5-8). Thrombosis develops thrombotic diseases, such as myocardial infarction and cerebral infarction. To prevent or ameliorate thrombosis and its related diseases, it is considered that investigations of food or nutrients for maintaining or activating VEC's function are important and beneficial.

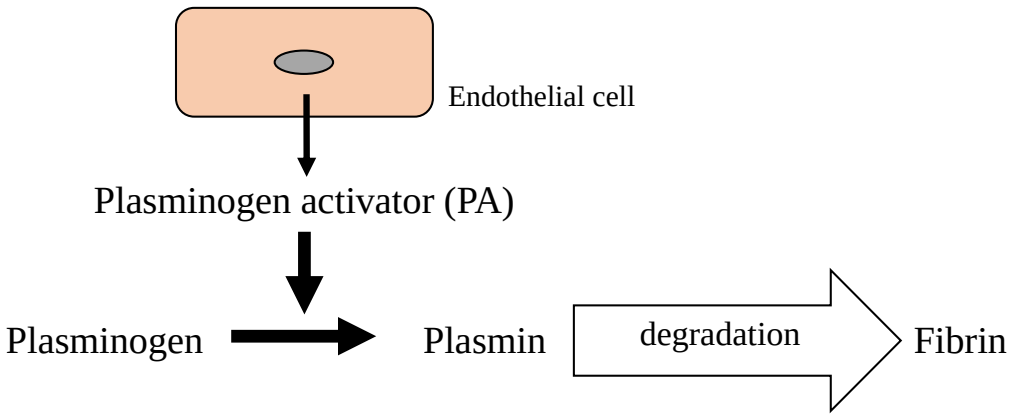

Fig. 1 Antithrombogenicity of endothelial cell.

Vascular complications due to obesity and diabetes are also important in discussing VEC's function. Vascular complications include macrovascular complications such as cerebrovascular disease and myocardial infarction, and microvascular complications such as nephropathy, retinopathy, and neuropathy.

Obesity is one of the common causes of chronic kidney disease (CKD), independent of glycemic control (9). It is suggested that body mass index is associated

with the incidence of CKD (10). Metabolic abnormalities caused by obesity may play an important role in the increasing vascular endothelial growth factor (VEGF) and eventually in the development of CKD (11). Furthermore, insulin resistance observed in obesity has been associated with cardiovascular disease (12). These results suggest that abnormal metabolites induced by obesity can accelerate the development of CKD.

It is reported that 537 million adults were diagnosed with diabetes in 2021 and approximately 783 million adults are expected to be diabetic by 2045 (13). Diabetic kidney disease (DKD) is one of the major CKD that requires renal replacement therapy (14). Moreover, the number of patients with end-stage renal disease (ESRD) requiring dialysis due to DKD is increasing (15). It is reported that endothelial to mesenchymal transition (EndMT) is associated with the development of renal fibrosis in DKD (16). EndMT is the process by which endothelial cells acquire a fibroblastic phenotype and endothelial cell phenotype declines. As EndMT progresses, the expression of endothelial cell markers, such as CD31 and VE-cadherin are decreased, while the expression of mesenchymal markers, such as SM22α and αSMA are increased. Cell adhesion molecules are decreased, and cell motility and migration activity are increased in EndMT (Fig.2).

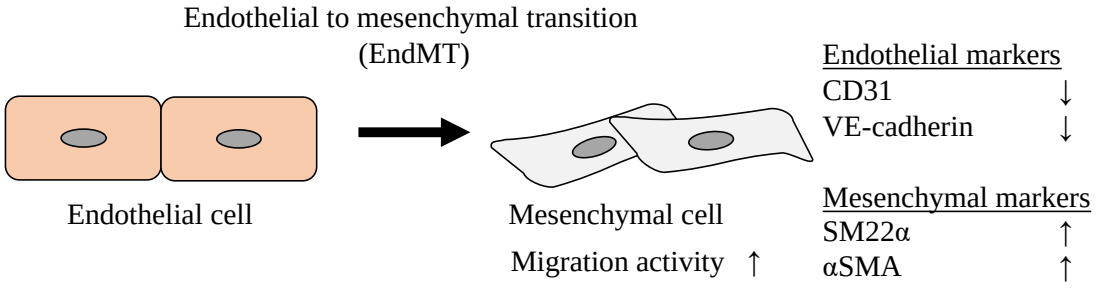

Fig. 2 Endothelial to mesenchymal transition (EndMT) in endothelial cells.

VEC play an important role of maintenance of systemic homeostasis. Dysfunction of VEC can lead to lifestyle-related diseases. Therefore, nutritional studies on VEC's function will promote prevention and treatment of lifestyle-related diseases. In the present study, VEC's function and food function in lifestyle-related diseases were investigated. The effect of food ingredients (mozuku) on antithrombogenicity of VEC was assessed. I also investigated the effect of nutritional status and eicosapentaenoic acid (EPA) on kidney disease using obesity model and diabetic model.

2. Antithrombotic effect of mozuku (*Cladosiphon okamuranus* Tokida, brown algae) in carotid arterial thrombosis rat.

This chapter is based on a paper previously published in *J. Nutr. Sci. Vitaminol.* (17).

2.1. INTRODUCTION

Anticoagulant and fibrinolytic activities are the major function of VEC. Thrombotic diseases, such as myocardial infarction and cerebral infarction could be prevented by activating the antithrombogenicity of VEC. Brown algaee had various nutraceutical and pharmacological functions including anti-inflammatory, anti-oxidative, anti-angiogenic, antihyperlipidemic and anticoagulant activity (18-22). Fucoidans from brown algae inhibited thrombotic activity and prolonged activated partial thromboplastin time *in vitro* (23, 24). Intravenous administration of sulfated galactofucan from brown algae showed the antithrombotic activity in the rat vena cava ligation thrombosis model (25). Thus, polysaccharides from brown algae might be useful for prevention of thrombosis via anticoagulation. However, the effect of polysaccharides from brown algae on fibrinolysis is not well clarified.

Okinawa mozuku (brown algae, *Cladosiphon Okamuranus* Tokida) is very popular in Japanese food. Okinawa mozuku abundantly contains fucoidan. It is reported that the fucoidan from Okinawa mozuku is absorbed through the small intestine *in vitro* and *in vivo* (26). However, the anticoagulant effects of Okinawa mozuku were not shown (23, 24). Moreover, the effects of oral administration of Okinawa mozuku on the fibrinolysis were not clear. In this study, the effects of Okinawa mozuku on fibrinolytic activity of cultured endothelial cells and the antithrombotic effects of oral administration

of Okinawa mozuku on carotid arterial thrombosis rat induced by ferric chloride were investigated.

2.2. METHODS

2.2.1 Okinawa mozuku extract

Okinawa mozuku (*Cladosiphon Okamuranus* Tokida) was purchased from commercially available products (Iki mozuku; Itosan Co. Ltd., Okinawa, Japan). Mozuku and distilled water of its equal weight were mixed and autoclaved for 15 min. It was centrifuged at 1,200 ×g for 10 min and supernatant was collected as Okinawa mozuku extract.

2.2.2 Vascular endothelial cells

The vascular endothelial cell line (TKM-33) that were established from human umbilical VEC (HUVEC) (27) were used. TKM-33 were placed onto 24 well plate (3×10^4 cells/well) and cultured in RPMI-1640 (Nissui, pharmaceutical, Tokyo, Japan) containing 10% fetal bovine serum (FBS, Thermo Fisher Scientific, MA, USA). Next, the cells were incubated with FBS-free RPMI-1640 with or without 1% of Okinawa mozuku extract. After incubation for twenty-four hours, conditioned medium and cell lysate were collected for assay of u-PA activity.

2.2.3 Fibrin zymography

u-PA activity was measured by fibrin zymography as described elsewhere (28). Briefly, protein samples from conditioned medium and cell lysate were separated by 10% polyacrylamide gel contained 0.55 mg/mL bovine plasminogen-rich fibrinogen (Organon

Teknika, Dublin, Ireland) and 0.056 U/mL thrombin (Midori juji, Osaka, Japan), subsequently soaked in 2.5% Triton X-100 for 60 min, and then incubated in glycine buffer (0.1 mol/L Glycine-HCl, pH 8.4) at 37°C for 18 hr. After that, the gel was stained with Coomassie Blue G-250 (FUJIFILM Wako Pure Chemical Corporation, Osaka, Japan) for 30 min and destained with multiple changes of destain solution (44% methanol, 11% acetic acid) until lysis bands appeared.

2.2.4 Animal experiments

All animal experimental procedures were approved by the Kindai University Experimental Animal Committee (approval number: KAAG-26-009) and conducted by the animal experiment guideline of Kindai University. Male Sprague-Dawley rats of 5 weeks of age were used (CLEA Japan, Tokyo, Japan). The rats had been freely fed and given water while they were kept in an environment with a 12 hr light/dark cycle at 22 ± 2°C. The rats were divided into two groups. Rats were given tap water or 5% Okinawa mozuku extract in tap water. After 8 weeks of treatments, the rats were provided for the carotid arterial thrombosis model. The blood samples were collected for measurements of platelet aggregation activity, activated partial thromboplastin time (APTT), u-PA activity in euglobulin fraction, plasma active PAI-1 levels.

2.2.5 Preparation of the euglobulin fraction

Plasma (0.5 mL) was mixed with 9.5 mL of 0.016% acetic acid, and incubated on ice for 20 min. After centrifugation at 2,000 ×g at 4°C for 15 min, the supernatant was discarded and the precipitated euglobulin fraction was resuspended in 0.4 mL of 309

mmol/L NaCl containing 5.3 mmol/L barbital buffer (pH 7.4). The euglobulin fraction was used for fibrin zymography.

2.2.6 The Carotid arterial thrombosis model

Rats were anesthetized and the right carotid artery was exposed. The filter paper (10 × 5 mm) was placed under the right carotid artery. FLO-C1 (OMEGAWAVE, INC. Tokyo, Japan) probe was attached to the carotid artery to monitor blood flow. Then, vascular injuries were induced by applying 40% $FeCl_3$ on a filter paper. Carotid artery blood flow (mL/min/100 g) was monitored continuously for 30 min.

2.2.7 Measurement of platelet aggregation

The blood samples were centrifuged for 10 min (300 ×g at 4°C) and supernatant was collected as platelet rich plasma (PRP). After collecting PRP, the blood samples were subjected to further centrifugation for 15 min (1,200 ×g at 4°C) and supernatant was collected as platelet poor plasma (PPP). Platelet aggregation in PRP was initiated by 1 mg/mL of collagen reagent Horm® (Moriya Sangyo K.K. Tokyo, Japan) and monitored using platelet aggregation analyzer, TPA-4C (Tokyo photoelectric Co., Ltd. Tokyo, Japan).

2.2.8 Activated partial thromboplastin time (APTT), PAI-1

APTT was measured using commercial APTT kit (Thrombocheck APTT; Sysmex, Hyogo, Japan). 0.1 mL of APTT reagent and 0.1 mL of PPP were mixed in test tube and warmed at 37°C for 2 min. Then, prewarmed (37°C) 0.1 mL of 0.02 mol/L $CaCl_2$

was added, and coagulation time was measured. Active PAI-1 level was measured using commercial ELISA kit (INR, MI, USA).

2.2.9 Statistics

All statistical analyses were performed using Microsoft Excel (Microsoft Corporation, Redmond, WA, USA) and the add-in software Statcel 3 (OMS Publishing Inc., Saitama, Japan). The data were shown as means ± SD for each group. Statistical analysis was performed by Student's t-test. All results were considered statistically significant at $p < 0.05$.

2.3. RESULTS

2.3.1 Effect of Okinawa mozuku extract on cultured vascular endothelial cells

To evaluate the effect of Okinawa mozuku extract on fibrinolytic activity of VEC *in vitro*, TKM-33 cells were incubated with or without Okinawa mozuku extract. And then, u-PA activities in the conditioned medium and the cell lysate were measured. The u-PA activity in conditioned medium of vascular endothelial cells (TKM-33) was significantly increased by the addition of Okinawa mozuku extract (Fig. 3a). However, Okinawa mozuku extract reduced u-PA activity in the cell lysate, compared with control (Fig. 3b). These results showed that the addition of Okinawa mozuku extract enhanced secretion of u-PA from inside of endothelial cells to outside.

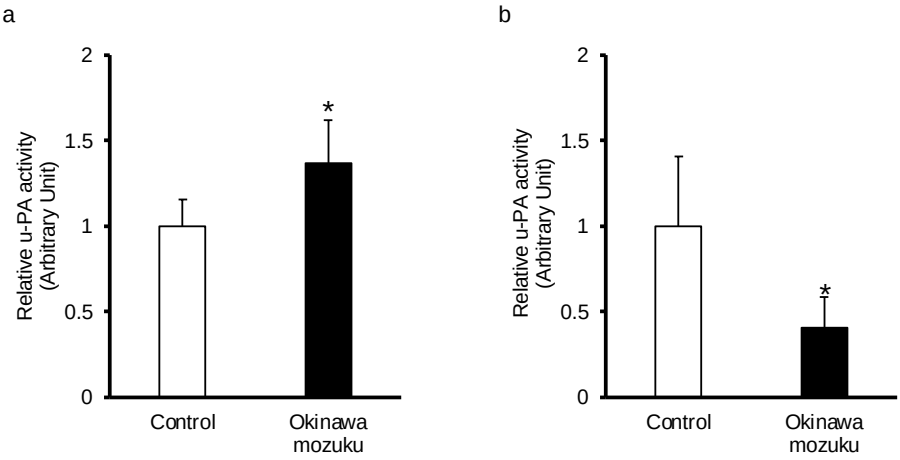

Fig. 3 Effects of Okinawa mozuku extract on u-PA activity in the conditioned medium and the cell lysate of TKM-33. Relative u-PA activity in the conditioned medium (a) and the cell lysate (b) were measured by using fibrin zymography. Control, n = 4; Okinawa mozuku, n = 4 were analyzed. Values are shown as mean ± SD. *p<0.05. This figure is reproduced from the figure previously published in *J. Nutr. Sci. Vitaminol.* (17).

2.3.2 Body weight, food intake, and water intake

The effect of oral administration of Okinawa mozuku extract on antithrombotic activity in rats was investigated. No statistically significant differences in body weight, food intake and water intake were observed between control and Okinawa mozuku groups (Table 1).

Table 1. Body weight, food intakes and water intakes in the experimental period.

	Control	Okinawa mozuku
Initial body weight (g)	331.3 ± 13.4	332.0 ± 17.6
Final body weight (g)	563.1 ± 36.2	576.1 ± 39.7
Food intake (g/day)	28.4 ± 0.3	30.2 ± 0.3
Water intake (g/day)	59.6 ± 0.6	60.5 ± 0.4

Values are shown as mean ± SD, n=6. This table is reproduced from the table previously published in *J. Nutr. Sci. Vitaminol.* (17).

2.3.3 Effect of Okinawa mozuku extract on blood coagulation parameters.

To evaluate the effect of Okinawa mozuku extract on blood coagulation parameters, platelet aggregation activity and APTT were measured. There were no significant differences in platelet maximum aggregation rate, appearance time of maximum aggregation rate, and the area under the curve (AUC) for platelet aggregation between control and Okinawa mozuku groups (Table 2). The oral administration of Okinawa mozuku extract did not affect the APTT (Fig. 4).

Table 2. Effect of Okinawa mozuku extract on platelet aggregation

	Control	Okinawa mozuku
Maximum aggregation rate (%)	80.1 ± 3.0	83.1 ± 9.1
Appearance time of maximum aggregation rate (sec.)	583 ± 11	570 ± 33
Area under the curve for platelet aggregation (AU)	13.7 ± 2.4	14.3 ± 4.7

Values are shown as mean ± SD, n=6. This table is reproduced from the table previously published in *J. Nutr. Sci. Vitaminol.* (17).

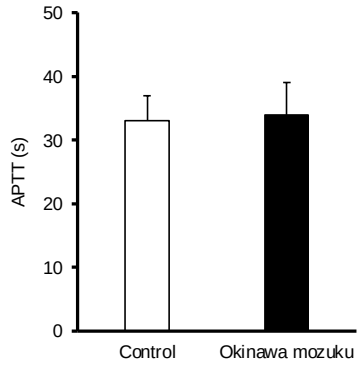

Fig. 4 Effect of Okinawa mozuku extract on APTT. The rats were fed with or without Okinawa mozuku extract for 8 weeks. Subsequently, the blood samples were collected for measurement of APTT. APTT was measured using commercial APTT reagents. Control, n = 5; Okinawa mozuku, n = 5 were analyzed. Values are shown as mean ± SD. This figure is reproduced from the figure previously published in *J. Nutr. Sci. Vitaminol.* (17).

2.3.4 Effect of Okinawa mozuku extract on $FeCl_3$-induced carotid artery thrombosis model

To evaluate the preventive effect of Okinawa mozuku on thrombosis, the effect of oral administration of Okinawa mozuku extract on carotid artery thrombosis rat induced by 40% $FeCl_3$ injury was measured. Rats were fed with or without Okinawa mozuku extract for 8 weeks before induction of thrombosis. After application of 40% $FeCl_3$ to carotid artery, blood flow was gradually decreased. However, the decrease of blood flow in Okinawa mozuku group was less than that in control group (Fig. 5a). The area under the curve for blood flow was significantly higher in Okinawa mozuku group, compared with control group (Fig. 5b). These results suggested that oral administration of Okinawa mozuku extract inhibited carotid arterial occlusion induced by $FeCl_3$ injury.

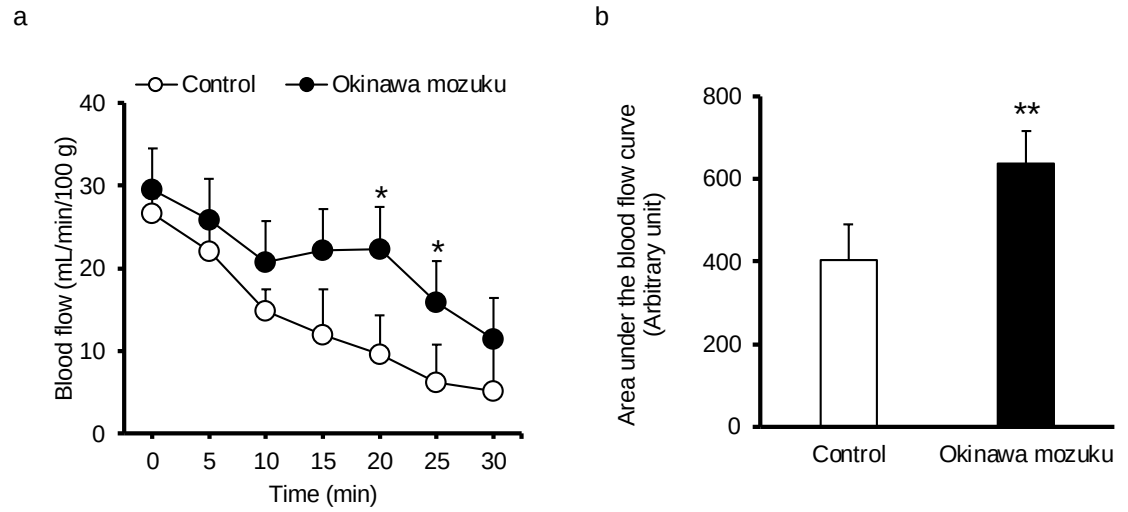

Fig. 5 Effects of Okinawa mozuku extract on blood flow in $FeCl_3$ induced carotid artery thrombosis model. Rats were fed with or without Okinawa mozuku extract for 8 weeks. Subsequently, 40% of $FeCl_3$ was applied to initiate thrombosis in carotid artery and blood flow of it after application was monitored (a). The decrease of blood flow in Okinawa mozuku extract group was less than that in control group. Moreover, the area under the blood flow curve for Okinawa mozuku extract group was compared with that for control (b). The area under the blood flow curve for Okinawa mozuku extract group was significantly higher than that for control group. Control, n=4; Okinawa mozuku, n=5 were analyzed. Values are shown as mean ± SD. *$p<0.05$, **$p<0.01$. This figure is reproduced from the figure previously published in *J. Nutr. Sci. Vitaminol.* (17).

2.3.5 Effect of Okinawa mozuku extract on fibrinolytic factors

To assess the effect of oral administration of Okinawa mozuku on fibrinolytic system, the activity of u-PA in euglobulin fraction and active PAI-1 levels in plasma were measured. In rats fed with Okinawa mozuku extract, the activity of u-PA in euglobulin fraction was significantly increased compared to control rats (Fig. 6a). On the other hand, Okinawa mozuku extract did not affect active PAI-1 levels in plasma (Fig. 6b).

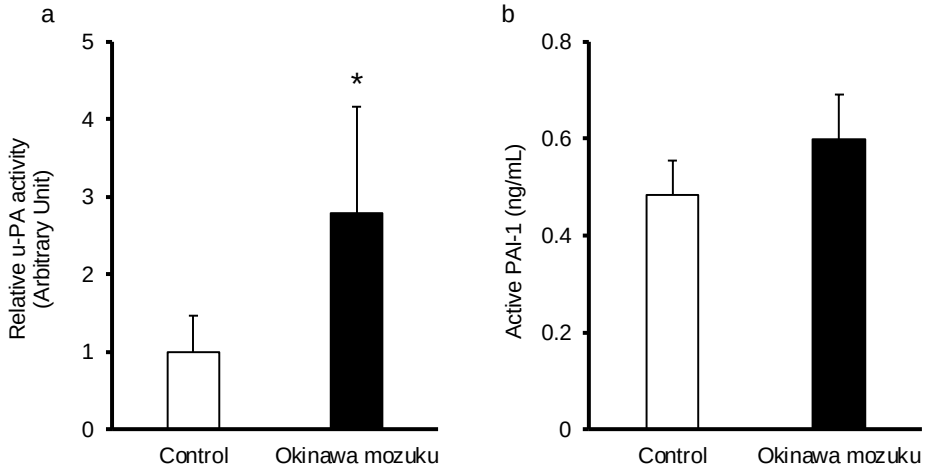

Fig. 6 Effects of Okinawa mozuku extract on u-PA activity and active PAI-1 levels in plasma. Relative u-PA activities in euglobulin fractions of rats fed with or without Okinawa mozuku were measured by using fibrin zymography (a). Control, n = 6; Okinawa mozuku, n = 6 were analyzed. Plasma active PAI-1 levels in rats fed with or without Okinawa mozuku were measured by ELISA (b). Control, n = 3; Okinawa mozuku, n = 6 were analyzed. Values are shown as mean ± SD. *$p<0.05$. This figure is reproduced from the figure previously published in *J. Nutr. Sci. Vitaminol.* (17).

2.4. DISCUSSION

The major function of VEC are blood coagulation and fibrinolysis. Plasminogen activator released from VEC promotes fibrinolysis. *In vitro* study showed that Okinawa mozuku increased u-PA activity in the conditioned medium of VEC (Fig. 3). It is speculated that Okinawa mozuku enhances the release of u-PA from endothelial cell. The u-PA is used as fibrinolytic agent for thrombotic diseases such as stroke and acute myocardial infarction (29, 30). The time to occlusion after $FeCl_3$-induced carotid artery injury in u-PA knockout mouse was shorter than that in wild-type mouse or t-PA knockout mouse (31). Moreover, the patency rate of occluded artery in u-PA knockout mouse was lower than that in wild-type mouse or t-PA knockout mouse (31). Therefore, it is thought that u-PA is more important for early blood clot resolution and vascular recanalization than t-PA. The augmented release of u-PA from VEC by Okinawa mozuku extract may contribute to prevent thrombus formation and promote fibrinolysis.

To evaluate the effect of oral administration of Okinawa mozuku extract on thrombosis, $FeCl_3$-induced carotid arterial thrombosis rat was used. $FeCl_3$-induced thrombosis model has been well used as the experimental arterial thrombosis model (32-34). In this model $FeCl_3$, an oxidizing agent, induces denudation of endothelial cells and exposes the subendothelium such as collagen. Then, coagulation cascade proceeds, and thrombus is formed. The FLO-C1 has been used to evaluate thrombosed vessel blood flow (35, 36). This study showed that Okinawa mozuku prevented the thrombotic occlusion due to $FeCl_3$-induced carotid artery injury (Fig. 5a and 5b). Furthermore, the oral administration of Okinawa mozuku extract increased u-PA activity in plasma euglobulin fraction (Fig. 6a). This phenomenon was supported by the *in vitro* study (Fig.

3a). These data suggested the antithrombotic effect of Okinawa mozuku via augment of u-PA activity.

There are no statistically significant differences in platelet aggregation and APTT between control group and Okinawa mozuku group (Table 2 and Fig. 5). These data indicated that Okinawa mozuku did not affect the platelet function and coagulation factors. Moreover, previously report supports these results (23).

PAI-1 is a main inhibitor of u-PA and regulates fibrinolytic system. PAI-1 blocks the activation of plasminogen to plasmin via inhibition of u-PA activity. PAI-1 is a risk factor for arterial thrombosis (37). In this study, Okinawa mozuku extract did not affect plasma PAI-1 levels (Fig. 6b). Therefore, it is considered that PAI-1 is not involved in the antithrombotic effect of Okinawa mozuku extract.

Many attempts have been made to develop chemical compounds that promote t-PA release from endothelial cells for the treatment of thrombosis (38, 39). However, these compounds have undesirable side effect, such as bleeding. Therefore, Okinawa mozuku has attracted attention because of their safety. Furthermore, because of the previous study in which the time to occlusion after $FeCl_3$-induced carotid artery injury in u-PA deficient mouse was shorter than t-PA deficient mouse as described above (13), it is speculated that u-PA releaser may be more efficient to prevent thrombus formation or promote clot lysis than t-PA releaser.

Since fucoidan is water-soluble, it is thought that Okinawa mozuku extract conteins fucoidan. The absorption of fucoidan, which is viscos polysaccharide in blown algae, is reported (26, 40). Oral administration of fucoidan from Laminaria Japonica prolonged the time to occlusion of blood vessel in electrical induced arterial thrombosis model. This phenomenon was accompanied with anticoagulation activity,

downregulation of thromboxane B_2, upregulation of 6-keto prostaglandin F1α, antiplatelet activity and effective fibrinolysis (40). The mechanism of the antithrombotic activity of fucoidan depends on its molecular weight (40). Although the main components of fucoidan are fucose and sulfate, fucoidan contains uronic acids and monosaccharides such as mannose, galactose, glucose, and xylose (41). The chemical property of fucoidan and bioactivity of fucoidan differ depending on the origin of seaweed species, and have some relation with sulfate content and position, molecular weight, and sugar composition. (23, 41). In this study, Okinawa mozuku extract did not possess anticoagulation activity but enhanced fibrinolytic activity. These findings suggest that molecular weight and/or chemical property of fucoidan from *Cladosiphon Okamuranus* are not similar to those from *Laminaria Japonica*.

The limitation of this study is that components of Okinawa mozuku extract are unclear and effective ingredients are unknown. Because the Okinawa mozuku extract has high viscosity, it is considered that it is rich in fucoidan and alginic acid, which are the main viscous polysaccharides of Okinawa mozuku. Although it is reported that alginic acid prevents thrombin generation (42), the involvement of alginic acid in fibrinolysis is unclear. In order to clarify this involvement, further study will be need.

In conclusion, it was demonstrated that Okinawa mozuku extract possessed the ability to enhance u-PA activity through an increase in u-PA release from endothelial cells both *in vitro* and *in vivo*. Furthermore, I also showed the antithrombotic effect of oral administration of Okinawa mozuku extract on rat carotid arterial $FeCl_3$-induced thrombosis model. It may be a beneficial food or supplement for the prevention of thrombosis and its related diseases.

3. The effect of inflammation and oxidative stress on albuminuria in obesity.

This chapter is based on a paper previously published in *FEBS Open Bio* (43).

3.1 INTRODUCTION

Obesity associated with microvascular complications, such as CKD. Obesity is one of the risk factors for CKD. Albuminuria is an early abnormal feature of CKD and has been recognized as a marker of systemic endothelial dysfunction (44). Albuminuria could reflect worsening renal function, cardiovascular disease, and increased risk of mortality (45). Data from the Prevention of Renal and Vascular End Stage Disease (PREVEND) study clearly show that increased albuminuria not only follows overt diabetic kidney disease but is also a marker of the progression of diabetes (46). It is reported that increases in inflammation and oxidative stress are recognized in the glomerular endothelial cells in insulin resistant conditions induced by diabetes and obesity (11). Recent studies indicate that inflammatory markers are closely related to endothelial dysfunction, which has been shown to indicate the development of diabetes (47-49).

This study characterized the mechanism of albuminuria caused by inflammation and oxidative stress in the glomeruli of obese rats.

3.2 METHODS

3.2.1 Animal experiments

All animal protocols were approved by the Kindai University and Joslin Diabetes Center's Animal Care Committee in accordance with the National Institutes of Health guidelines. Age matched male ZF, lean ZL rats, and C57BL/6J mice (Shimizu, Kyoto, Japan) were used. To determine nuclear factor κB (NF-κB) activation in the glomeruli,

NF-κB-dependent enhanced green fluorescent protein (GFP) transgenic mice (cis-NF-κB^{EGFP}) were used (50). These mice were produced as described previously and kindly provided by Steve Shoelson and Jongsoon Lee at the Joslin Diabetes Center. Obesity and insulin-resistant states were induced in 8-week-C57BL/6J and 8-week-cis-NF-κB^{EGFP} mice by feeding them a high-fat diet (45% and 42% from fat; Shimizu, Kyoto, Japan and Harlan Tekland, Indianapolis, IN, USA, respectively) or a normal diet for 2 months. Eight-week- cis-NF-κB^{EGFP} mice were the same group as published in previous study (50).

3.2.2 Isolation of glomeruli

Rat glomeruli were isolated from the renal cortex by the sieving method as described elsewhere (11).

3.2.3 Measurement of urinary albumin

Urinary albumin excretion in rat was measured by Nephrat (Exocell Inc., Philadelphia, PA, USA) using 24 hours urine collection samples from rat housed in individual metabolic cages. Urinary albumin excretion in mouse was measured by Albuwell (Exocell Inc., Philadelphia, PA, USA) using 24 hours urine collection samples from mouse housed in individual metabolic cages.

3.2.4 Serum triglyceride, serum total cholesterol, and plasma insulin

Serum triglyceride was measured by LabAssay Triglyceride (FUJIFILM Wako Pure Chemical Corporation, Osaka, Japan). Serum total cholesterol was measured by LabAssay Cholesterol (FUJIFILM Wako Pure Chemical Corporation, Osaka, Japan).

Plasma insulin was measured by Ultra-Sensitive Rat Insulin ELISA Kit (Morinaga Institute of Biological Science, Yokohama, Japan).

3.2.5 Real-time PCR analysis

Total RNA was isolated from the glomeruli using an RNAeasy microcolumn with DNase treatment (Qiagen, Valencia, CA, USA). Quantification of RNA was performed with the NanoDrop ND-1000 spectrophotometer (Thermo Scientific, Wilmington, DE, USA). cDNA was synthesized using Superscript III reverse transcriptase (Invitrogen, Carlsbad, CA, USA). mRNA expression in the glomeruli was evaluated by a SYBR green procedure (Applied Biosystems, Foster City, CA, USA). Amplification and detection were performed using the Step One Plus system (Applied Biosystems). Expression levels were normalized to levels of GAPDH. PCR primers were shown in table 3.

Table 3. PCR primers

	Forward Primer	Reverse Primer
TNF-α	AAATGGGCTCCCTCTCATCAGTTC	TCTGCTTGGTTTGCTACGAC
IL-6	TCCTACCCCAACTTCCAATGCTC	TTGGATGGTCTTGGTCCTTAGCC
CCR2	CTTGTGGCCCTTATTTTCCA	GAATTCCTGGAAGGTGGTCA
GAPDH	GTATTGGGCGCCTGGTCACC	CGCTCCTGGAAGATGGTGATGG

3.2.6 Histological study

Kidney samples for light microscopy analysis were fixed in 4% paraformaldehyde phosphate buffer. Kidney sections (2 μm) were stained with periodic acid–Schiff. Glomeruli were digitally photographed, and the images were imported into imagej software (National Institutes of Health, Bethesda, MD, USA;

https://imagej.nih.gov/ij/) and analyzed morphometrically. Dissected glomeruli from obese and control cis-NF-κB^{EGFP} mice were fixed in acetone and observed by digital fluorescence microscopy.

3.2.7 Statistics

Data are expressed as mean ± SD. Comparisons among more than two groups were performed by one-way ANOVA, followed by post hoc analysis with paired or unpaired t-test to evaluate statistical significance. All analyses were performed using StatView (SAS Institute, Cary, CA, USA). Statistical significance was defined as $P < 0.05$.

3.3 RESULTS

3.3.1 Physiological characteristics of experimental groups

Body weight was significantly increased in ZF rats when compared to ZL rats. Like ZF rats, mice fed with high-fat diet showed increases in body weight when compared to mice fed with normal diet (Tables 4 and 5). Serum triglyceride and cholesterol levels in ZF rats were significantly higher than those in ZL rats. However, there were no significant statistical differences in the levels of plasma insulin (Table 6). Initially, there were no significant differences in urinary albumin excretion between ZF and ZL rats (Fig. 7a). After 2 months of feeding, urinary albumin excretion was significantly increased in ZF rats when compared to ZL rats (Fig. 7b). Like rat experiments, there were no significant differences in urinary albumin excretion in mice, but when mice fed with high-fat diet after 2 months significantly increased in urinary albumin excretion when compared to normal diet (Fig. 7c, d).

Table 4. General characteristics of the rat experimental groups

	ZL	ZF
Number	6	4
Initial body weight (g)	169 ± 13	217 ± 7*
Body weight at 2 months (g)	303 ± 17	482 ± 10*

Values are shown as mean ± SD. *p<0.05 versus ZL rats. This table is reproduced from a table previously published in *FEBS Open Bio* (43). with modifications.

Table 5. General characteristics of the mice experimental groups

	Normal diet	High fat diet
Number	6	4
Initial body weight (g)	25 ± 2	25 ± 2
Body weight at 5 months (g)	34 ± 4	46 ± 2*

Values are shown as mean ± SD. *p<0.05 versus normal diet. This table is reproduced from a table previously published in *FEBS Open Bio* (43) with modifications.

Table 6. Serum triglyceride, serum total cholesterol, and plasma insulin

	ZL	ZF
Triglyceride (mg/dL)	28.1 ± 14.3	195.7 ± 23.6*
Total cholesterol (mg/dL)	51.2 ± 5.9	77.5 ± 7.0*
Insulin (ng/mL)	21.9 ± 0.5	19.9 ± 0.5

Values are shown as mean ± SD. *p<0.05 versus ZL rats. This table is reproduced from a table previously published in *FEBS Open Bio* (43) with modifications.

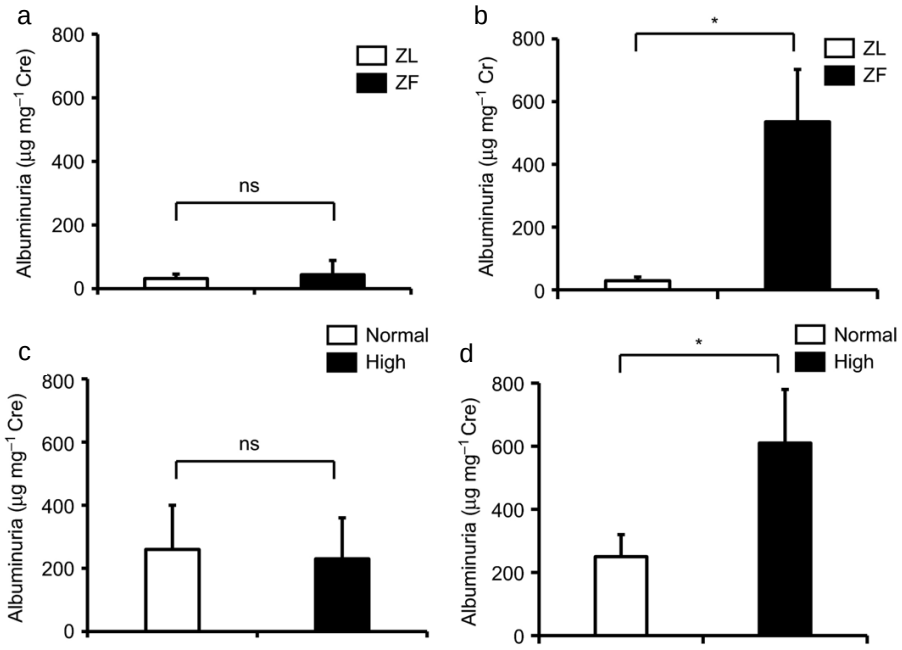

Fig. 7 Albuminuria in experimental groups. (a) Albuminuria in ZL and ZF rats at the start of experiment. (b) Albuminuria in ZL and ZF rats at 2 months. (c) Albuminuria in mice at the start of experiment. (d) Albuminuria in mice fed with high-fat diet after 2 months. *$p<0.05$. ns, not significant. ZL, n = 6; ZF, n = 4; Normal, n = 6; High, n = 4 were analyzed. Values are shown as mean ± SD. This figure is reproduced from a figure previously published in *FEBS Open Bio* (43).

3.3.2 Glomerular inflammation in experimental groups

Inflammatory markers were characterized in the glomeruli with the induction of obesity. Expression of TNF-α mRNA and CCR2 mRNA in the glomeruli of ZF rats were higher than those in the glomeruli of ZL rats (Fig. 8a, b). However, there were no statistically significant differences in expression of IL-6 mRNA between the glomeruli of ZL rats and ZF rats (Fig. 8c), which was consistent with previous report (50).

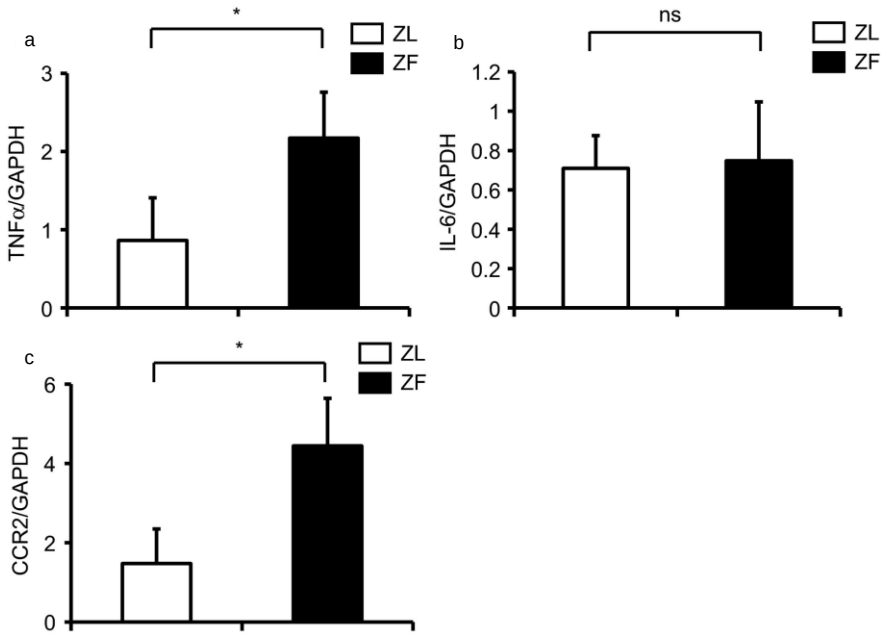

Fig. 8 Evaluation of inflammatory markers in the glomeruli of ZL and ZF rats. (a) TNF-α mRNA expression in the glomeruli of ZL and ZF rats. (b) IL-6 mRNA expression in the glomeruli of ZL and ZF rats. (c) CCR2 mRNA expression in the glomeruli of ZL and ZF rats. *$p<0.05$. ns, not significant. ZL, n = 6; ZF, n = 4 were analyzed. Values are shown as mean ± SD. This figure is reproduced from a figure previously published in *FEBS Open Bio* (43).

3.3.3 Renal histology in experimental groups

Morphometric analysis of glomerular area was performed. There were no statistically significant differences in the glomerular area between ZL and ZF rats (Fig. 9).

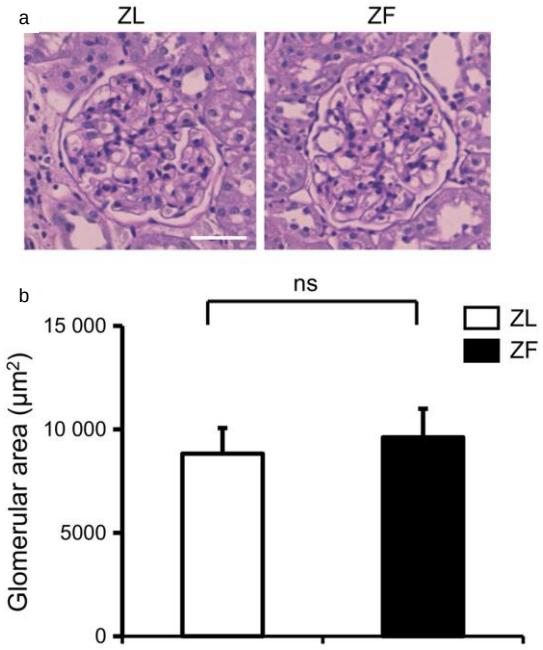

Fig. 9 Renal morphology in the experimental groups. (a) Representative light microscopic appearance of glomeruli (periodic acid-Schiff) for ZL and ZF rats. Bar = 50 μm. (b) Morphometric analysis of glomerular area. ns, not significant. ZL, n = 6; ZF, n = 4 were analyzed. Values are shown as mean ± SD. This figure is reproduced from a figure previously published in *FEBS Open Bio* (43).

3.3.4 Immunohistochemistry of NF-κB activation in the glomeruli of mice fed a high-fat diet

As inflammation and oxidative stress can activate NF-κB in obesity and the insulin-resistant state (51), NF-κB activity in the glomeruli of cis-NF-κB^{EGFP} mice were analyzed. GFP-positive areas were detected in the glomeruli of mice fed a high-fat diet for 2 months, indicating NF-κB activation (Fig. 10).

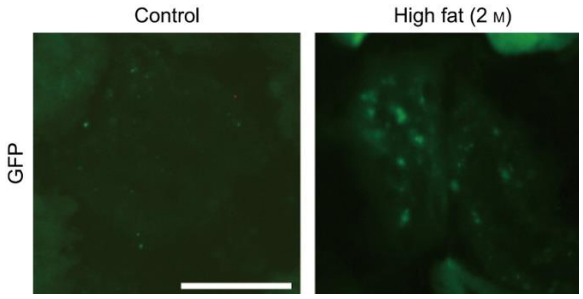

Fig. 10 Activation of NF-κB in the glomeruli of cis-NF-κB^{EGFP} transgenic mice. cis-NF-κB^{EGFP} transgenic mice were fed a high-fat diet for 2 months, after which EGFP fluorescence was assessed using digital fluorescence microscopy. Bar = 50 μm. This figure is reproduced from a figure previously published in *FEBS Open Bio* (43).

3.4 DISCUSSION

This study reports for the first time that obesity and the insulin-resistant state increase albuminuria, which is correlated with inflammation or oxidative stress. However, 2 months of metabolic abnormality was not enough to cause glomerular pathological changes. Previous reports have primarily focused on the activation of inflammation and oxidative stress by diabetes alone. Several studies have associated changes in inflammation and oxidative stress with albuminuria in CKD (52, 53). However, it has not

been reported that inflammation and oxidative stress can increase albuminuria, in the absence of renal pathological changes.

Quantitative PCR data showed increase of TNF-α and CCR2, but not IL-6 in the glomeruli of obese rats. It is reported that levels of TNF-α and IL-6 mRNA are increased by diabetes, but not by insulin resistance in retina (50). Also, it is reported that obesity-induced increases in IL-6 did not correlate with the incidence rate of acute kidney injury, while oxidative stress marker plasma F2-isoprostanes was increased in those patients (54). Expression of IL-6 mRNA was mainly recognized in moderate mesangial expansion area and the interstitial expression correlated with the degree of interstitial damages in DKD (55). Thus, increases in IL-6 level could be recognized in the kidney that was damaged to some extent by insulin-resistant state or diabetes. These findings could support the expression discrepancy between TNF-α and IL-6 mRNA in this study.

This study showed that obesity could increase TNF-α and CCR2 in the kidney when hyperinsulinemia is not present. Recent studies clearly show that TNF-α and its receptors, TNF receptors 1 and 2, are correlated with estimated glomerular filtration rate (56). Interestingly, these markers of inflammation are significantly increased in CKD patients without diabetes (57).

The mechanism for obesity-induced proteinuria appears to be via TNF-α activation. Among the inflammatory cytokines that were activated in the glomeruli, TNF-α appears to be the primary contributor to increased proteinuria. Previous studies indicated that TNF-α could change membrane permeability (58) resulting in proteinuria (59). Clinically, inhibition of TNF-α using the TNF-α neutralizing antibody, tocilizumab, results in decreased proteinuria.

Some reports have suggested that high-fat feeding over a prolonged time could develop mesangial expansion (60). However, glomerular histological changes were not recognized in this study. Observation period was only 2 months, while previous studies that showed high-fat diet-induced renal injuries were more than 3 months. Furthermore, they used the diet 60% from fat, while 42% in this study.

The monocyte chemoattractant protein (MCP)-1/CCR2 pathway may also play an important role in developing DKD (61, 62). It is reported that the inhibition of MCP-1/CCR2 pathway by CCR2 antagonist, propagermanium ameliorated the progression of DKD (63). Furthermore, CCR2 inhibitor CCX140-B showed renoprotective effects, reducing albuminuria in DKD patients (64). Present study supports the idea that inflammatory cytokines may be elevated before developing renal pathological changes and inhibiting cytokine action as a possible therapeutic target could improve and prevent DKD.

Previous report indicated that PKC activation selectively inhibits insulin/insulin receptor substrate (IRS)1 signaling, increasing inflammation and oxidative stress in the glomerulus of ZF rats (11). Here, this study demonstrates that obesity, without diabetes, induced by a high-fat diet was able to activate NF-κB in the glomerulus. In addition, increased TNF-α in the glomerulus can induce albuminuria after 2 months of obesity in ZF rats. Activation of the tyrosine phosphatase, Src homology-domain-containing phosphatase-1 (SHP-1), which is increased by diabetes and PKC-δ, causes VEGF resistance-induced podocyte apoptosis (65). Mechanistically, this pathway is independent of inflammation, oxidative stress, and NF-κB.

This study suggested that feeding of high fat diet for only 2 months duration can cause albuminuria in obese animals, due to increased inflammation or oxidative stress,

but may not be long enough to develop renal pathological changes. Further studies of the NF-κB, TNF-α, and CCR2 pathways could lead to effective interventions for obesity-induced CKD.

4. The effect of eicosapentaenoic acid on endothelial to mesenchymal transition in diabetes

This chapter is based on the paper previously published in *J. Diabetes Res.* (66).

4.1 INTRODUCTION

In chapter 3, two months of obesity did not cause histological changes in kidney. Therefore, to examine the endothelial function and the effect of nutrient in CKD, STZ-induced diabetic mice fed with high fat diet were used.

Several large clinical studies such as the action in diabetes and vascular disease: Preterax and Diamicron modified release controlled evaluation (ADVANCE) study, the UK prospective diabetes study (UKPDS), and the action to control cardiovascular risk in diabetes (ACCORD) trial indicated that intensive glycemic control could reduce the risk of DKD (67-70). On the other hand, large randomized controlled studies including the ADVANCE study, ACCORD trial, and outcome reduction with initial glargine intervention (ORIGIN trial) showed severe hypoglycemia, serious adverse events, renal impairment, and increased mortality (68, 70, 71). Thus, there is an urgent need to establish the new approach to treat DKD without hypoglycemia risk.

Extracellular matrix (ECM) accumulation, inducing mesangial expansion is a critical process in the glomerular pathology induced by diabetic condition (72). Type IV collagen (Col4) and smooth muscle actin are known as a common molecular marker of phenotypic changes of mesangial cells in DKD (73). It is reported that the transforming growth factor-β (TGF-β)/Smad1 pathway transcriptionally regulates the expression of Col4 and α-smooth muscle actin (αSMA) (74-77). Previous reports indicated that EndMT in the endothelial cells induced by the TGF-β signaling caused to glomerulosclerosis in the diabetic kidney (16). Recent reports suggest that supplementation with fish oil, which

is a major source of the n-3 polyunsaturated fatty acids (PUFA) eicosapentaenoic acid has been suggested to prevent glomerulonephritis and type-2 diabetes (78, 79). However, the mechanistic of action of ethyl eicosapentaenoic acid (EPA-E) on the glomerular cells is unclear.

In this study, the effects of EPA-E on albuminuria and EndMT in diabetic mice was analyzed. Further, the effect of adipocyte hypertrophy on EndMT in cultured VEC and the effect of EPA on its EndMT were evaluated.

4.2 METHODS

4.2.1 Animal experiments

All animal experiments were approved by the Animal Experiment Committee of Kindai University (approval number: KAAG-26-010) and performed by the animal experimental guideline of Kindai University. Male C57/BL6 mice (Shimizu, Kyoto, Japan) were used. Diabetes was induced in 11-week-old C57/BL6 mice by intraperitoneal injection of streptozotocin (STZ; 50 mg/kg body weight: Sigma, St Louis, MO) in 0.05 mol/l citrate buffer (pH 4.5) or citrate buffer for controls for 5 consecutive days. Control mice (Non-diabetic; NDM) were fed a control diet (MF diet, Oriental Yeast, Tokyo, Japan), and diabetic mice (DM) were fed a high-fat diet (60% from fat; HFD-60, Oriental Yeast, Tokyo, Japan). Two weeks after of injection of STZ, some diabetic mice were fed with a high-fat diet were orally administrated EPA-E (Mochida Pharmaceutical, Tokyo, Japan) at a dose of 1000 mg/ kg body weight/day in the diet for 19 weeks (DM + EPA-E) (80, 81). The systolic, mean, and diastolic blood pressure was measured by the tail-cuff method (BP-98A; Softron, Tokyo, Japan). After 19 weeks of treatment with EPA-E,

kidney samples were collected for histological analysis, malondialdehyde assay, western blotting, and real-time PCR assay.

4.2.2 Intraperitoneal glucose tolerance test

The intraperitoneal glucose tolerance test (IPGTT) was performed after 12 weeks of the EPA administration (25 weeks of age). After 16 hours of fasting, the mice were intraperitoneally treated with glucose (2 g/kg body weight), which was followed by blood sampling from the tail vein at intervals of 0, 30, 60, 90, and 120 minutes. The blood glucose level was measured by the glucose analyzer (Sanwa Kagaku, Aichi, Japan).

4.2.3 Measurement of the urinary albumin and creatinine

The urinary albumin and creatinine were measured using the Albuwell (Exocell Inc., PA, USA) and by creatinine colorimetric detection kit (Enzo Life Science, NY, USA), respectively. The urine samples were collected from the mice housed in individual metabolic cages for 24 hours. Urinary albumin and creatinine were measured at 11 weeks old (before treatment of EPA-E) and 28 weeks old (after 15 weeks of EPA-E treatment).

4.2.4 Plasma triglyceride and non-esterified fatty acid

After 19 weeks of EPA-E treatment, blood samples were collected for measurements of plasma triglyceride and non-esterified fatty acid. The plasma triglyceride and non-esterified fatty acid were measured using the LabAssay Triglyceride (FUJIFILM Wako Pure Chemical Corporation, Osaka, Japan) and LabAssay NEFA (FUJIFILM Wako Pure Chemical Corporation, Osaka, Japan), respectively.

4.2.5 Malondialdehyde assay

Malondialdehyde in the renal cortex was measured using the TBARS assay kit (Cell Biolabs, San Diego, CA, USA), according to the manufacturer's instructions.

4.2.6 Histological analysis

Kidney sections for light microscopy analysis were fixed in 4% paraformaldehyde phosphate buffer. Sections were stained with periodic acid-Schiff. Glomeruli were digitally photographed, and the images were imported to the ImageJ software (National Institutes of Health, Bethesda, MD, USA; https://imagej.nih.gov/ij/) and analyzed morphometrically (82). For immunohistochemistry, the tissue sections were de-paraffined using xylene and rehydrated through an ethanol series and PBS. The antigen retrieval was performed by microwave treatment, with Citrate buffer, pH 6. Endogenous peroxidase was blocked with 0.3% H2O2 in methanol for 30 min, followed by incubation with the G-Block (Genostaff, Tokyo, Japan) and avidin/biotin blocking kit (Vector, CA, USA). The sections were incubated with an anti-CD31 rabbit monoclonal antibody (Cell Signaling, MA, USA) at 4°C overnight. They were incubated with biotin-conjugated anti-rabbit Ig (Dako, CA, USA), for 30 min at room temperature, followed by the addition of peroxidase-conjugated streptavidin (Nichirei, Tokyo, Japan) for 5 min. The peroxidase activity was visualized using diaminobenzidine. The sections were counterstained with Mayer's Hematoxylin (MUTO, Tokyo, Japan), dehydrated, and then mounted with Malinol (MUTO).

4.2.7 3T3-L1 differentiation for adipocyte

The mouse 3T3-L1 preadipocytes were cultured in DMEM (FUJIFILM Wako Pure Chemical Corporation, Osaka, Japan) containing 10% fetal bovine serum (FBS) at 37°C, 5% CO2. The differentiation for adipocytes was induced by a commercial kit (AdipoInducer Reagent, Takara Bio, Shiga, Japan). Two days post confluency, 3T3-L1 preadipocytes were cultured using differentiation medium (DMEM containing 10 µg/mL insulin, 2.5 µM dexamethasone, and 0.5 mM 3-isobutyl-1methylxanthine) for 48 hours. Then, the differentiation medium was replaced with a maintenance medium (DMEM containing 10 µg/mL insulin). Thereafter, the maintenance medium was replaced every two days. After differentiation, the medium was collected on the 4th and 8th days, as the adipocyte-conditioned medium for stimulating the endothelial cells.

4.2.8 Oil red O stain

To evaluate the lipid accumulation of 3T3-L1 adipocyte, the Oil red O staining was performed. The cells were washed by PBS and fixed in 2.5% glutaraldehyde for 10 min. After washing with PBS, the cells were stained by Oil red O solution (FUJIFILM Wako Pure Chemical Corporation, Osaka, Japan) for 15 min. The stained cells were visualized under an optical microscope. Then, the Oil red O stained lipid was extracted by isopropanol and quantified by measuring the absorbance at 492 nm using a microplate reader (Thermo Fisher Scientific, MA, USA).

4.2.9 Endothelial cell culture

The cell line (bEnd.3) that was established from the mouse microvascular endothelial cells were used. EPA-E was dissolved in 100% ethanol to make stock solution.

The cells were plated onto a 6-well plate and cultured in DMEM containing 10% FBS and 5.6 mM glucose. After reaching sub-confluence, the medium was replaced by a 3T3-L1 adipocyte conditioned medium containing 5.6 mM glucose and 2% fatty acid-free BSA (FUJIFILM Wako Pure Chemical Corporation, Osaka, Japan) with or without a 200 μM EPA-E (Mochida Pharmaceutical, Tokyo, Japan). The same amount of ethanol as EPA-E solution was used for the vehicle. After incubation for 48 hours, the protein lysate was harvested for western blot analysis.

4.2.10 Adipocyte conditioned medium-induced cell migration assay

The cell culture inserts (Greiner Bio-One Co. Ltd, Tokyo, Japan) with an 8 μm pore membrane were used for the cell migration assay as previously described with modifications (16, 83). The endothelial cells were passaged in the upper chamber. Twenty-four hours after passage, the medium was changed to the 3T3-L1 adipocyte conditioned medium containing 5.6 mM glucose and 2% fatty acid-free BSA with or without of 200 μM EPA-E. After incubation for 48 hours, the nonmigratory cells were removed with a cotton swab. The migrated cells were stained with DAPI and counted. Five different areas were evaluated in each group.

4.2.11 High glucose-induced endothelial cell migration

The cell culture inserts (Greiner Bio-One Co. Ltd, Tokyo, Japan) with 8 μm pore membrane were used for cell migration assay. The endothelial cells were passaged in upper chamber. Twenty-four hours after passage, the medium was changed to low glucose (5.6 mM glucose and 19.4 mM mannitol) or high glucose medium (25mM glucose) with or without of 50 μM EPA-E. After 24 h, the nonmigratory cells were removed with a

cotton swab. The migration cells were stained with DAPI and counted. Five different areas were evaluated in each group.

4.2.12 Western blotting

In vivo experiments, protein samples were isolated from renal cortex. The protein lysates were separated by 10% SDS-polyacrylamide gels and blotted onto polyvinylidene fluoride (PVDF) membranes. After blocking, the membranes were incubated with anti-CD31 (Cell Signaling, MA, USA), anti-SM22α (Abcam, Cambridge, UK), anti-Erk1/2 (Cell Signaling, MA, USA), anti-pErk1/2 (Cell Signaling, MA, USA), anti-PAI-1 (Abcam, Cambridge, UK), TGF-β (Cell Signaling, MA, USA), anti-Snail (Cell Signaling, MA, USA), anti-TGF-β (Cell Signaling, MA, USA) and anti-β-actin (Cell Signaling, MA, USA) at 4°C overnight. The membranes were washed and incubated with horseradish peroxidase-conjugated secondary antibodies for 1 h at room temperature. The protein-antibody complex was detected using the ECL reagent (SuperSignalTM West Dura Extended Duration Substrate, Thermo Fisher Scientific, MA, USA) and the signals were detected using LAS 4000mini biomolecular imager (FUJIFILM, Tokyo, Japan). Membranes are cut prior to hybridization with antibodies, so these are not images of full-length blots.

4.2.13 RNA and microRNA isolation and real-time PCR assay

The total RNA was isolated from renal cortex using the RNeasy Mini Kit (Qiagen, German). The complementary DNA was synthesized using the SuperScript III reverse transcriptase (Invitrogen, Carlsbad, CA, USA). The real-time PCR was performed on a StepOne Plus real-time PCR system (Thermo Fisher Scientific, MA, USA) using the

SYBR Green Master Mix (Applied Biosystems, Foster City, CA, USA). The expression levels were normalized to levels of GAPDH. PCR primers were shown in table 7.

Table 7. PCR primers

	Forward Primer	Reverse Primer
Collagen IV	GCCAAGTGTGCATGAGAAGA	AGCGGGGTGTGTTAGTTACG
TGF-β	TGCTTCAGCTCCACAGAGAA	TGGTTGTAGAGGGCAAGGAC
PKCβ	GGGATTCCAGTGTCAAGTCTGCT	AGGACTGGAGTACGTGTGGATCTT
p47phox	ACCTTCATTCGCCATATCGCCCT	TTCTGTAGACCACCTTCTCCGACA
Nox2	TGCAGCCTGCCTGAATTTCAACTG	AGATGTGCAATTGTGTGGATGGCG
Nox4	GAACCTCAACTGCAGCCTGATC	CTTTTGTCCAACAATCTTCTTGTTCTC
GAPDH	ATGTTCCAGTATGACTCCACTCACG	GAAGACACCAGTAGACTCCACGACA

The primers for Mm_miR-29b and Mm_let-7a were from the miScript Primer Assay designed by Qiagen. The mature microRNA sequences were as follows:
Mm_miR-29b: UAGCACCAUUUGAAAUCAGUGUU;
Mm_let-7a: UGAGGUAGUAGGUUGUAUAGUU. All of the experiments were performed in triplicates, and Hs_RNU6-2_1 (Qiagen) was used as an endogenous control for normalization.

4.2.14 Statistics

All statistical analyses were performed using Microsoft Excel (Microsoft Corporation, Redmond, WA, USA) and the add-in software Statcel 3 (OMS Publishing Inc., Saitama, Japan). The data are shown as the mean ± SD for each group. Statistical analysis was performed by one-way analysis of variance (ANOVA) post hoc Tukey—

Kramer multiple comparisons, or Student's t-test. All results were considered statistically significant at $p < 0.05$.

4.3 RESULTS

4.3.1 Characteristic of the experimental group

Blood glucose significantly increased in in the diabetic mice fed a high-fat diet compared to the control mice after 5 months of diabetes. The final body weights of experimental groups did not change. Kidney weight per body weight increased in diabetic mice compared to the control mice. However, there were no statistically significant differences between these two groups (Table 8). Systolic blood pressure was significantly increased in diabetic mice compared to the control mice. Serum triglyceride and non-esterified fatty acid were increased in diabetic mice compared to the control mice. However, there were no statistically significant differences between these two groups (Table 9). The effects of diabetes and high-fat diet on the systemic insulin resistance evaluated by IPGTT showed a significant increase in glucose in a step-wise manner with maximum levels on diabetic mice fed a high-fat diet reached at 1 h with levels > 500 mg/dL (Fig. 10).

Table 8. General characteristics of the experimental groups

	NDM	DM+HF	DM+HF+EPA-E
Number	8	4	6
Bodyweight (g)			
10 weeks old	25.1 ± 2.0	24.5 ± 3.9	24.3 ± 2.7
32 weeks old	34.7 ± 4.0$^{\#}$	33.0 ± 9.9	33.8 ± 5.8
rKW/BW (g/100 g BW)	1.06 ± 0.18	1.19 ± 0.38	1.13 ± 0.16
Blood glucose (mg/dL)	98.5 ± 14.9	314 ± 100*	274 ± 92*

NDM, non-diabetic mice; DM, mice with STZ-induced diabetes fed a high fat diet; DM+EPA-E, STZ-induced diabetic mice fed a high fat diet treated with EPA-E; EPA-E, ethyl eicosapentaenoate; rKW/BW, right kidney weight/body weight. Values are shown as mean ± SD. $^{*}p < 0.05$ vs. NDM, $^{\#}p < 0.01$ vs. NDM 10 weeks old. This table is reproduced from a table previously published in *J. Diabetes Res.* (66).

Table 9. Metabolic characteristics of experimental groups

	NDM	DM+HF	DM+HF+EPA-E
Number	8	3	4
TG (mg/dL)	85.3 ± 23.4	123 ± 140	68.9 ± 26.2
NEFA (mEq/L)	0.52 ± 0.13	0.75 ± 0.83	0.33 ± 0.16
SBP (mmHg)	113 ± 8	126 ± 1*	113 ± 6

NDM, non-diabetic mice; DM, mice with STZ-induced diabetes fed a high fat diet; DM+EPA-E, STZ-induced diabetic mice treated with EPA-E; EPA-E, ethyl eicosapentaenoate; TG, triglyceride; NEFA, non-esterified fatty acid, SBP; systolic blood pressure. Values are shown as mean ± SD. $^{*}p < 0.05$ vs. NDM. Blood sampling and blood pressure measurement could not be performed on all mice due to their conditions. This table is reproduced from a table previously published in *J. Diabetes Res.* (66).

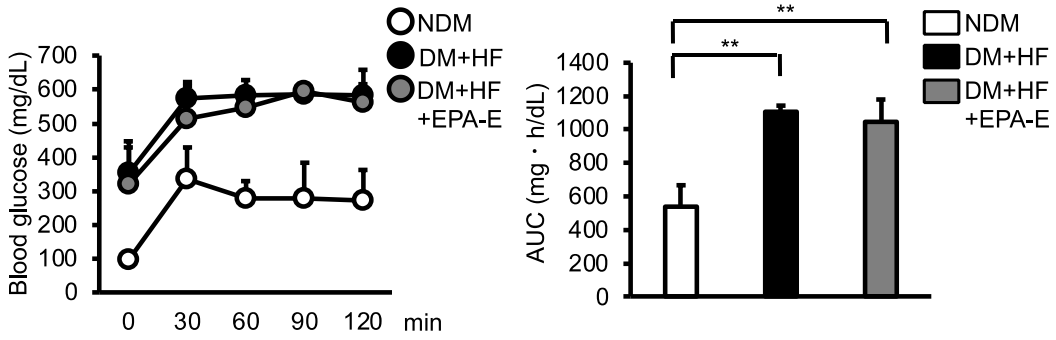

Fig. 10 Effects of EPA-E on blood glucose in the experimental groups. Intraperitoneal glucose tolerance tests were performed in the experimental groups. Time-course measurements of blood glucose is shown. The area under the curve is derived from the intraperitoneal glucose tolerance tests. **p<0.01. NDM, n = 8; DM+HF, n = 4; DM+HF+EPA-E, n = 6 were analyzed. Values are shown as mean ± SD. NDM, non-diabetic mice; DM+HF, mice with STZ-induced diabetes were fed a high-fat diet; DM+HF+EPA-E, STZ-induced diabetic mice were fed a high-fat diet treated with EPA-E. This figure is reproduced from a figure previously published in *J. Diabetes Res.* (66) with modifications.

4.3.2 Effect of EPA-E on the kidney of high fat-fed diabetic mice

Urinary albumin excretion was significantly increased in diabetic mice compared to the control mice. Administration of EPA-E significantly decreased albuminuria compared to diabetic mice (Fig. 11). The glomerular area was significantly increased in the diabetic mice fed a high-fat diet compared to the control mice. Administration of EPA-E significantly decreased glomerular area compared to the diabetic mice (Fig. 12a). The immunohistochemical analysis showed that the positive cell number of CD31 in glomeruli was significantly decreased in diabetic mice compared to the control mice. EPA-E treatment significantly increased the positive cell number of CD31 compared to the diabetic mice (Fig. 12b).

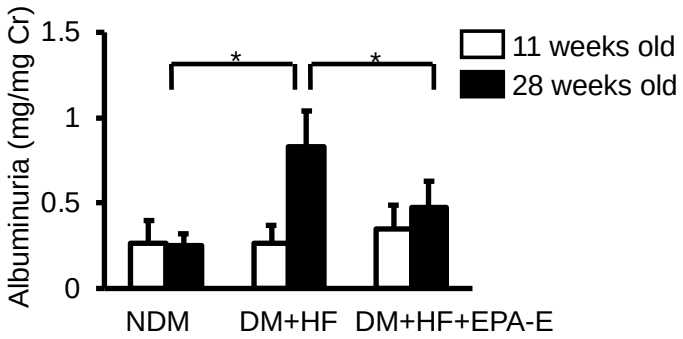

Fig. 11 Effects of EPA-E on albuminuria in the experimental groups. Albuminuria was measured by the Albuwell. *$p<0.05$. NDM, n = 8; DM+HF, n = 4; DM+HF+EPA-E, n = 6 were analyzed. Values are shown as mean ± SD. NDM, non-diabetic mice; DM+HF, mice with STZ-induced diabetes were fed a high-fat diet; DM+HF+EPA-E, STZ-induced diabetic mice were fed a high-fat diet treated with EPA-E. This figure is reproduced from a figure previously published in *J. Diabetes Res.* (66) with modifications.

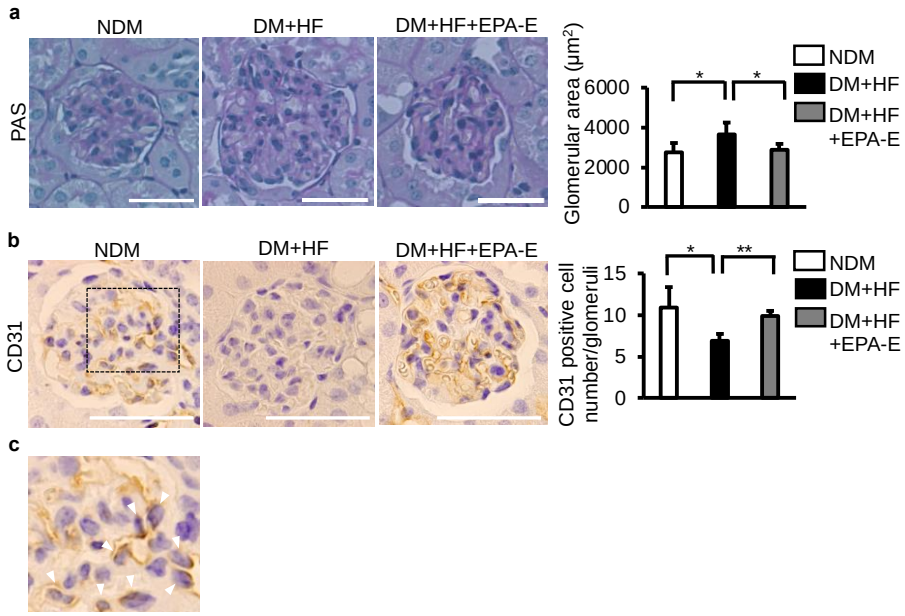

Fig. 12 Effects of EPA-E on renal morphology and immunohistochemical staining of CD31. (a) Representative light microscopic appearance of glomeruli (periodic acid-Schiff) for experimental groups. Morphometric analysis of the glomerular area. Bar = 50 μm. (b) Representative immunohistochemistry of CD31 in the glomeruli. Sections were counterstained with hematoxylin solution. Bar = 50 μm. (c) Enlarged glomerular image of the box in d. Positive nuclear staining for CD31 was localized in endocapillary area (white triangle). *$p<0.05$. **$p< 0.01$. NDM, n = 8; DM+HF, n = 4; DM+HF+EPA-E, n = 6 were analyzed. Values are shown as mean ± SD. NDM, non-diabetic mice; DM+HF, mice with STZ-induced diabetes were fed a high-fat diet; DM+HF+EPA-E, STZ-induced diabetic mice were fed a high-fat diet treated with EPA-E. This figure is reproduced from a figure previously published in *J. Diabetes Res.* (66) with modifications.

The protein expression of αSMA in the renal cortex was significantly increased in the diabetic mice. EPA-E treatment significantly decreased the protein expression of αSMA (Fig. 13a). The mRNA expression of Col4 was significantly increased in the diabetic mice compared to the control mice. EPA-E treatment significantly decreased the mRNA expression of Col4 (Fig. 13b). Phosphorylation of Erk1/2 (pErk1/2) was significantly increased in diabetic mice compared with control mice (Fig. 14a). The expression of pErk1/2 was decreased by the administration of EPA-E. However, there were no statistically significant differences (Fig. 14a). TGF-β and PKCβ mRNA were significantly increased in diabetic mice (Fig. 14b and 14c). There was a similar trend for a beneficial effect of EPA-E in these mRNA levels. However, no statistically significant differences were observed between these mice (Fig. 14b and 14c).

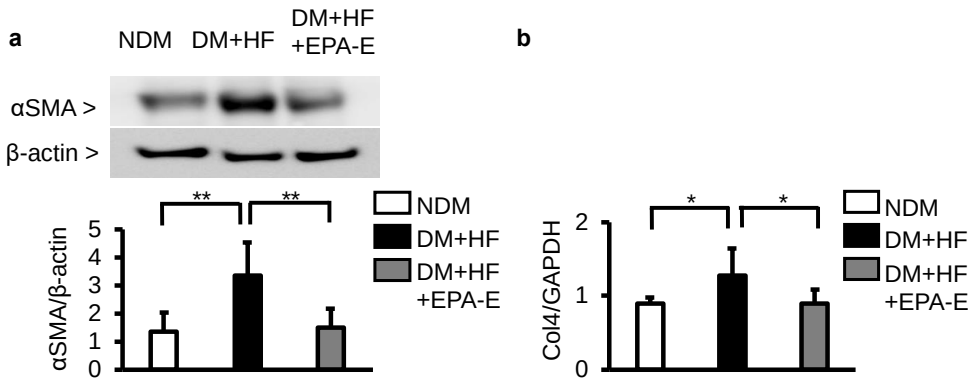

Fig. 13 Effect of EPA-E on extracellular matrix in the experimental groups. (a) Immunoblot analysis of αSMA in the renal cortex. (b) *Type 4 collagen* mRNA expression in the renal cortex of the experimental groups. *p< 0.05. **p< 0.01. NDM, n = 8; DM+HF, n = 4; DM+HF+EPA-E, n = 6 were analyzed. Values are shown as mean ± SD. NDM, non-diabetic mice; DM+HF, mice with STZ-induced diabetes were fed a high-fat diet; DM+HF+EPA-E, STZ-induced diabetic mice were fed a high-fat diet treated with EPA-E. This figure is reproduced from a figure previously published in *J. Diabetes Res.* (66) with modifications.

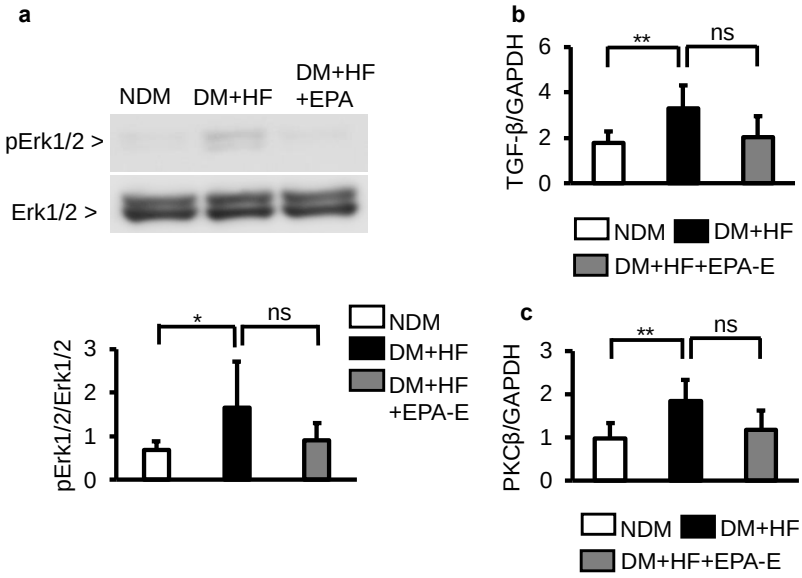

Fig. 14 Effect of EPA-E on phosphorylation of Erk1/2, TGF-β, and PKCβ in the experimental groups. (a) Immunoblot analysis of phosphor-Erk1/2 in the renal cortex of the experimental groups. (b) TGF-β (c) and PKCβmRNA expression in the renal cortex of the experimental groups. *p< 0.05. **p<0.01. ns; not significant. NDM, n = 8; DM+HF, n = 4; DM+HF+EPA-E, n = 6 were analyzed. Values are shown as mean ± SD. NDM, non-diabetic mice; DM+HF, mice with STZ-induced diabetes were fed a high-fat diet; DM+HF+EPA-E, STZ-induced diabetic mice were fed a high-fat diet treated with EPA-E. This figure is reproduced from a figure previously published in *J. Diabetes Res.* (66). with modifications.

4.3.3 Oxidative stress in renal cortex

The markers of oxidative stress, which could contribute to developing DKD (43, 84-86) were evaluated. Malondialdehyde (MDA) levels was significantly increased in renal cortex of diabetic mice compared to control mice. Although the results are not statistically significant, EPA-E treatment decreased MDA levels in renal cortex of diabetic mice (Fig. 15). The expression of mRNA of p47phox, Nox2, and Nox4 in the renal cortex were significantly increased in diabetic mice. Similarly, EPA-E decreased these expressions. However, there were no statistically significant differences between these mice (Fig.16a, 16b, and 16c).

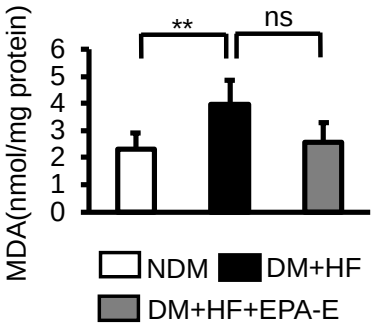

Fig. 15 Effect of EPA-E malondialdehyde in the experimental groups. Malondialdehyde is measured by the thiobarbituric acid reactive substance assay. **p<0.01. ns; not significant. NDM, n = 8; DM+HF, n = 4; DM+HF+EPA-E, n = 6 were analyzed. Values are shown as mean ± SD. NDM, non-diabetic mice; DM+HF, mice with STZ-induced diabetes were fed a high-fat diet; DM+HF+EPA-E, STZ-induced diabetic mice were fed a high-fat diet treated with EPA-E. This figure is reproduced from a figure previously published in *J. Diabetes Res.* (66) with modifications.

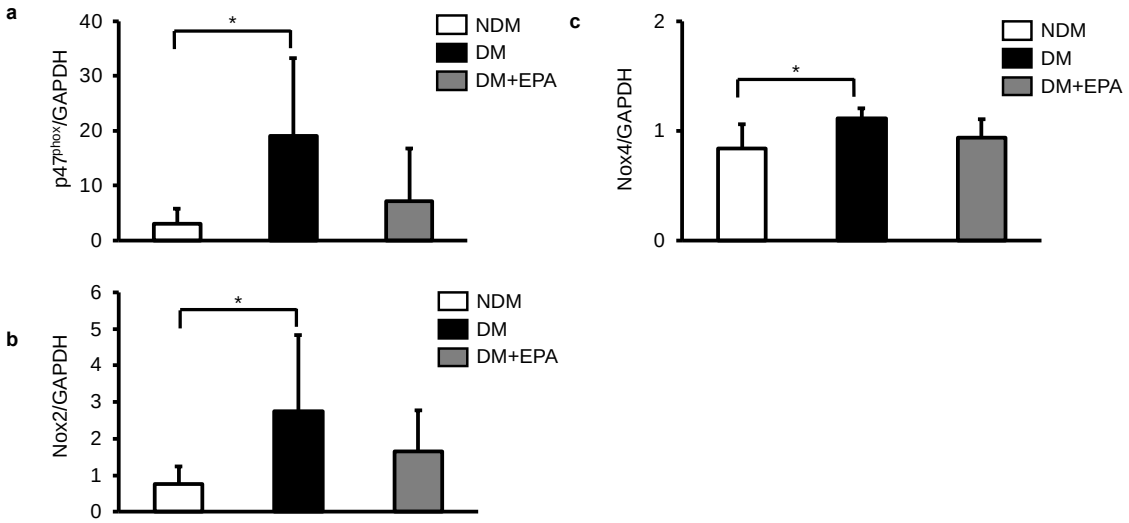

Fig. 16 Evaluation of the oxidative stress in the renal cortex. (a−c) Characterization of the changes in the mRNA levels of p47phox, (a), Nox2, (b), and Nox4 (c) expression in the renal cortex of the non-diabetic mice, STZ-induced diabetic mice, and STZ-induced diabetic mice treated with EPA-E. *p< 0.05. ns; not significant. NDM, n = 8; DM+HF, n = 4; DM+HF+EPA-E, n = 6 were analyzed. Values are shown as mean ± SD. NDM, non-diabetic mice; DM+HF, mice with STZ-induced diabetes were fed a high-fat diet; DM+HF+EPA-E, STZ-induced diabetic mice were fed a high-fat diet treated with EPA-E. This figure is reproduced from a figure previously published in *J. Diabetes Res.* (66) with modifications.

4. 3.4 The effect of adipocyte hypertrophy on EndMT in cultured endothelial cells.

To determine whether a high-fat condition can cause EndMT due to the process of adipogenic differentiation, the 3T3-L1 preadipocyte cells were used. As shown in this results, oil red O staining increased gradually from 0 to 8 days (Fig. 17). The protein levels of TGF-β were significantly increased in 3T3-L1 cells (Fig. 18a). Expression of TGF-β mRNA was also significantly increased in the same manner (Fig. 18b). The cell migration assay was performed by using double chamber methods. The addition of the conditioned medium from adipocyte significantly increased the number of migrated cells

in 8 days compared to 0 days. The addition of EPA-E significantly decreased the number of migrated cells in 8 days (Fig. 19). In addition, high glucose condition significantly increased the number of migrated cells compared to low glucose condition. Addition of EPA-E significantly decreased the number of migrated cells in high glucose condition (Fig. 20). It is reported that TGF-β induced EndMT by causing downregulation of CD31 and upregulation of SM22α in endothelial cells (87). To evaluate the effect of adipocyte hypertrophy on EndMT, endothelial cells were stimulated with adipocyte conditioned medium. Adipocyte conditioned medium significantly decreased the expression of CD31 (Fig. 21a). On the other hand, the expression of SM22α was significantly increased by adipocyte conditioned medium (Fig. 21b). EPA-E partially normalized CD31 expression SM22α expression (Fig. 21a and 21b). As activation of the Erk1/2-PAI-1 pathway plays a significant role in developing DKD following EndMT (82, 88), phosphorylation of Erk1/2 and PAI-1 expression were measured. Adipocyte conditioned medium significantly increased phosphorylation of ErK1/2 and PAI-1 expression (Fig. 22a and 22b). These increases of pErk1/2 and PAI-1 expression were significantly suppressed by EPA-E (Fig. 22a and 22b). The expression of Snail, a transcription factor that regulates EndMT, was measured. Adipocyte conditioned medium significantly increased Snail expression. However, the expression of Snail was significantly decreased by EPA-E (Fig. 22c).

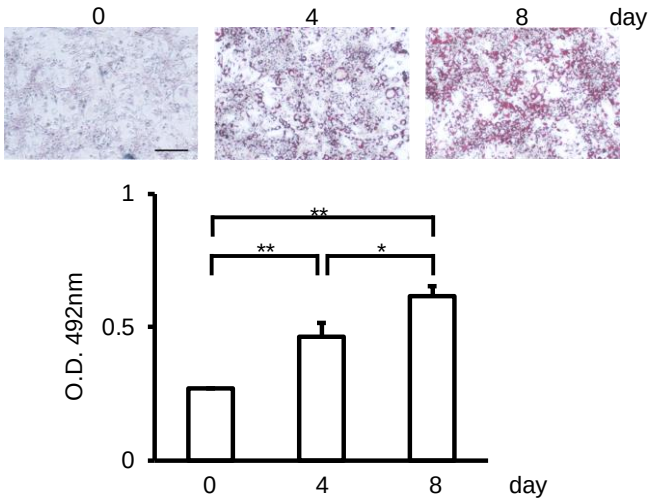

Fig. 17 Accumulation of lipids by differentiation of 3T3-L1 cells. The 3T3-L1 cells were cultured in differentiation medium for 8 days. Cells that were differentiated into adipocytes were stained with Oil red O staining. Oil red O staining was evaluated by measuring the absorbance of the eluate. Bar = 100 μm. *p< 0.05. **p< 0.01. n = 3 were analyzed. Values are shown as mean ± SD. This figure is reproduced from a figure previously published in *J. Diabetes Res.* (66) with modifications.

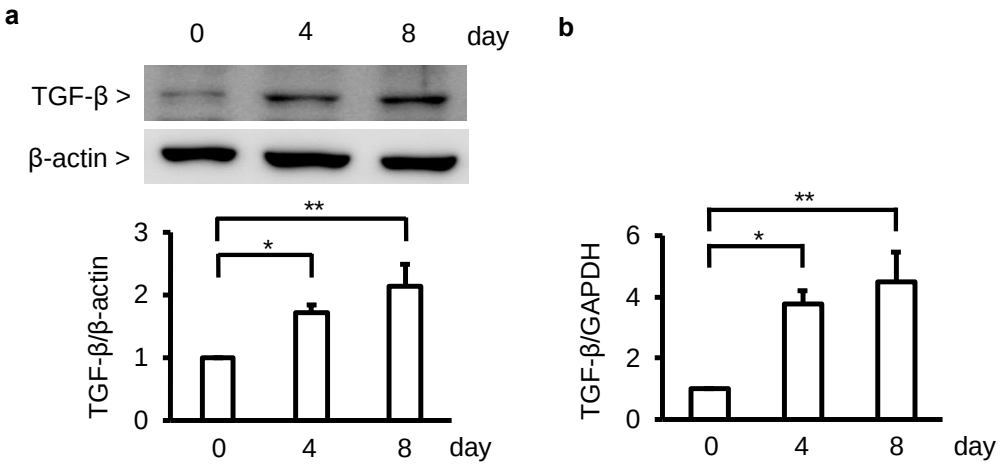

Fig. 18 TGF-β expression of 3T3-L1 cells. (a) Protein expression of TGF-β and (b) mRNA expression of TGF-β in 3T3-L1 cells were evaluated. *p< 0.05. **p< 0.01. n = 3 were analyzed. Values are shown as mean ± SD. This figure is reproduced from a figure previously published in *J. Diabetes Res.* (66) with modifications.

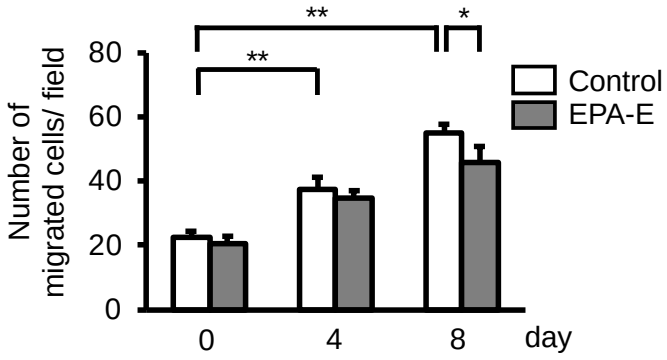

Fig. 19 The effect of adipocyte conditioned medium on migration of endothelial cells. Endothelial cells migration was measured using the Boyden chamber assay for evaluation of EndMT. *p< 0.05. **p< 0.01. n = 3 were analyzed. Values are shown as mean ± SD. This figure is reproduced from a figure previously published in *J. Diabetes Res.* (66) with modifications.

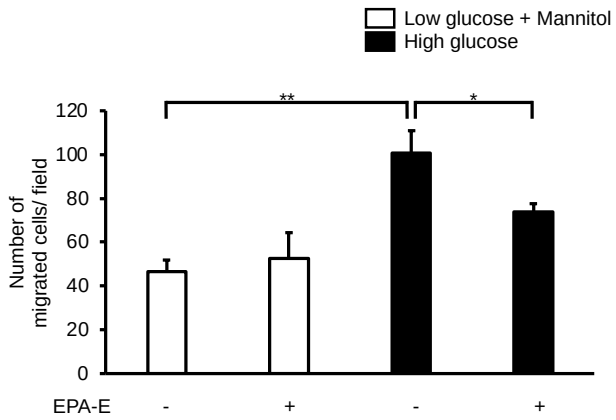

Fig. 20 High glucose promotes EndMT, and EPA-E inhibits its effect. EndMT was evaluated using the Boyden chamber assay. The endothelial cells were passaged in upper chamber. Twenty-four hours after passage, the medium was changed to low glucose (5.6 mM glucose and 19.4 mM mannitol) or high glucose medium (25mM glucose) with or without of 50 μM EPA-E. The migration cells were stained with DAPI and counted. *p< 0.05. **p< 0.01. n = 3 were analyzed. Values are shown as mean ± SD. This figure is reproduced from a figure previously published in *J. Diabetes Res.* (66) with modifications.

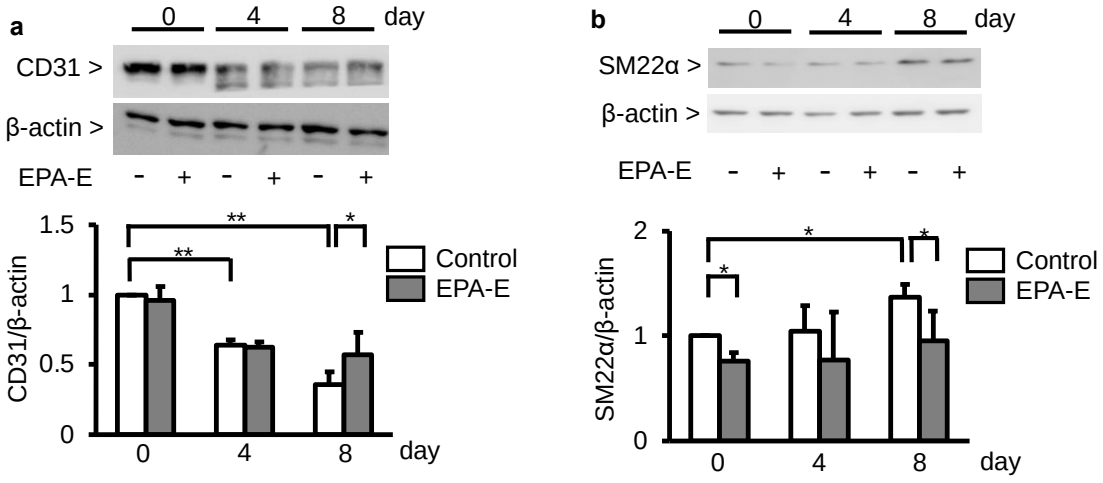

Fig. 21 The effect of EPA-E on expression of CD31 and SM22α in endothelial cells. (a) CD31 expression and (b) SM22α expression in endothelial cells incubated in the adipocyte conditioned medium with or without EPA-E (200 μM). *p< 0.05. **p< 0.01. n = 3 were analyzed. Values are shown as mean ± SD. This figure is reproduced from a figure previously published in *J. Diabetes Res.* (66) with modifications.

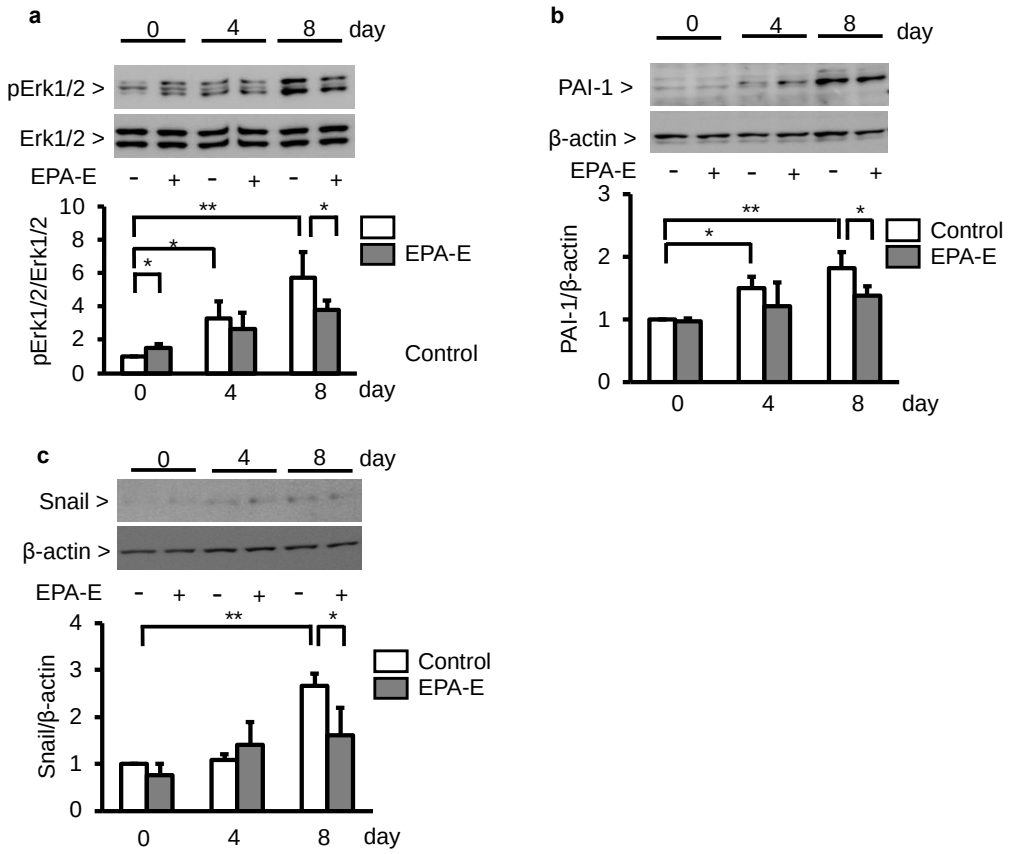

Fig. 22 The effect of EPA-E on expression of phosphorylation of Erk1/2, PAI-1, and Snail in endothelial cells. (a) pErk1/2 expression, (b) PAI-1 expression, and (c) Snail expression in endothelial cells incubated in the adipocyte conditioned medium with or without EPA-E (200 μM). *p< 0.05. **p< 0.01. n = 3 were analyzed. Values are shown as mean ± SD. This figure is reproduced from a figure previously published in *J. Diabetes Res.* (66) with modifications.

To assess the effect of TGF-β in adipocyte conditioned medium on EndMT, LY364947, selective inhibitor of TGF-βRI, was used. The expression of CD31 in endothelial cells was significantly decreased by adipocyte conditioned medium. However, addition of LY364947 did not restore CD31 expression (LY364947; 1 μM and 10 μM, respectively, Fig. 23).

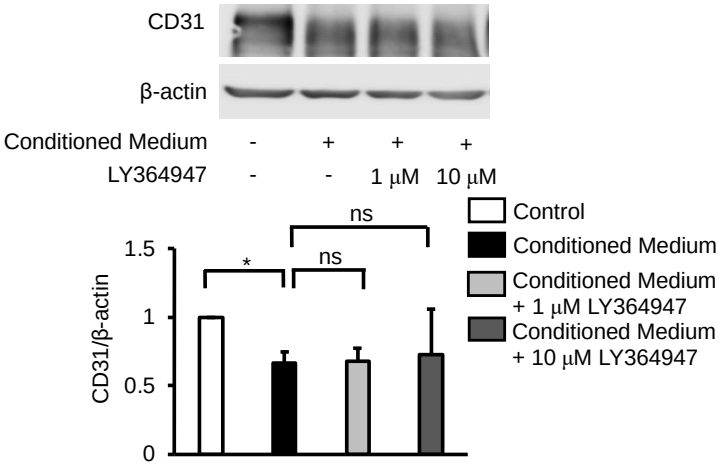

Fig. 23 Effect of selective inhibitor of TGF-βR1, LY36497 on CD31 expression in endothelial cells. Immunoblot analysis of CD3l. Endothelial cells were incubated in the adipocyte conditioned medium 1μM or 10μM LY36497. *p< 0.05. ns; not significant. n = 3 were analyzed. Values are shown as mean ± SD. Regarding immunoblot, membranes are cut prior to hybridization with antibodies, so these are not images of full-length blots. This figure is reproduced from a figure previously published in *J. Diabetes Res.* (66) with modifications.

4.3.5 Expression of Mm_miR-29b and Mm_let-7a in the renal cortex of diabetic mice

Mm_miR-29b and Mm_let-7a exhibit renal protective effects, acts as a negative regulator of the EndMT via inhibition of TGF-β signaling, while these expressions decrease in renal injury (89-91). No statistically significant differences in the expression of Mm_miR-29b in the renal cortex were observed between control mice and diabetic mice (Fig. 24a). The expression of Mm_let-7a in diabetic mice was significantly decreased compared to control mice (Fig. 24b). Next, the effect of the administration of EPA-E on Mm_miR-29b and Mm_let-7a expression was evaluated. However, EPA-E did not affect any of these expressions (Fig. 24a and 24b).

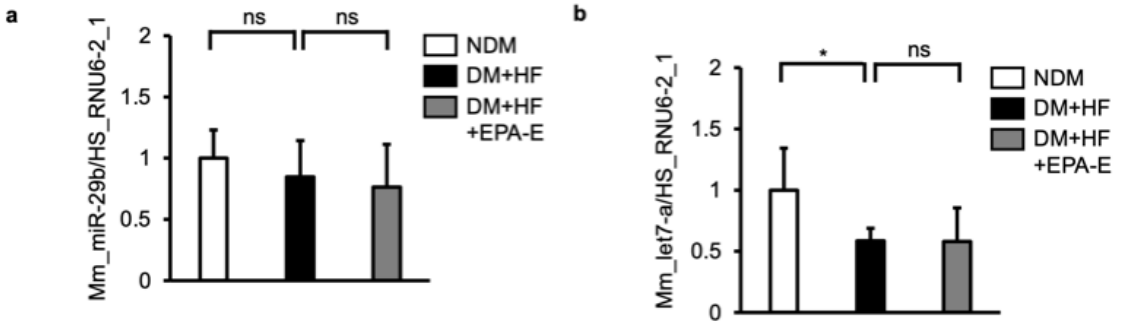

Fig. 24 Mm_miR-29b and Mm_let-7a reveal trends of suppression in the renal cortex. (a, b) MiRNAs alterations in the renal cortex of the non-diabetic mice, STZ-induced diabetic mice, and STZ-induced diabetic mice treated with EPA-E were evaluated. (a) Mm_miR-29b. (b) Mm_let-7a. *p< 0.05. ns; not significant. NDM, n = 8; DM+HF, n = 4; DM+HF+EPA-E, n = 6 were analyzed. Values are shown as mean ± SD. NDM, non-diabetic mice; DM+HF, mice with STZ-induced diabetes were fed a high-fat diet; DM+HF+EPA-E, STZ-induced diabetic mice were fed a high-fat diet treated with EPA-E. This figure is reproduced from a figure previously published in *J. Diabetes Res.* (66) with modifications.

4.4 DISCUSSION

This study demonstrated that progression of EndMT may be occurred in the glomeruli of diabetic mice, leading to DKD. Furthermore, EPA-E ameliorated the mesangial expansion and albuminuria through the inhibition of EndMT.

Extracellular matrix, such as type I and IV collagen, or αSMA, which is regulated by TGF-β and bone morphogenetic protein 4 (BMP4), is increased in the glomeruli of patients with type-2 diabetes and one of the important features of DKD (92). Notably, the expression of TGF-β-induced EndMT in the endothelial cells is recognized in diabetic conditions, which could be suppressed by the linagliptin-mediated microRNA 29 induction (16). However, bEnd.3 which is derived from the mouse microvascular endothelial cells was used. Thus, the results of this study may not reflect the effects on renal glomeruli.

In the Reduction of Cardiovascular Events with Icosapent Ethyl-Intervention (REDUCE-IT) and the Japan EPA Lipid Intervention Study (JELIS), noted a tendency toward the use of high-dose n-3 PUFA, EPA significantly reduced the risk of cardiovascular diseases (93, 94). Although not directly assessing patients with DKD, many patients in REDUCE-IT had diabetes and thus the effects of EPA treatment in diabetic models may be relevant to these other studies.

DHA-E reduces blood pressure (95, 96), heart rate (97, 98), and platelet aggregation (99, 100) more efficiently than EPA-E. DHA-E has a longer carbon chain and additional double bonds than EPA-E, it undergoes rapid isomerization, which increases membrane fluidity rather than stability, resulting in a rapid decrease in antioxidant capacity (101-103). Hence, the effects of EPA-E and DHA-E may be different. Further study will be needed to clarify.

It is reported that plasma level of EPA-E is 62 μg/mL when the rat was treated with EPA-E at 1000mg/kg/day for 4 weeks, which is less than in humans given a clinical dose of EPA-E (1800mg/day) for 3 months (143 μg/mL) (80, 81). Thus, 1000 mg/kg/day is considered to be an appropriate dose for *in vivo* experiments of the pharmacological effects of EPA-E in mice.

The activation of PKCβ has been identified to lead to the inhibition of glomeruli endothelial cell function (11, 82). The diminution of the endothelial nitric oxide synthase activation and endothelial dysfunction in the glomeruli could contribute to the loss of antioxidative and inflammatory effects of nitric oxide (11, 84). The phosphorylation of Erk and increase in PKCβ are recognized in diabetic mice which is consistent with the previous report (82, 104). The increase in phosphorylation of Erk in the diabetic condition is presumably because of the activation of PKCβ, which can increase MAPK (82).

Reflecting on the emergence of glomeruli endothelial dysfunction and EndMT, the number of CD31-positive cells were decreased, and αSMA expression were increased in the glomeruli of the diabetic mice. EndMT is characterized by the reduced expression of the endothelial markers, such as CD31 and VE-cadherin, and increases the expression of mesenchymal markers, such as SM22α and αSMA (105). Thus, cell adhesion molecules are decreased, while cell migration ability is increased in EndMT. It has been reported that EndMT is controlled by a variety of stimuli, including TGF-β, high glucose, oxidative stress, TNF-α, and IL-1β (106). However, the relationship between adipocyte differentiation and EndMT has not been clear. These results indicate that there was a decrease in CD31 expression and an increase in SM22α expression in the cultured endothelial cells during adipocyte hypertrophic differentiation. Further, cell migration assay in this study revealed that both adipocytes conditioned medium and high glucose

could induce endothelial cell migration, leading to EndMT. However, there are few reports regarding cell migration assay in diabetic condition (107). Although convincing, there is a limitation in this point.

TGF-β induces EndMT through the Smad, MEK/ERK, PI3K, and p38MAPK signaling pathways and increases the expression of Snail, which is the cell adhesion suppressing transcription factor. Mima et al. have previously reported that TGF-β/BMP4-Smad1 pathway upregulates the expression of Col4 and αSMA (74, 76, 91). Further, the inhibition of phosphorylation of Erk1/2 prevents the TGF-β-induced EndMT via the suppression of Snail expression (108). TGF-β regulated-Snail decreases the endothelial cell characteristics and, counterintuitively increases the expression of mesenchymal markers such as αSMA and SM22α (109, 110). However, these data may not be enough to affirm that EPA-E acts through EndMT and TGF-β-mediated renal fibrosis because no statistically significant difference was found. This problem may have occurred owing to the small samples. Therefore, further study will be needed to clarify this.

This study indicated that suppression of TGF-β alone is not sufficient to suppress EndMT. As shown in this results, TGF-β suppression by EPA-E was partial, while EPA-E completely reduced snail expression, which is more involved in EndMT. Not only TGF-β signaling but other signals such as notch signaling are involved in the increase of snail (111, 112). Thus, EPA-E-induced reduction of snail expression may be the result of strong suppression of signals other than TGF-β signaling. Previous reports indicated that 3T3-L1 adipocyte secretes a variety of adipokines and lipids, resulting in increases in TGF-β (113, 114). Therefore, the secretion of adipokines and other factors induced by the differentiation process of 3T3-L1cells into adipocytes could give rise to EndMT.

The vascular endothelial (VE)-cadherin is an accurately endothelial-specific adhesion molecule located at the junctions between the endothelial cells (82, 115, 116). The cancer cell-conditioned medium decreased the expression of VE-cadherin in the endothelial cells by the binding of Snail to the VE-cadherin promoter (117). This study showed that EPA-E suppressed the expression of Snail and the phosphorylation of Erk1/2 by the adipocyte conditioned medium. Thus, EPA-E regulated the expression of CD31 and SM22α by suppressing the phosphorylation of Erk1/2 and TGF-β-Snail signaling.

There is substantial evidence indicating that the reactive oxygen species (ROS) is increased in the retina, kidney, and endothelial cells either when exposed to diabetic conditions or in the diabetic rodent model (50). Further, ROS regulates the TGF-β-induced expression of αSMA and Nox4 in human cardiac fibroblasts. In contrast, the knockdown of Nox4 with siRNA reduced the oxidative stress and expression of αSMA by TGF-β (118). This study showed an increase in the MDA levels, expression of p47phox, Nox2, and Nox4 mRNAs in the diabetic kidney, although the increase was modest in the EPA-E-treated mice compared to the control mice. The administration of EPA-E has been found to decrease albuminuria without affecting glycemic control, serum lipid level, and blood pressure in patients with type-2 diabetes (119). Previous reports indicate that the intraperitoneal injection of EPA-E ameliorated the mesangial matrix expansion and decreased the phosphorylation of Erk1/2 in KKAy/Ta mice (120). EPA-E also suppressed the diabetes-induced upregulation of MCP-1 and TGF-β expression, along with the reduction of MDA (121).

The results obtained from the conditioned medium from the cultured adipocyte demonstrated that the PKC activation increased the phosphorylation of Erk1/2, which leads to the activation of PAI-1. In contrast, EPA-E inhibited the increase in the

phosphorylation of Erk1/2, PAI-1 expression in the endothelial cells, and the ability of the endothelial cell to migrate. PAI-1 increased the ECM accumulation through inhibition of proteolysis and promotion of ECM synthesis by TGF-β in the diabetic kidney, while inhibition of PAI-1 decreased ECM accumulation with the suppression of Col4 expression (122, 123). PAI-1 also promoted endothelial cell migration through inhibition of integrin-mediated cell adhesion (124). These results indicate that EPA-E not only suppresses EndMT but may also directly the signal to increase extracellular matrix.

MicroRNAs (miRNAs) are well known for their regulatory effects on several diseases such as diabetes, cancer cells, and renal fibrosis (16, 125, 126). The differential miRNA expression indicated a role of altered miRNA in the pathogenesis of the renal disease (127, 128). Mm_miR-29b is downstream of Smad3 and can inhibit the upstream TGF-β-Smad3 signaling by the Mm_miR-29b-regulated negative feedback, decreasing the type I and III collagen (89). Similarly, the Mm_let-7 family including Mm_let-7a inhibits the TGF-β signaling in renal fibrosis (90, 129, 130). In this study, both Mm_miR-29b and Mm_ let-7a were reduced in diabetic mice, but the differences were not statistically significant; Mm_ let-7a was in fact significantly reduced in diabetic mice, but Mm_miR-29b was not significantly reduced as indicated in fig. 24. Furthermore, the increase in these miRNAs upon EPA-E treatment was not evident. Thus, EndMT inhibition by EPA-E treatment may result from the direct inhibition of the PKCβ/TGF-β/PAI-1 signaling, but not via miRNAs.

5. The effects of linagliptin on high glucose-induced podocyte apoptosis and glomerular insulin signaling in diabetic mouse.

This chapter is based on the paper previously published in *Sci. Rep.* (131).

5.1 INTRODUCTION

DKD is the most common cause of CKD and ESRD (132). Glomerular endothelial dysfunction and podocyte apoptosis are involved in the progression of DKD, including increased albuminuria (11). Insulin/(IRS1) signaling can increase nitric oxide (NO) production, which is mediated by the PI3K/Akt pathway, thereby increasing anti-inflammatory effects (11). NO induces vasodilatation and inhibits podocyte apoptosis (133). Diabetes can inhibit insulin/IRS1 signaling in mesangial and glomerular endothelial cells, probably through the PKC β2 pathway (11). Furthermore, diabetes could increase podocyte apoptosis in DKD via activation of PKCδ/p38 mitogen-activated protein (MAPK) to enhance SHP-1 expression, which in turn resulted in VEGF resistance (65). Thus, it is likely that the loss of effect of insulin on glomeruli may contribute to the development of DKD.

Incretins are the family of gut hormones including glucagon like peptide-1 (GLP-1) and glucose-dependent insulinotropic polypeptide. Recent study indicated that a GLP-1 analogue improved diabetes-induced inflammation, preventing mesangial expansion and glomerulosclerosis beyond glycemic control (82). As GLP-1 is rapidly degraded by dipeptidyl peptidase-4 (DPP-4), DPP-4 inhibitors that are widely used to treat type 2 diabetes could be a potential treatment for DKD in part because of their pleiotropic actions. A recently published large clinical trial, CArdiovascular safety and Renal Microvascular outcomE study with LINAgliptin in patients with type 2 diabetes at high vascular risk (CARMELINA®), established hard renal endpoints using DPP-4

inhibitors for the first time and clearly showed that linagliptin administration prevented the progression of microalbuminuria to overt proteinuria in patients with type 2 diabetes (134).

Based on the above findings indicating the effect of incretins on insulin signaling, the hypothesis that linagliptin may decrease high glucose-induced podocyte apoptosis through enhancement of insulin/IRS1 signaling in podocytes was investigated. Furthermore, it has been reported that interaction between Kelch-like ECH-associated protein 1 (Keap1) and nuclear factor erythroid 2-related factor 2 (Nrf2) can increase anti-inflammatory effects (135). Previous reports have also reported that diabetes-induced inflammation and oxidative stress could induce intrinsic antioxidant response through the Keap1/Nrf2 pathway (136, 137). Incretin-related drugs decreased inflammatory status and enhanced Nrf2 system in DKD (138). Therefore, the effects of linagliptin on high glucose-induced podocyte apoptosis and insulin/IRS1 signaling in diabetic mice and cultured podocyte were investigated.

5.2 METHODS

5.2.1 Animal experiments

All animal protocols were approved by the Kindai University in accordance with the National Institutes of Health guidelines (approval number: KAAG-26-010). Age-matched male Sprague-Dawley (SD) rats (Shimizu, Kyoto, Japan) were used. Diabetes was induced in 7-week-old SD rats by a single intravenous injection of STZ (50mg/kg body weight; Sigma, St Louis, MO) in 0.05mol/l citrate buffer (pH 4.5) or citrate buffer for controls. Blood glucose levels, determined 1 week after the injections by glucose analyser (Sanwa Kagaku, Aichi, Japan) and levels >16.7mmmol/l, were defined as having

diabetes. One week after diabetes, linagliptin (3mg/kg body weight; Boehringer Ingelheim, Ingelheim, Germany) or vehicle were administered for 4 weeks. Doses of linagliptin was decided based on the previous reports (16, 139). Regular human insulin (10mU/g; Lilly, Indianapolis, IN) or diluents were injected into the inferior vena cava for 10 min to study insulin signaling.

5.2.2 Cell culture and reagents

Podocytes from a conditionally immortalised cell line were provided by P. Mundel and cultured as described previously (65). Briefly, podocytes were cultured in RPMI-1640 (Sigma, St. Lois, MO, USA) medium containing 10% foetal calf serum (FCS), 100 U/mL penicillin, 0.1 mg/mL streptomycin, and 2 mM L-glutamine. For propagation, podocytes were cultivated with a culture medium supplemented with 50 U/mL recombinant mouseγ-interferon (PeproTech, London, UK) at 33°C with 5% CO2. To induce differentiation, the cells were cultured on 10-cm culture dishes coated with type I collagen at 37°C without γ-interferon. Podocytes were cultured in RPMI-1640 containing 10% FCS. After reaching subconfluence, the cells were exposed to low glucose (5.5 mM + 19.5 mM mannitol) or high glucose (25 mM) with linagliptin (50 nM) in RPMI containing 0.1% FCS for 96h. Stimulation with insulin (10 nM) was carried out in RPMI containing 0.1% FCS for 5 min. Endothelial cell lines TKD2 were purchased from National Institutes of Biomedical Innovation, Health and Nutrition (Osaka, Japan). Endothelial cells were cultured in RITC80-7 containing 2% FCS. D-(+)-glucose was purchased from Sigma. Linagliptin was provided by Boehringer Ingelheim (Ingelheim, Germany) and doses of linagliptin for *in vitro* study was decided based on the previous reports (16).

5.2.3 Isolation of Glomeruli

Rat glomeruli were isolated from the renal cortex by the sieving method as described elsewhere (11).

5.2.4 Adenoviral vector infection

Adenoviral vectors containing green fluorescent protein (GFP, Ad-IRS1) were constructed. These adenoviral vectors were used to infect podocytes as reported elsewhere (11).

5.2.5 Small interfering RNA studies

Small interfering RNA (siRNA) against IRS1 (siIRS1) and scrambled control siRNA (siControl) were purchased from Santa Cruz. Differentiated podocytes were seeded in to 6-cm culture dishes and were grown until they were 60% to 80% confluent. The cells were transfected with siRNA using siRNA transfection system (Santa Cruz) according to the recommended protocol. After 48h of transfection, cells were exposed to low glucose (5.5 mM) or high glucose (25 mM).

5.2.6 Immunoblot analysis

Samples were dissolved in 0.5% NP-40, which was used after optimisation studies. Proteins were separated by sodium dodecyl sulphate-polyacrylamide gel electrophoresis (SDS-PAGE). Blots were subsequently incubated with anti-IRS1 (Cell Signaling, Danvers, MA, USA), anti-phospho-IRS (Merck Millipore, MA, USA), anti-Akt (Cell Signaling), anti-phospho-Akt (Cell Signaling), anti-DPP-4 (Abcam, Cambridge,

UK), anti-Keap1 (Cell Signaling), anti-Nrf2 (Cell Signaling), and anti-β-actin (Cell Signaling).

5.2.7 Real-time PCR analysis

IRS1 mRNA was assayed by Real-time PCR and normalized to GAPDH. PCR primers were shown in table 10.

Table 10. PCR primers

	Forward Primer	Reverse Primer
IRS1	CACACGGATGATGGCTACATG	GTTTGTCCACAGCTT TCCATAG
GAPDH	ATGTTCCAGTATGACTCCACTCACG	GAAGACACCAGTAGACTCCACGACA

5.2.8 DNA fragmentation analysis

DNA fragmentation was measured by quantitation of cytosolic oligonucleosome-bound DNA using ELISA kit, according to the manufacturer's instructions (Roche Diagnostics, Indianapolis, IN, USA).

5.2.9 Immunocytochemistry

For immunocytochemical analysis, the cells were fixed with 2% paraformaldehyde and permeabilised with 0.1% Triton X. Apoptotic cells were detected using TdT-mediated dUTP nick end (TUNEL) labelling kit, according to the manufacturer's instructions (Merck Millipore). 4',6-Diamino-2-phenylindole (DAPI) staining was performed as described previously (11).

5.2.10 Histological studies

Kidney sections for light microscopy analysis were fixed in 4% paraformaldehyde phosphate buffer. Sections were stained with periodic acid-Schiff. Glomeruli were digitally photographed, and the images were imported to ImageJ software (National Institutes of Health, Bethesda, MD, USA; https://imagej.nih.gov/ij/) and analysed morphometrically.

5.2.11 Statistics

Data are expressed as mean ± standard deviation (SD). Comparisons among more than two groups were performed by one-way ANOVA, followed by post hoc analysis with paired or unpaired t test to evaluate statistical significance. All analyses were performed using StatView (SAS Institute, Cary, CA, USA). Values of $P < 0.05$ were considered statistically significant.

5.3 RESULTS

5.3.1 Linagliptin inhibited podocyte apoptosis induced by high glucose.

Expression of nephrin protein was confirmed in the cultured podocytes by immunoblotting. On the other hand, its expression was not confirmed in the cultured endothelial cells (Fig.25). DNA fragmentation in podocytes exposed to high glucose (25 mM) levels increased when compared to DNA fragmentation in podocytes exposed to low glucose (5.5 mM) conditions. Linagliptin (50 nM) reduced high glucose-induced podocyte apoptosis (Fig. 26a). However, D-mannitol-induced hyperosmolality did not affect DNA fragmentation (Fig. 26b). Immunocytochemical staining of podocytes showed that the number of TUNEL/DAPI double-positive cells increased in high-glucose

conditions compared to that in low-glucose conditions. However, the addition of linagliptin reduced this increase (Fig. 26c).

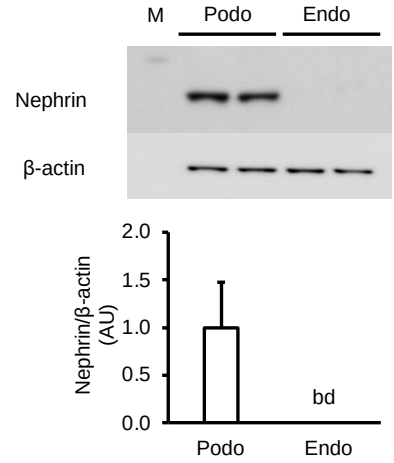

Fig. 25 The expression of nephrin in cultured podocytes. Immunoblot analyses of nephrin in cultured podocytes and endothelial cells. Podo; podocytes. Endo; endothelial cells. bd; below detection limit. n = 3 were analyzed. Values are shown as mean ± SD. Results are representative of one of three independent experiments. This figure is reproduced from a figure previously published in *Sci. Rep.* (131) with modifications.

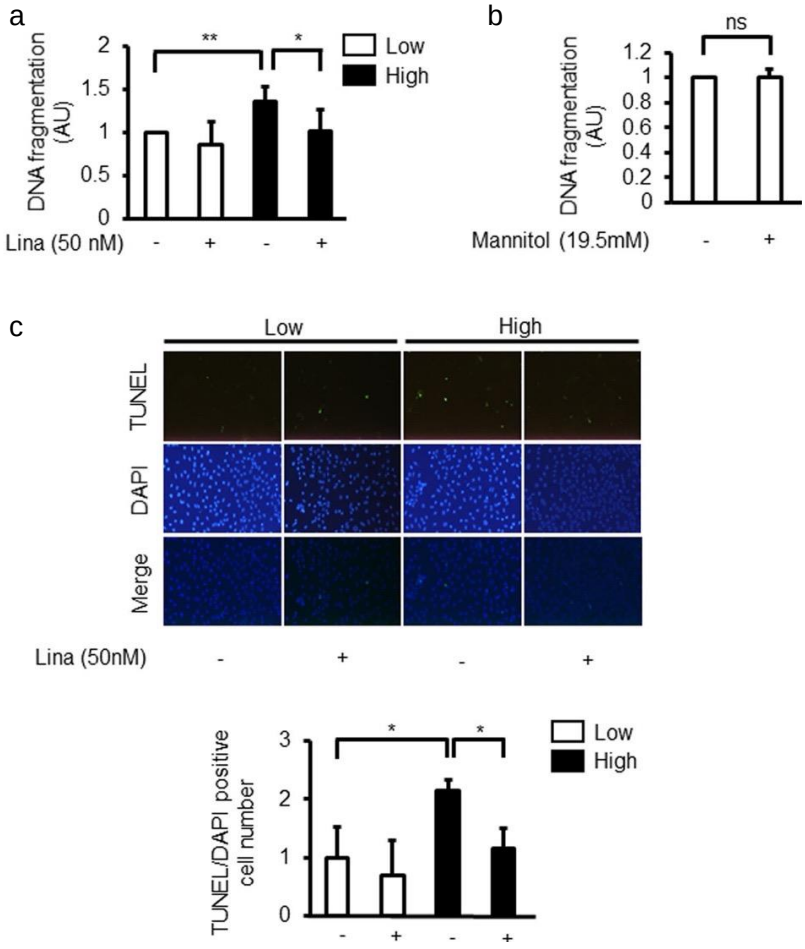

Fig. 26 Effect of high glucose and linagliptin on apoptosis in cultured podocytes. (a) DNA fragmentation in podocytes incubated with low glucose (5.5 mM) or high glucose (25 mM) for 96 h in the absence or presence of linagliptin (50 nM). Lina; linagliptin. (b) Effect of D-mannitol-induced hyperosmolality on DNA fragmentation. Low; low glucose. High; high glucose. Lina; linagliptin. ns; not significant. (c) Immunocytochemical staining with TdT-mediated dUTP nick end (TUNEL) and 4′,6-diamino-2-phenylindole (DAPI) (merged image). Magnification: X40. Data from upper panel were revealed as lower panel. Low; low glucose. High; high glucose. Lina; linagliptin. *$p < 0.05$. **$p < 0.01$. $n = 3$ were analyzed. Values are shown as mean ± SD. Results are representative of one of three independent experiments. This figure is reproduced from a figure previously published in *Sci. Rep.* (131) with modifications.

5.3.2 Effect of high glucose on DPP-4 expression and insulin signaling in podocyte.

First, the effect of high glucose on DPP-4 expression in cultured podocytes was evaluated. The expression of DPP-4 protein was significantly increased by high glucose in podocytes (Fig. 27). As Akt activation is known to exert anti-apoptotic effects and it is inhibited in glomerular endothelial cells by diabetes, the effects of high glucose on IRS1 activation and Akt activation were evaluated in podocytes. The phosphorylation of Akt (pAkt) was significantly increased by insulin. However, the increase of pAkt was inhibited by high glucose. Linagliptin partially normalized insulin-induced pAkt compared with that in high-glucose conditions without linagliptin (Fig. 28). The expression of tyrosine phosphorylation of IRS1 (pIRS1) was significantly increased by insulin. In contrast, high glucose condition significantly reduced IRS1 activation in podocytes when compared with low glucose condition. The addition of linagliptin significantly reversed the inhibitory effect of high glucose on IRS1 activation (Fig. 29).

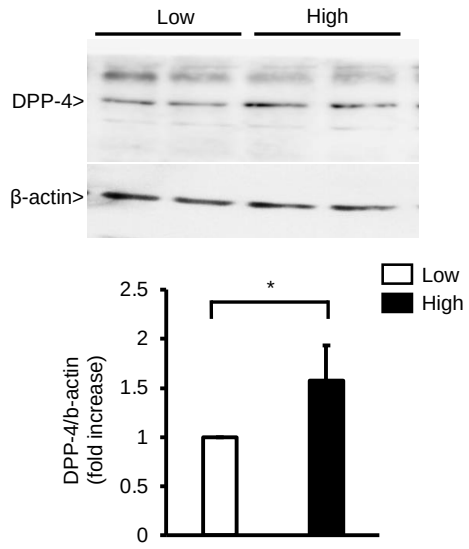

Fig. 27. Effect of high glucose on DPP-4 in cultured podocytes. Immunoblot analysis of DPP-4. Podocytes were incubated with low glucose (5.5 mM) or high glucose (25 mM). Low; low glucose. High; high glucose. *$p < 0.05$. $n = 3$ were analyzed. Values are shown as mean ± SD. Results are representative of one of three independent experiments. This figure is reproduced from a figure previously published in *Sci. Rep.* (131) with modifications.

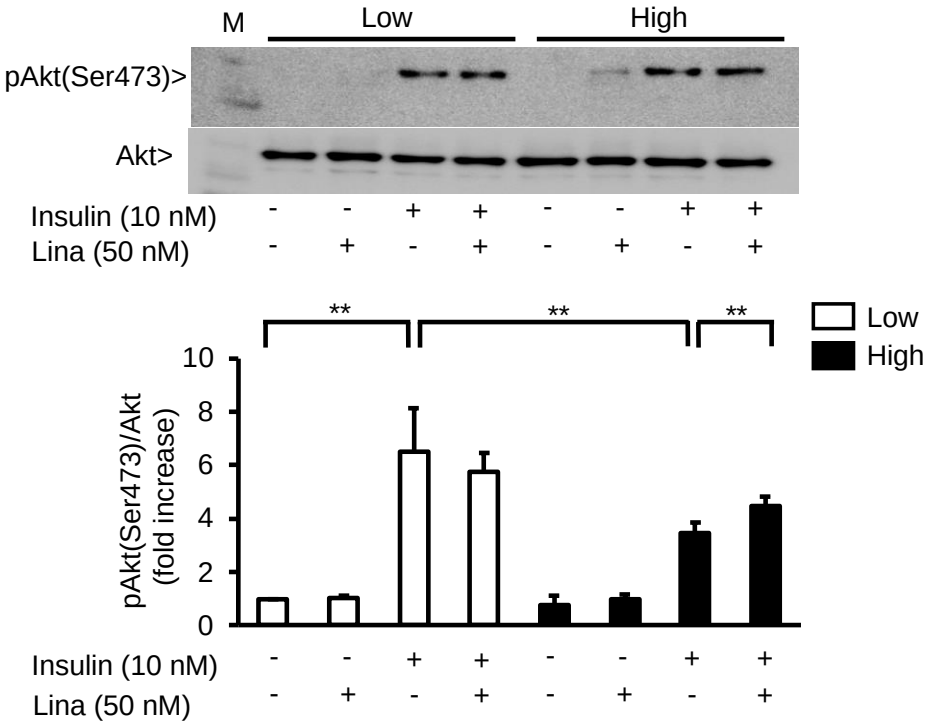

Fig. 28 Effect of linagliptin on phosphorylation of Akt in cultured podocytes. Podocytes were incubated with low glucose (5.5 mM) or high glucose (25 mM). Immunoblot analysis of Akt phosphorylation. After 96 h of exposure to low glucose (5.5 mM) or high glucose (25 mM), podocytes were incubated with insulin (10 nM, 5 min) in the absence or presence of linagliptin (50 nM). Low; low glucose. High; high glucose. Lina; linagliptin. **p< 0.01. n = 3 were analyzed. Values are shown as mean ± SD. Results are representative of one of three independent experiments. This figure is reproduced from a figure previously published in *Sci. Rep.* (131) with modifications.

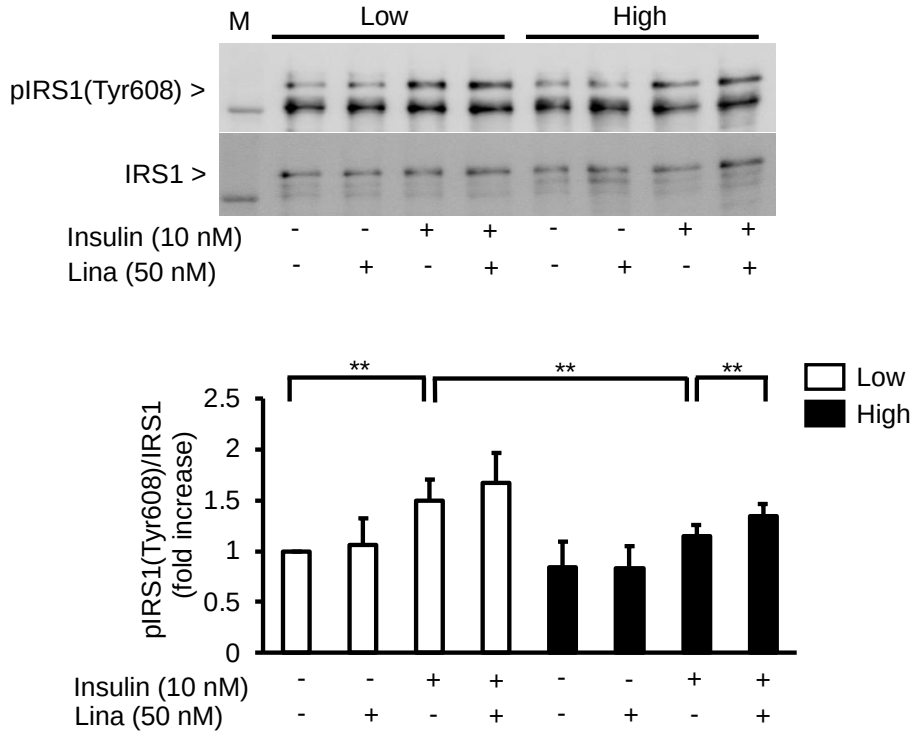

Fig. 29 Effect of linagliptin on phosphorylation of IRS1 in cultured podocytes. Podocytes were incubated with low glucose (5.5 mM) or high glucose (25 mM). Immunoblot analysis of IRS1 phosphorylation. After 96 h of exposure to low glucose (5.5 mM) or high glucose (25 mM), podocytes were incubated with insulin (10 nM, 5 min) in the absence or presence of linagliptin (50 nM). Low; low glucose. High; high glucose. Lina; linagliptin. **p< 0.01. n = 3 were analyzed. Values are shown as mean ± SD. Results are representative of one of three independent experiments. This figure is reproduced from a figure previously published in *Sci. Rep.* (131) with modifications.

5.3.3 Effect of linagliptin on insulin signaling in the glomeruli of diabetic rat.

After 5 weeks of injection of STZ, blood glucose levels were significantly increased and kidney weight per body weight was significantly increased in diabetic rats compared to control rats (Table 11). Histological analysis of the glomeruli (PAS staining) revealed that glomerular areas were significantly increased in diabetic rats than those in control rats (Fig. 30). Linagliptin treatment significantly reduced glomerular area compared to untreated diabetic rats (Fig. 30). In diabetic rats, Akt activation induced by insulin was significantly reduced compared to control rats (Fig. 31a). Moreover, insulin stimulated pIRS1 expression was significantly increased in control rats. Like pAkt, insulin stimulated pIRS1 levels were reduced in diabetic rats compared to control rats. However, no statistically significant differences were found between control rats and diabetic rats (Fig. 31b). Linagliptin treatment significantly increased pAkt in the glomeruli of diabetic rats when compared to untreated diabetic rat (Fig. 31a). The phosphorylation of IRS1 was increased by linagliptin treatment. However, no statistically significant differences were found between diabetic rats and linagliptin treated diabetic rats (Fig. 31b).

Table 11. General characteristics of the experimental groups

	NDM	DM	DM + Lina
Number	5	3	4
Bodyweight (g)	418.5 ± 31.4	333.3 ± 31.8**	289.6 ± 22.6**
Blood glucose (mg/dL)	102.2 ± 6.9	398.0 ± 95.3**	433.0 ± 82.1**
rKW/BW (g/100 g BW)	0.80 ± 0.10	1.20 ± 0.27*	1.26 ± 0.20*
Serum insulin (ng/mL)	3.32 ± 0.62	0.90 ± 0.16**	0.75 ± 0.13**

NDM, nondiabetic rats; DM, STZ-induced diabetic rats; Lina, linagliptin; rKW/BW, right kidney weight/body weight. Values are shown as mean ± SD. *p < 0.05. **p< 0.01. vs. NDM SD. This table is reproduced from a table previously published in *Sci. Rep.* (131) with modifications.

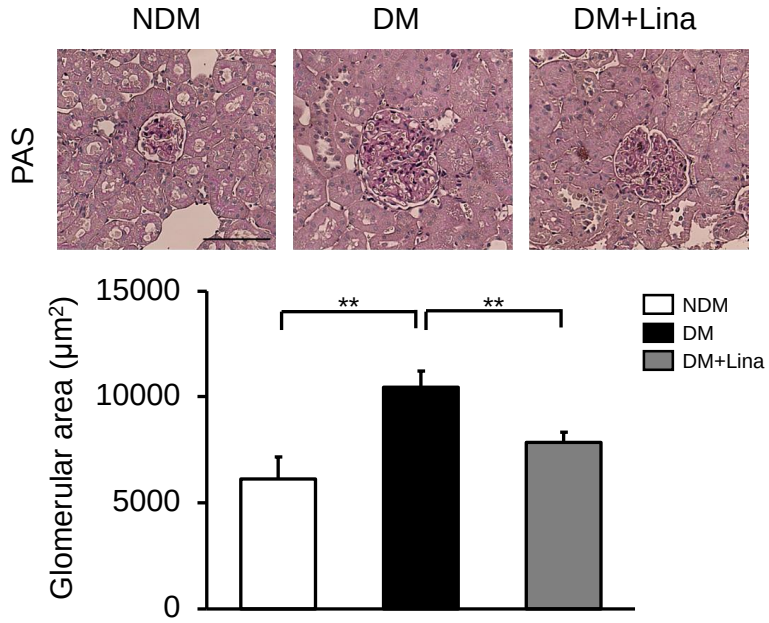

Fig. 30 Effect of linagliptin on the glomeruli of diabetic rats. Representative light microscopic appearance of glomeruli (PAS staining) and morphometric analysis of glomerular area. NDM; nondiabetic rats, DM; STZ-induced diabetic rats; Lina, linagliptin. Bar=100 μm. **p< 0.01. NDM, n = 5; DM, n = 3; DM+Lina, n = 4 were analyzed. Values are shown as mean ± SD. This figure is reproduced from a figure previously published in *Sci. Rep.* (131) with modifications.

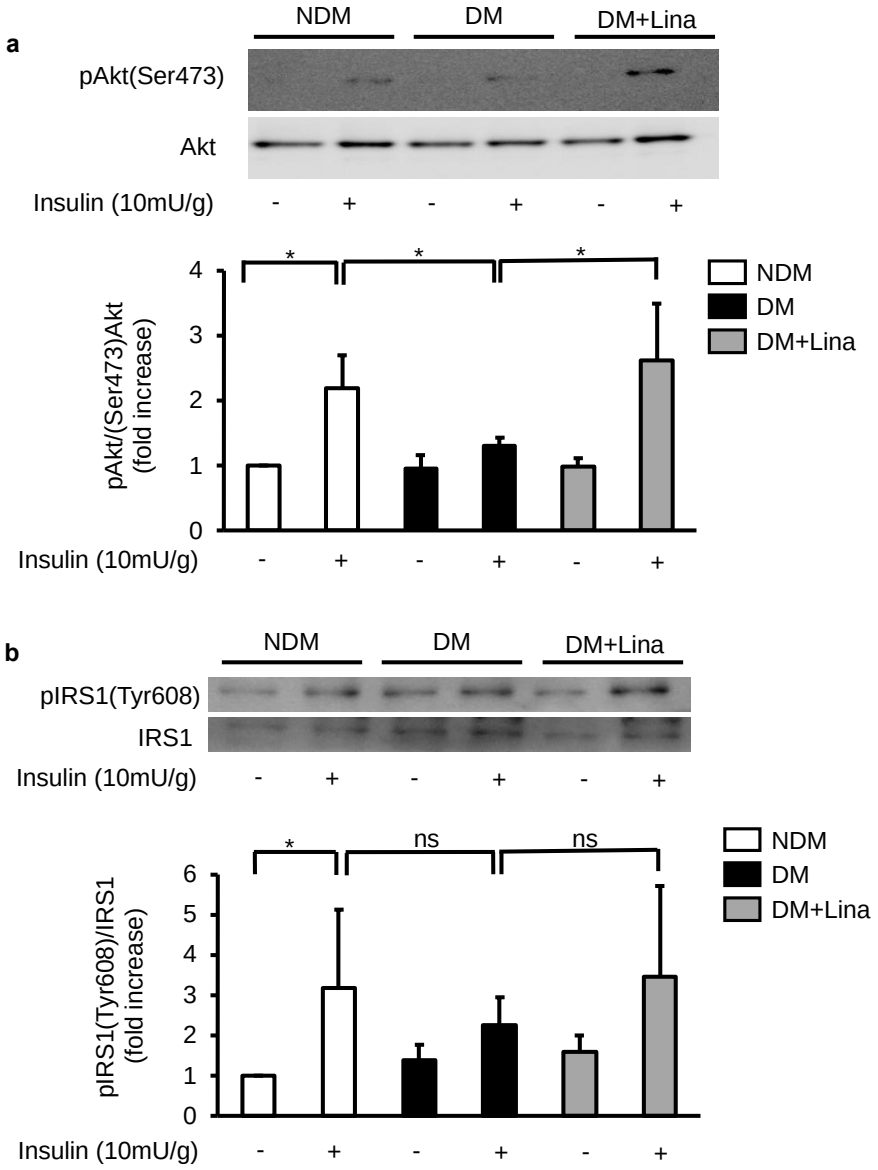

Fig. 31 Effect of linagliptin on Akt and IRS1 in the glomeruli of diabetic rats. (a) Representative immunoblots of tyrosine phosphorylation of Akt and (b) IRS1 from glomeruli. Solubilized glomeruli were subjected to immunoprecipitation followed by immunoblotting. NDM; nondiabetic rats, DM; STZ-induced diabetic rats; Lina, linagliptin. *$p < 0.05$. ns; not significant. NDM, n = 5; DM, n = 3; DM+Lina, n = 4 were analyzed. Values are shown as mean ± SD. This figure is reproduced from a figure previously published in *Sci. Rep.* (131) with modifications.

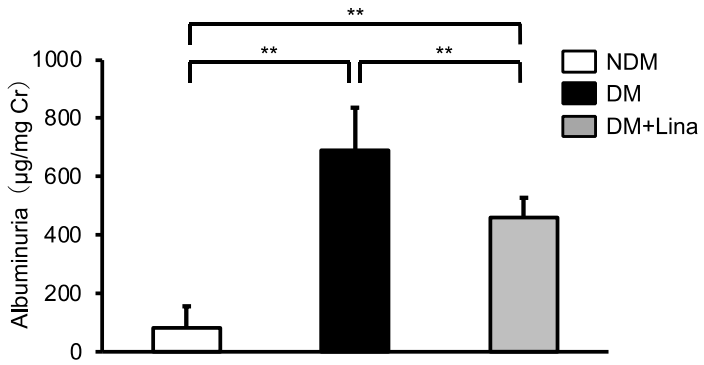

Fig. 32 Effect of linagliptin on albuminuria in diabetic rats. Albuminuria was measured by Nephrat. NDM; nondiabetic rats, DM; STZ-induced diabetic rats; Lina, linagliptin. **p< 0.01. NDM, n = 5; DM, n = 3; DM+Lina, n = 4 were analyzed. Values are shown as mean ± SD. This figure is reproduced from a figure previously published in *Sci. Rep.* (131) with modifications.

5.3.4 IRS1 overexpression reduced DPP-4 expression and apoptosis in podocyte.

To evaluate the effect of IRS1 on podocyte apoptosis, IRS1 was overexpressed by Ad-IRS1. IRS1 expression in podocyte was significantly increased by infection with Ad-IRS1 (Fig. 33a). When IRS1 overexpressed in podocyte, DPP-4 expression was significantly decreased (Fig. 33b). Infection with Ad-IRS1 significantly decreased DNA fragmentation induced by high glucose (Fig. 33c). The mRNA expression and protein expression of IRS1 was downregulated by siIRS1 in podocyte (Fig. 33d and 33e). The downregulation of IRS1 by siIRS1 increased podocyte apoptosis even in low glucose conditions (Fig. 33f).

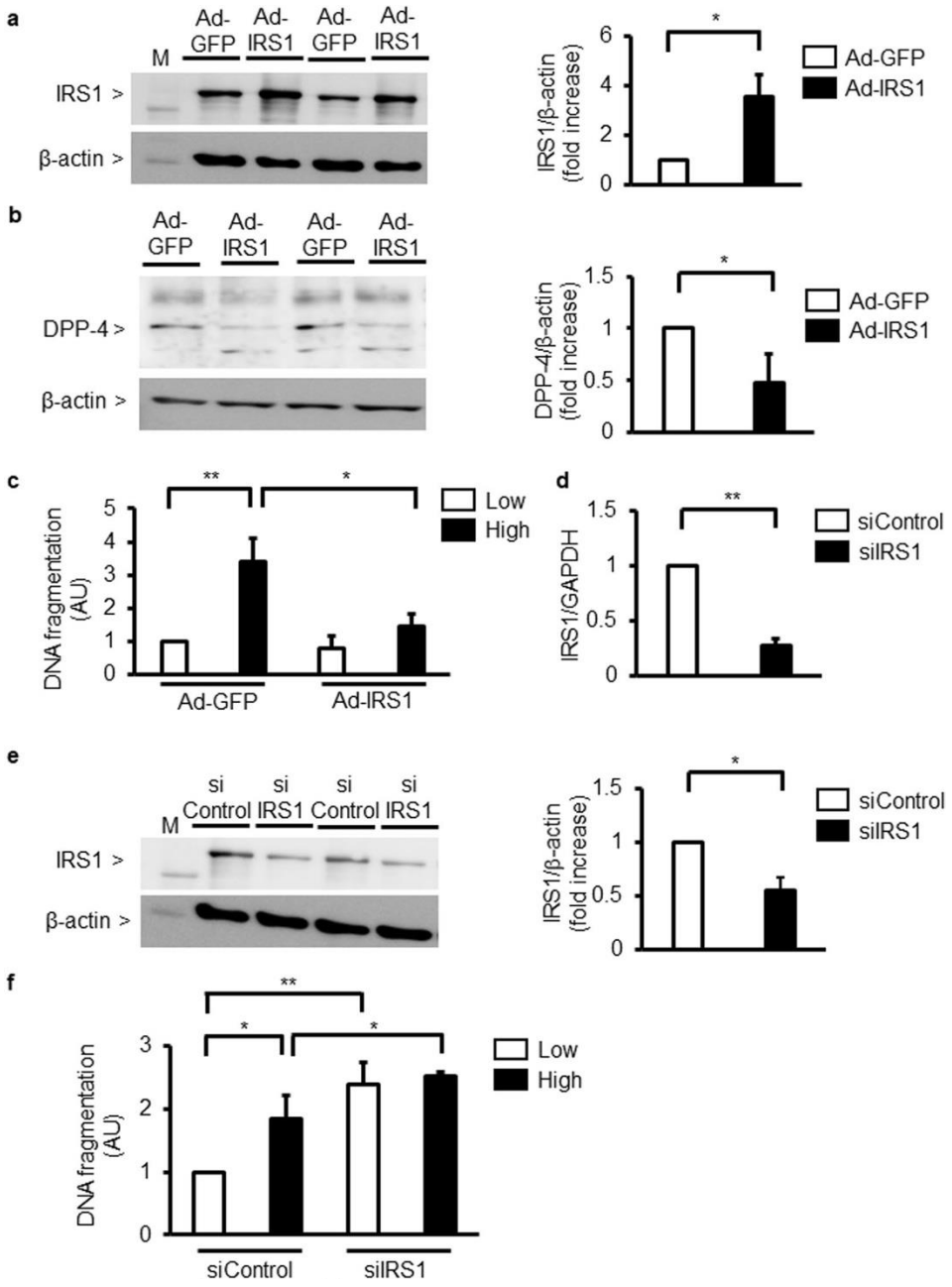

Fig. 33 Effect of IRS1 on glucose-induced podocyte apoptosis. (a) Immunoblot analysis of IRS1. Podocytes were transfected with adenoviral vectors containing green fluorescent (Ad-GFP or Ad-IRS1) protein. (b) Immunoblot analysis of DPP-4. Podocytes were transfected with Ad-GFP or Ad-IRS1. (c) Podocytes were transfected with Ad-GFP or Ad-IRS1 and then incubated with low glucose (5.5 mM) or high glucose (25 mM). Podocyte apoptosis was measured by DNA fragmentation. (d) IRS1 mRNA expression in podocytes. Podocytes were transfected scrambled control siRNA (siControl) or small interfering RNA (siRNA)

against IRS1 (siIRS1). (e) Immunoblot analysis of IRS1. Podocytes were transfected with siControl or siIRS1. (f) Podocytes were transfected with siControl or siRNA and then incubated with low glucose (5.5 mM) or high glucose (25 mM). Podocyte apoptosis was measured by DNA fragmentation. Low; low glucose. High; high glucose. *$p < 0.05$. **$p< 0.01$. NDM, n = 5; DM, n = 3; DM+Lina, n = 4 were analyzed. Values are shown as mean ± SD. Results are representative of one of three independent experiments. This figure is reproduced from a figure previously published in *Sci. Rep.* (131) with modifications.

5.3.5 Effect of linagliptin on Keap1/Nrf2 pathway

The addition of linagliptin (50 nM) did not change DNA fragmentation in IRS1 silencing podocytes (Fig. 34a). The expression of Nrf2 in podocyte was increased in high glucose conditions compared with low glucose conditions. Furthermore, the addition of linagliptin significantly increased the expression of Nrf2 in low glucose conditions (Fig. 34b). However, linagliptin or overexpression of IRS1 did not affect the protein expression of Keap1 (Fig. 34b, 34c and 34d). Knockdown of IRS1 in podocyte with siRNA did not affect the protein expression of Keap1 and Nrf2. (Fig. 34e).

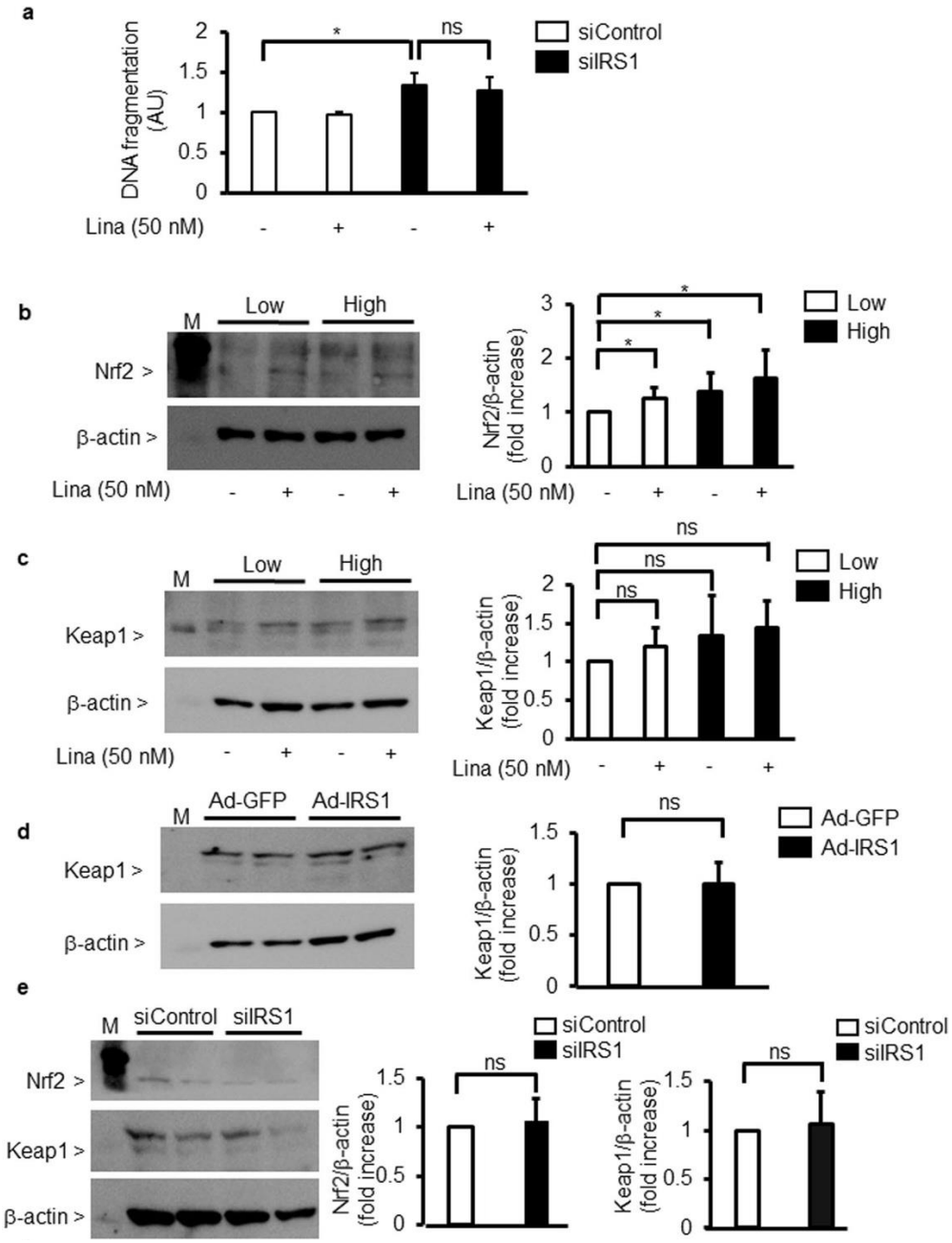

Fig. 34 Effect of linagliptin on Nrf2/Keap1. (a) Podocytes were transfected with siControl or siIRS1 in the absence or presence of linagliptin (50 nM). Podocyte apoptosis was measured by DNA fragmentation. Lina, linagliptin. (b, c) Immunoblot analysis of Nrf2 andKeap1. After 96 h of exposure to low glucose (5.5 mM) or high glucose (25 mM), podocytes were incubated with or without linagliptin (50 nM). (b) Nrf2. (c) Keap1. (d) Immunoblot analysis of Keap1. Podocytes were transfected with Ad-GFP or Ad-IRS1. (e) Immunoblot analysis of Nrf2 and Keap1. Podocytes were transfected with siControl or siRNA. ns; not significant. *p < 0.05. NDM, n = 5;

DM, n = 3; DM+Lina, n = 4 were analyzed. Values are shown as mean ± SD. Results are representative of one of three independent experiments. This figure is reproduced from a figure previously published in *Sci. Rep.* (131) with modifications.

5.4 DISCUSSION

In this study, the effects of linagliptin on high glucose-induced podocyte apoptosis and IRS1/insulin signaling in DKD were evaluated. The possible explanation for linagliptin-induced renal protective effects is that (i) high glucose-induced podocyte apoptosis was recovered by overexpression of IRS1 and (ii) addition of linagliptin reversed high glucose-induced inhibition of insulin-induced tyrosine phosphorylation of IRS1. This is the first study to report the biochemical pathway by which insulin/IRS1 exerts protective action in podocytes. Podocyte loss is one of the important features of DKD. Podocyte apoptosis is an early stage of DKD progression and therefore, evaluation of podocyte apoptosis could be the best early prognostic marker of DKD (140, 141). Although the mechanism of diabetes-induced podocyte apoptosis is still unclear, previous reports clearly showed that inhibition of insulin and VEGF actions by SHP-1 plays a key role in development of podocyte apoptosis (65, 142, 143). In addition, VEGF-induced tyrosine phosphorylation of nephrin was inhibited in the podocytes of diabetic rats (65).

Similar to glomerular endothelial cells, resistance to insulin signaling and actions for podocytes is also selective for the activation of insulin/IRS1/Akt cascade, which is clearly supported by overexpression of IRS1 using adenoviral vector or knocking down IRS1 using siRNA in the present study. In addition, this study demonstrated that linagliptin reversed high glucose-induced podocyte apoptosis through enhancing insulin/IRS1/Akt signaling.

Previous reports indicated that linagliptin ameliorated renal pathological changes and albuminuria in CKD mouse models without affecting blood glucose levels (144). Extracellular matrix, such as type I and IV collagen, or α-smooth muscle actin, which is regulated by transforming growth factor-β (TGF-β) and bone morphogenetic protein 4, is increased in the glomeruli of DKD (92). Linagliptin suppressed TGF-β-induced EndMT in endothelial cells in diabetic conditions (16). It has been reported that both soluble and membrane-anchored forms of DPP-4 are increased in the rodent models of diabetic nephropathy (16, 145). In contrast, another study suggested that the great majority of soluble DPP-4 is the bone marrow rather than kidney (146). Soluble DPP-4 can activate mannose-6-phosphate/insulin-like growth factor II receptor (M6P/IGF-IIR), increasing the interaction of advanced glycation end product (AGE) with its receptor, RAGE (147). Membrane-anchored DPP-4 can affect cation-independent mannose 6-phosphate receptor (CIM6PR), activating the TGF-β/Smad signaling pathway (148). Thus, both DPP-4 pathway could develop diabetic nephropathy. Linagliptin may reduce both signaling pathway, decreasing albuminuria and renal fibrosis.

Previous reports indicated that linagliptin could attenuate glomerular area expansion in diabetic rodents without changes in blood glucose, insulin level and body weight (149). These findings may explain increases in DPP-4 enzyme is recognized in the kidney of diabetes. Further, it is possible that monocyte chemoattractant protein (MCP)-1/CCR2 pathway and invasion of inflammatory cells in kidney can be a pivotal role in developing diabetic nephropathy (62). Linagliptin could decrease AGE/RAGE, reducing inflammation and reactive oxygen species (150). Considering these results, linagliptin may have pleiotropic effects beyond glycemic control. This study showed that mannitol-induced osmotic stress did not increase podocyte apoptosis. These results mean

diabetic conditions, not high osmolarity could increase podocyte apoptosis. Further, our laboratory and others have published data previously regarding the increases in inflammation and oxidative stress, increasing podocyte apoptosis in the kidney of diabetic rodents (64, 151). Clinically, kidney biopsies from patients with type diabetes showed that loss of podocytes (140). Previous study indicates loss of insulin signaling in the glomeruli of diabetic rats play a significant role in developing diabetic nephropathy (11). The novelty of new findings is due to linagliptin's effects on insulin signaling, preventing podocyte apoptosis in diabetic nephropathy. The concentration of linagliptin that used in the clinic is up to 100μg/kg BW, while the concentration *in vitro* study was very low. Although convincing, there is a limitation in this point.

Several clinical trials using DPP-4 inhibitors showed decreased rates of microalbuminuria progression. A recent sub-analysis study of Saxagliptin Assessment of Vascular Outcomes Recorded in Patients with Diabetes Mellitus-Thrombolysis in Myocardial Infarction (SAVOR-TIMI) 53 indicated that saxagliptin markedly decreased both overt proteinuria and microalbuminuria (152). Unlike SAVOR-TIMI 53, the Efficacy, Safety and Modification of Albuminuria in Type 2 Diabetes Subjects Renal Disease with LINAgliptin (MARLINA-T2D) study did not show substantial renal improvements owing to the small sample size (153). The cardiovascular and kidney clinical trial CARMELINA® clarified the renal outcomes of linagliptin. For the first time, this trial set the renal endpoint using DPP-4 inhibitors: composite renal endpoint [renal death, sustained ESRD, sustained decrease of 40% or more in estimated glomerular filtration rate (GFR)]. The study demonstrated not only cardiovascular safety, but also marked reduction in albuminuria and microvascular composite outcomes, including diabetic retinopathy in patients with type 2 diabetes. However, no significant effects

regarding ESRD, death due to kidney disease, and kidney composite outcome were observed in this study (134).

The glomerular capillary tuft, which is a highly complex and specialised microvascular bed that filters plasma and protects from losing protein to urine, comprises podocytes, endothelial cells, and basement membrane. In contrast, increase in glomerular area could be associated with declining GFR in DKD (154).

Several large-scale clinical studies, including CARMELINA, reported that DPP-4 inhibitors could ameliorate albuminuria without affecting GFR (134). These results suggest that DPP-4 inhibitors induced renoprotective effects mainly on podocytes and endothelial cells, rather than mesangial cells. This study and previous reports showed that linagliptin directly affected both podocytes and endothelial cells, decreasing albuminuria. However, the effect of linagliptin on mesangial cells, which in turn may affect GFR, is still unclear. Therefore, further study will be needed to clarify this.

Nrf2 is a master modulator of cellular detoxification responses, and the induction of antioxidant responses occurs through the activation of Nrf2 transcription signal (135, 155, 156). Bardoxolone methyl, a synthetic oleanane triterpenoid that activates Nrf2, has been found to interact with cysteine residues on Keap1, resulting in Nrf2 translocation to the nucleus. However, a phase 3 clinical trial of bardoxolone methyl in patients with DKD was terminated owing to cardiovascular safety concerns. In contrast, a phase 2 clinical trial of bardoxolone methyl (The TSUBAKI study) improved renal function without safety concerns in patients with DKD (American Society of Nephrology Kidney week 2017). Thus, Nrf2 activation seems to be a potential therapeutic target for DKD. Unlike previous reports using DPP-4 inhibitors, these results showed that linagliptin increased protein expression of Nrf2, while Keap1 levels remained unchanged. Linagliptin affected

upstream antioxidant signaling, and downregulation of endogenous antioxidant response was observed. Furthermore, linagliptin could not affect protein expression of Keap1, which induces ubiquitination of Nrf2. Previous reports showed that phosphorylation of Akt and GSK3β increased Nrf2 activation without Keap1 system (157). Thus, linagliptin-induced increase in Nrf2 expression might be mediated by mechanisms other than ubiquitin-proteasome system.

6. Summary and perspectives

Lifestyle changes have led to a rapid increase in the number of patients with lifestyle-related diseases, which has become a problem both in Japan and abroad. VEC play an important role of maintenance of systemic homeostasis. Disorder of VEC's function is related to the progression of lifestyle-related diseases. As the lifestyle-related diseases, thromboembolic diseases such as myocardial infarction and cerebral infarction, and diabetic diseases were focused. In the present study, VEC's functions in these lifestyle-related diseases and beneficial effects of foods or nutrients on maintaining VEC's functions to prevent these diseases were investigated. The antithrombotic effect of Okinawa mozuku was evaluated by using cultured vascular endothelial cells and rat carotid arterial thrombosis model induced by FeCl3. Since obesity was caused by unhealthful nutritional status, the influences of obesity on diabetic complications were also investigated. Furthermore, the effect of EPA on diabetic nephropathy was studied by using diabetic animal model.

Okinawa mozuku extract significantly augmented u-PA activity in the conditioned medium. The decrease of carotid artery blood flow induced by $FeCl_3$ injury in rats fed with Okinawa mozuku extract was less than that in control rats. Thus, oral administration of Okinawa mozuku extract prevented thrombus formation in this model. Oral administration of Okinawa mozuku extract significantly increased u-PA activity in euglobulin fraction, compared with control group. On the other hand, platelet aggregation activity, activated partial thromboplastin time, and active PAI-1 level in plasma exhibited no significant differences between control and Okinawa mozuku groups. These results indicate that oral administration of brown algae augments fibrinolytic activity of endothelial cells and prevents thrombus formation which is induced by injury of VEC.

Obesity is one of the risk factors for diabetes mellitus and diabetic complication, CKD, but the precise mechanism involved is unclear. This study characterizes the pathological influences of obesity on glomerular inflammation, oxidative stress, and albuminuria in obese rats. After feeding of high fat diet for 2 months, body weight and albuminuria were significantly increased in ZF rat when compared to ZL rat. Expression of the markers of inflammation, TNF-α mRNA and CCR2 mRNA, was significantly increased in the glomeruli of ZF rat when compared to ZL rat. Histological analysis of kidney showed no glomerular expansion. As inflammatory and oxidative stress markers were associated with NF-κB, NF-κB activation was analyzed in the glomeruli of mice fed with high fat diet. The augmentation of NF-κB activation in the glomeruli was observed when mice were fed with high fat diet. These results suggest that feeding of high fat diet for only 2 months duration can cause albuminuria in ZF rat, due to increased inflammation or oxidative stress, but may not be long enough to develop renal pathological changes. Further understanding of the NF-κB, TNF-α, and CCR2 pathways could lead to effective interventions for obesity-induced CKD.

Diabetes-induced endothelial pathologic changes are hypothesized to lead to the progression of DKD. The EndMT possibly induces fibrosis, leading to glomerulosclerosis in the kidney. Furthermore, this could lead to albuminuria in DKD due to glomerular endothelial dysfunction. This study has clarified the mechanism by which EPA-E can protect the glomerular endothelial cells by inhibiting EndMT followed by the PKCβ/TGF-β/PAI-1 signaling. Further, it is demonstrated that these inhibitory effects by EPA-E regulated independently of the miRNAs. These findings suggest that EPA-E exerts renal protective effects on endothelial cells, by preventing EndMT followed by the

PKCβ/TGF-β/PAI-1 signaling. Thus, EPA-E has the potential for imparting renal protection by regulating EndMT in DKD.

Diabetes-induced podocyte apoptosis is considered to play a critical role in the pathogenesis of DKD. It was suggested that hyperglycemia can induce podocyte apoptosis by inhibiting the action of podocyte survival factors, thus inactivating the cellular effects of insulin signaling. In this study, the effects of linagliptin, DPP-4 inhibitor, on high glucose-induced podocyte apoptosis were investigated. Diabetes inhibited insulin/IRS1/Akt signaling in podocytes, resulting in podocyte apoptosis. Upregulation of IRS1 expression or addition of linagliptin reversed this inhibition, thereby protecting against podocyte apoptosis. Thus, linagliptin may induce protective effects in patients with DKD in real-world clinical situations, and increasing IRS1 levels could be a potential therapeutic target in DKD. In this way, this study has clarified the pathophysiology of DKD, and this clarification has enabled search for food ingredients that inhibit the worsening of DKD. Furthermore, DPP-4 inhibitors have been reported to be effective in type 2 diabetic patients with high serum eicosapentaenoic acid concentrations (158). In chapter 4, it is demonstrated the renoprotective effect of EPA-E in diabetes rat. Therefore, it is expected to be effective in combination therapy with EPA-E.

In conclusion, this study showed that Okinawa mozuku extract inhibited thrombosis caused by VEC injury. Furthermore, diabetes-induced EndMT leading to glomerulosclerosis in the kidney was inhibited by EPA-E. Thus, it was demonstrated that food ingredients had the potential effects for improving VEC's function. On the other hand, study of VEC's function is important for understanding the pathophysiology of thrombotic disease and kidney disease and may lead to the development of novel

protective or therapeutic approaches. It may be possible that preventing these diseases by improvement of VEC's function through nutrition and food ingredients also leads to the useful treatment.

7. Abbreviations

VEC	Vascular endothelial cells
t-PA	tissue-type plasminogen activator
u-PA	urokinase-type plasminogen activator
PAI-1	Inhibitor of plasminogen activator
CKD	Chronic kidney disease
DKD	Diabetic kidney disease
EndMT	Endothelial to mesenchymal transition
APTT	Activated partial thromboplastin time
ZL	Zucker lean
ZF	Zucker fatty
TNF-α	Tumor necrosis factor-α
CCR2	C-C Motif Chemokine Receptor 2
EPA	Eicosapentaenoic acid
TGF-β	Transforming growth factor-β
STZ	Streptozotocin

8. Acknowledgments

I would like to express my sincere gratitude to Prof. Shigeru Ueshima for his support, careful guidance, and advice. I would like to thank Prof. Tatsuki Itoh for his supervision. I would like to thank Prof. Nobuhiro Zaima and Prof. Seiji Masuda for kind reviewing and advising on this manuscript. Advice and comments given by Prof. Akira Mima has been a great help in this work.

Finally, I would like to show my greatest appreciation to all those which, supported, helped, and encourage my PhD work.

9. References

1) Gao Y, Galis ZS. Exploring the role of endothelial cell resilience in cardiovascular health and disease. *Arterioscler. Thromb. Vasc. Biol.* 2021; 41: 179-185.
2) Schwingshackl L, Morze J, Hoffmann G. Mediterranean diet and health status: Active ingredients and pharmacological mechanisms. *Br. J. Pharmacol.* 2020; 177: 1241-1257.
3) Dahlbäck B. Blood coagulation and its regulation by anticoagulant pathways: genetic pathogenesis of bleeding and thrombotic diseases. *J. Intern. Med.* 2005; 257: 209-223.
4) Weitz JI. Heparan sulfate: antithrombotic or not? *J. Clin. Invest.* 2003; 111: 952-954.
5) Li PC, Yang CC, Hsu SP, Chien CT. Repetitive progressive thermal preconditioning hinders thrombosis by reinforcing phosphatidylinositol 3-kinase/Akt-dependent heat-shock protein/endothelial nitric oxide synthase signaling. *J. Vasc. Surg.* 2012 56: 159-170.
6) Xian X, Ding Y, Zhang L, Wang Y, McNutt MA, Ross C, Hayden MR, Deng X, Liu G. Enhanced atherothrombotic formation after oxidative injury by FeCl3 to the common carotid artery in severe combined hyperlipidemic mice. *Biochem. Biophys. Res. Commun.* 2009; 385: 563-569.
7) Bonetti PO, Lilach OL, Amir L. Endothelial dysfunction a marker of atherosclerotic risk. *Arterioscler. Thromb. Vasc. Biol.* 2003; 23: 168-175.
8) Hadi HA, Carr CS, Al Suwaidi J. Endothelial dysfunction: cardiovascular risk factors, therapy, and outcome. *Vasc. Health. Risk. Manag.* 2005; 1: 183-198.

9) Madero M, Katz R, Murphy R, Newman A, Patel K, Ix J, Peralta C, Satterfield S, Fried L, Shlipak M, Sarnak M. Comparison between different measures of body fat with kidney function decline and incident CKD. *Clin. J. Am. Soc. Nephrol.* 2017; 12: 893–903.

10) Herrington WG, Smith M, Bankhead C, Matsushita K, Stevens S, Holt T, Hobbs FD, Coresh J, Woodward M. Smith M, Bankhead C. Body-mass index and risk of advanced chronic kidney disease: prospective analyses from a primary care cohort of 1.4 million adults in England. *PLoS One.* 2017; 12: e0173515.

11) Mima A, Ohshiro Y, Kitada M, Matsumoto M, Geraldes P, Li C, Li Q, White GS, Cahill C, Rask-Madsen C, King GL. Glomerular-specific protein kinase C-β-induced insulin receptor substrate-1 dysfunction and insulin resistance in rat models of diabetes and obesity. *Kidney Int.* 2011; 79: 883–896.

12) Ryden L, Mellbin L. New hope for people with dysglycemia and cardiovascular disease manifestations: reduction of acute coronary events with pioglitazone. *Circulation.* 2017; 135: 1894–1896.

13) International Diabetes Federation. Diabetes Atlas 2021. Brussels, Belgium: Diabetes Atlas 2021 [Available from: https://diabetesatlas.org/atlas/tenth-edition/]

14) Remuzzi G, Benigni A, Remuzzi A. Mechanisms of progression and regression of renal lesions of chronic nephropathies and diabetes. *J. Clin. Invest.* 2006; 116(2): 288-96.

15) Jones CA, Krolewski AS, Rogus J, Xue JL, Collins A, Warram JH. Epidemic of end-stage renal disease in people with diabetes in the United States population: do we know the cause? *Kidney Int.* 2005; 67(5): 1684-91.

16) Kanasaki K, Shi S, Kanasaki M, He J, Nagai T, Nakamura Y, Ishigaki Y, Kitada M, Srivastava SP, Koya D. Linagliptin-mediated DPP-4 inhibition ameliorates kidney fibrosis in streptozotocin-induced diabetic mice by inhibiting endothelial-to-mesenchymal transition in a therapeutic regimen. *Diabetes.* 2014; 63(6): 2120-31.

17) Yasuzawa T, Mima A, Ueshima S. Antithrombotic effect of oral administration of Mozuku (Cladosiphon okamuranus, Brown Seaweed) extract in rat. *J. Nutr. Sci. Vitaminol.* 2019; 65(2): 161-176.

18) Ruocco N, Costantini S, Guariniello S, Costantini M. Polysaccharides from the Marine Environment with Pharmacological, Cosmeceutical and Nutraceutical Potential. *Molecules.* 2016; 21: 551-567.

19) Wang J, Zhang Q, Zhang Z, Li Z. Antioxidant activity of sulfated polysaccharide fractions extracted from Laminaria japonica. *Int. J. Biol. Macromol.* 2008; 42: 127-132.

20) Wang J, Zhang Q, Zhang Z, Song H, Li P. Potential antioxidant and anticoagulant capacity of low molecular weight fucoidan fractions extracted from Laminaria japonica. *Int. J. Biol. Macromol.* 2010; 46: 6-12.

21) Amano H, Kakinuma M, Coury AD, Ohno H, Hara T. Effect of a seaweed mixture on serum lipid level and platelet aggregation in rats. *Fish Sci.* 2005; 71: 1160-1166.

22) Ren R, Azuma Y, Ojima T, Hashimoto T, Mizuno M, Nishitani Y, Yoshida M, Azuma T, Kanazawa K. Modulation of platelet aggregation-related eicosanoid production by dietary F-fucoidan from brown alga Laminaria japonica in human subjects. *Br J Nutr.* 2013; 110: 880-890.

23) Cumashi A, Ushakova NA, Preobrazhenskaya ME, D'Incecco A, Piccoli A, Totani L, Tinari N, Morozevich GE, Berman AE, Bilan MI, Usov AI, Ustyuzhanina NE,

Grachev AA, Sanderson CJ, Kelly M, Rabinovich GA, Iacobelli S, Nifantiev NE; Consorzio Interuniversitario Nazionale per la Bio-Oncologia, Italy. A comparative study of the anti-inflammatory, anticoagulant, antiangiogenic, and antiadhesive activities of nine different fucoidans from brown seaweeds. *Glycobiology.* 2007; 17: 541-552.

24) Ustyuzhanina NE, Ushakova NA, Zyuzina KA, Bilan MI, Elizarova AL, Somonova OV, Madzhuga AV, Krylov VB, Preobrazhenskaya ME, Usov AI, Kiselevskiy MV, Nifantiev NE. Influence of fucoidans on hemostatic system. *Mar. Drugs.* 2013; 11: 2444-2458.

25) Rocha HA, Moraes FA, Trindade ES, Franco CR, Torquato RJ, Veiga SS, Valente AP, Mourão PA, Leite EL, Nader HB, Dietrich CP. Structural and hemostatic activities of a sulfated galactofucan from the brown alga Spatoglossum schroederi. An ideal antithrombotic agent? *J. Biol. Chem.* 2005; 280: 41278-41288.

26) Nagamine T, Nakazato K, Tomioka S, Iha M, Nakajima K. Intestinal absorption of fucoidan extracted from brown seaweed, Cladosiphon okamuranus. *Mar. Drugs*. 2015; 13: 48-64.

27) Matsumoto H, Ueshima S, Fukao H, Mitsui Y, Matsuo O. Identification of urokinase-type plasminogen activator receptor in human endothelial cells and its modulation by phorbol myristate acetate. *Cell Struct. Funct.* 1995; 20: 429-437.

28) Matsumoto H, Ueshima S, Fukao H, Mitsui Y, Matsuo O. Effects of lipopolysaccharide on the expression of fibrinolytic factors in an established cell line from human endothelial cells. *Life Sci.* 1996; 59: 85-96.

29) Ogawa A, Mori E, Minematsu K, Taki W, Takahashi A, Nemoto S, Miyamoto S, Sasaki M, Inoue T; MELT Japan Study Group. Randomized trial of intraarterial

infusion of urokinase within 6 hours of middle cerebral artery stroke: the middle cerebral artery embolism local fibrinolytic intervention trial (MELT) Japan. *Stroke.* 2007; 38: 2633-2639.

30) Victor G. Therapeutic Fibrinolysis How Efficacy and Safety Can Be Improved. *J. Am. Coll. Cardiol.* 2016; 68: 2099-2106.

31) Schäfer K, Konstantinides S, Riedel C, Thinnes T, Müller K, Dellas C, Hasenfuss G, Loskutoff DJ. Different mechanisms of increased luminal stenosis after arterial injury in mice deficient for urokinase- or tissue-type plasminogen activator. *Circulation* 2002; 106: 1847-1852.

32) Qin YR, You SJ, Zhang Y, Li Q, Wang XH, Wang F, Hu LF, Liu CF. Hydrogen sulfide attenuates ferric chloride-induced arterial thrombosis in rats. *Free. Radic. Res.* 2016; 50: 654-665.

33) Wang X, mith PL, Hsu MY, Ogletree ML, Schumacher WA. Murine model of ferric chloride-induced vena cava thrombosis: evidence for effect of potato carboxypeptidase inhibitor. *J. Thromb. Haemost.* 2006; 4: 403-410.

34) Zhu W, Gregory JC, Org E, Buffa JA, Gupta N, Wang Z, Li L, Fu X, Wu Y, Mehrabian M, Sartor RB, McIntyre TM, Silverstein RL, Tang WHW, DiDonato JA, Brown JM, Lusis AJ, Hazen SL. Gut Microbial Metabolite TMAO Enhances Platelet Hyperreactivity and Thrombosis Risk. *Cell.* 2016; 165: 111-124.

35) Nosaka M, Ishida Y, Kimura A, Kuninaka Y, Inui M, Mukaida N, Kondo T. Absence of IFN-γ accelerates thrombus resolution through enhanced MMP-9 and VEGF expression in mice. *J. Clin. Invest.* 2011; 121: 2911-2920.

36) Lee J, Kwon G, Park J, Kim JK, Choe SY, Seo Y, Lim YH. An ethanol extract of Ramulus mori improves blood circulation by inhibiting platelet aggregation. *Biosci. Biotechnol. Biochem.* 2016; 80: 1410-1415.

37) Yasar Yildiz S, Kuru P, Toksoy Oner E, Agirbasli M. Functional stability of plasminogen activator inhibitor-1. *Sci. World J.* 2014: 858293.

38) Okayama T, Nakano M, Odake S, Hagiwara M, Morikawa T, Ueshima S, Okada K, Fukao H, Matsuo O. Synthetic dipeptide, N-Stearoyl-D-Ser-L-Pro-OEt, induces release of tissue-type plasminogen activator in cultured cells and in experimental animals. *Chem. Pharm. Bull.* 1994; 42: 1854-1858.

39) Ueshima S, Matsuno H, Hayashi M, Horibuchi K, Okada K, Fukao H, Uematsu T, Matsuo O. Function of tissue-type plasminogen activator releaser on vascular endothelial cells and thrombolysis in vivo. *Thromb. Haemost.* 2002; 87: 1069-1074.

40) Zhao X, Guo F, Hu J, Zhang L, Xue C, Zhang Z, Li B. Antithrombotic activity of oral administered low molecular weight fucoidan from Laminaria Japonica. *Thrombs. Res.* 2016; 144: 46-52.

41) Li B, Lu F, Wei X, Zhao R. Fucoidan: Structure and bioactivity. *Molecules*. 2008; 13: 1671-1695.

42) Keuren JF, Wielders SJ, Willems GM, Morra M, Cahalan L, Cahalan P, Lindhout T. Thrombogenicity of polysaccharide-coated surfaces. *Biomaterials*. 2003; 24: 1917-1924.

43) Mima A, Yasuzawa T, King GL, Ueshima S. Obesity-associated glomerular inflammation increases albuminuria without renal histological changes. *FEBS Open Bio*. 2018; 8(4): 664-70.

44) Siddiqi FS, Advani A. Endothelial-podocyte crosstalk: the missing link between endothelial dysfunction and albuminuria in diabetes. *Diabetes.* 2013; 62: 3647–3655.

45) Carrero JJ, Grams ME, Sang Y, Ärnlöv J, Gasparini A, Matsushita K, Qureshi AR, Evans M, Barany P, Lindholm B, Ballew SH, Levey AS, Gansevoort RT, Elinder CG, Coresh J. Albuminuria changes are associated with subsequent risk of end-stage renal disease and mortality. *Kidney Int.* 2017; 91: 244–251.

46) Brantsma AH, Bakker SJ, Hillege HL, de Zeeuw D, de Jong PE, Gansevoort RT; PREVEND Study Group. Urinary albumin excretion and its relation with C-reactive protein and the metabolic syndrome in the prediction of type 2 diabetes. *Diabetes Care.* 2005; 28" 2525– 2530.

47) Lin J, Hu FB, Rimm EB, Rifai N, Curhan GC. The association of serum lipids and inflammatory biomarkers with renal function in men with type II diabetes mellitus. *Kidney Int.* 2006; 69: 336–342.

48) Stehouwer CD, Fischer HR, van Kuijk AW, Polak BC, Donker AJ. Endothelial dysfunction precedes development of microalbuminuria in IDDM. *Diabetes*. 1995; 44: 561–564.

49) Schalkwijk CG, Poland DC, van Dijk W, Kok A, Emeis JJ, Dräger AM, Doni A, van Hinsbergh VW, Stehouwer CD. Plasma concentration of C- reactive protein is increased in type I diabetic patients without clinical macroangiopathy and correlates with markers of endothelial dysfunction: evidence for chronic inflammation. *Diabetologia.* 1999; 42: 351–357.

50) Mima A, Qi W, Hiraoka-Yamomoto J, Park K, Matsumoto M, Kitada M, Li Q, Mizutani K, Yu E, Shimada T, Lee J, Shoelson SE, Jobin C, Rask-Madsen C, King

GL. Retinal not systemic oxidative and inflammatory stress correlated with VEGF expression in rodent models of insulin resistance and diabetes. *Invest. Ophthalmol. Vis. Sci.* 2012; 53: 8424–8432.

51) Siebenlist U, Franzoso G, Brown K. Structure, regulation and function of NF-kappa B. *Annu. Rev. Cell. Biol*. 1994; 10: 405–455.

52) Wang H, Chen X, Su Y, Paueksakon P, Hu W, Zhang MZ, Harris RC, Blackwell TS, Zent R, Pozzi A. p47(phox) contributes to albuminuria and kidney fibrosis in mice. *Kidney Int.* 2015; 87: 948–962.

53) Giacco F, Du X, D'Agati VD, Milne R, Sui G, Geoffrion M, Brownlee M. Knockdown of glyoxalase 1 mimics diabetic nephropathy in nondiabetic mice. *Diabetes* 2014; 63: 291–299.

54) Billings FT 4th, Pretorius M, Schildcrout JS, Mercaldo ND, Byrne JG, Ikizler TA, Brown NJ. Obesity and oxidative stress predict AKI after cardiac surgery. *J. Am. Soc. Nephrol*. 2012; 23: 1221–1228.

55) Suzuki D, Miyazaki M, Naka R, Koji T, Yagame M, Jinde K, Endoh M, Nomoto Y, Sakai H. In situ hybridization of interleukin 6 in diabetic nephropathy. *Diabetes.* 1995; 44: 1233–1238.

56) Gohda T, Niewczas MA, Ficociello LH, Walker WH, Skupien J, Rosetti F, Cullere X, Johnson AC, Crabtree G, Smiles AM, Mayadas TN, Warram JH, Krolewski AS. Circulating TNF receptors 1 and 2 predict stage 3 CKD in type 1 diabetes. *J. Am. Soc. Nephrol.* 2012; 23: 516–524.

57) Gohda T, Maruyama S, Kamei N, Yamaguchi S, Shibata T, Murakoshi M, Horikoshi S, Tomino Y, Ohsawa I, Gotoh H, Nojiri S, Suzuki Y. Circulating TNF

receptors 1 and 2 predict mortality in patients with end- stage renal disease undergoing dialysis. *Sci. Rep.* 2017; 7: 43520.

58) Petecchia L, Sabatini F, Usai C, Caci E, Varesio L, Rossi GA. Cytokines induce tight junction disassembly in airway cells via an EGFR-dependent MAPK/ERK1/2-pathway. *Lab. Invest.* 2012; 92: 1140–1148.

59) Nakamura T, Kawagoe Y, Matsuda T, Ueda A, Ueda Y, Takahashi Y, Tanaka A, Koide H. Effect of granulocyte and monocyte adsorption apheresis on urinary albumin excretion and plasma endothelin-1 concentration in patients with active ulcerative colitis. *Blood Purif.* 2004; 22: 499–504.

60) Deji N, Kume S, Araki S, Soumura M, Sugimoto T, Isshiki K, Chin-Kanasaki M, Sakaguchi M, Koya D, Haneda M, Kashiwagi A, Uzu T. Structural and functional changes in the kidneys of high-fat diet-induced obese mice. *Am. J. Physiol. Renal. Physiol.* 2009; 296: F118–F126.

61) Vaidya VS, Niewczas MA, Ficociello LH, Johnson AC, Collings FB, Warram JH, Krolewski AS, Bonventre JV. Regression of microalbuminuria in type 1 diabetes is associated with lower levels of urinary tubular injury biomarkers, kidney injury molecule-1, and N-acetyl-beta-D-glucosaminidase. *Kidney Int.* 2011; 79: 464–470.

62) Reddy MA, Sumanth P, Lanting L, Yuan H, Wang M, Mar D, Alpers CE, Bomsztyk K, Natarajan R. Losartan reverses permissive epigenetic changes in renal glomeruli of diabetic db/db mice. *Kidney Int.* 2014; 85: 362–373.

63) Kanamori H, Matsubara T, Mima A, Sumi E, Nagai K, Takahashi T, Abe H, Iehara N, Fukatsu A, Okamoto H, Kita T, Doi T, Arai H. Inhibition of MCP-1/CCR2 pathway ameliorates the development of diabetic nephropathy. *Biochem. Biophys. Res. Commun.* 2007; 360: 772–777.

64) de Zeeuw D, Bekker P, Henkel E, Hasslacher C, Gouni-Berthold I, Mehling H, Potarca A, Tesar V, Heerspink HJ, Schall TJ; CCX140-B Diabetic Nephropathy Study Group. The effect of CCR2 inhibitor CCX140-B on residual albuminuria in patients with type 2 diabetes and nephropathy: a randomised trial. *Lancet Diabetes Endocrinol.* 2015; 3: 687– 696.

65) Mima A, Kitada M, Geraldes P, Li Q, Matsumoto M, Mizutani K, Qi W, Li C, Leitges M, Rask-Madsen C, King GL. Glomerular VEGF resistance induced by PKCdelta/SHP-1 activation and contribution to diabetic nephropathy. *FASEB J.* 2012; 26: 2963–2974.

66) Yasuzawa T, Nakamura T, Ueshima S, Mima A. Protective Effects of Eicosapentaenoic Acid on the Glomerular Endothelium via Inhibition of EndMT in Diabetes. *J. Diabetes Res.* 2021; 2182225.

67) Patel A; ADVANCE Collaborative Group, MacMahon S, Chalmers J, Neal B, Woodward M, Billot L, Harrap S, Poulter N, Marre M, Cooper M, Glasziou P, Grobbee DE, Hamet P, Heller S, Liu LS, Mancia G, Mogensen CE, Pan CY, Rodgers A, Williams B. Effects of a fixed combination of perindopril and indapamide on macrovascular and microvascular outcomes in patients with type 2 diabetes mellitus (the ADVANCE trial): a randomised controlled trial. *Lancet*. 2007; 370(9590):829-40.

68) Patel A, MacMahon S, Chalmers J, Neal B, Billot L, Woodward M, Marre M, Cooper M, Glasziou P, Grobbee D, Hamet P, Harrap S, Heller S, Liu L, Mancia G, Mogensen CE, Pan C, Poulter N, Rodgers A, Williams B, Bompoint S, de Galan BE, Joshi R, Travert F, ADVANCE Collaborative Group. Intensive blood glucose

control and vascular outcomes in patients with type 2 diabetes. *N. Engl. J. Med.* 2008; 358(24): 2560-72.

69) Holman RR, Paul SK, Bethel MA, Matthews DR, Neil HA. 10-year follow-up of intensive glucose control in type 2 diabetes. *N. Engl. J. Med.* 2008; 359(15): 1577-89.

70) Gerstein HC, Miller ME, Byington RP, Goff DC Jr, Bigger JT, Buse JB, Cushman WC, Genuth S, Ismail-Beigi F, Grimm RH Jr, Probstfield JL, Simons-Morton DG, Friedewald WT, Action to Control Cardiovascular Risk in Diabetes Study Group. Effects of intensive glucose lowering in type 2 diabetes. *N. Engl. J. Med.* 2008; 358(24): 2545-59.

71) Gerstein HC, Bosch J, Dagenais GR, Díaz R, Jung H, Maggioni AP, Pogue J, Probstfield J, Ramachandran A, Riddle MC, Rydén LE, Yusuf S, ORIGIN Trial Investigators. Basal insulin and cardiovascular and other outcomes in dysglycemia. *N. Engl. J. Med.* 2012; 367(4): 319-28.

72) Fogo A, Ichikawa I. Evidence for the central role of glomerular growth promoters in the development of sclerosis. *Semin. Nephrol.* 1989; 9(4): 329-42.

73) Kagami S, Border WA, Miller DE, Noble NA. Angiotensin II stimulates extracellular matrix protein synthesis through induction of transforming growth factor-beta expression in rat glomerular mesangial cells. *J. Clin. Invest.* 1994; 93(6): 2431-7.

74) Mima A, Matsubara T, Arai H, Abe H, Nagai K, Kanamori H, Sumi E, Takahashi T, Iehara N, Fukatsu A, Kita T, Doi T. Angiotensin II-dependent Src and Smad1 signaling pathway is crucial for the development of diabetic nephropathy. *Lab. Invest*. 2006; 86(9): 927-39.

75) Matsubara T, Abe H, Arai H, Nagai K, Mima A, Kanamori H, Sumi E, Takahashi T, Matsuura M, Iehara N, Fukatsu A, Kita T, Doi T. Expression of Smad1 is directly associated with mesangial matrix expansion in rat diabetic nephropathy. *Lab. Invest.* 2006; 86(4): 357-68.

76) Mima A, Abe H, Nagai K, Arai H, Matsubara T, Araki M, Torikoshi K, Tominaga T, Iehara N, Fukatsu A, Kita T, Doi T. Activation of Src mediates PDGF-induced Smad1 phosphorylation and contributes to the progression of glomerulosclerosis in glomerulonephritis. *PLoS One.* 2011; 6(3): e17929.

77) Mima A, Arai H, Matsubara T, Abe H, Nagai K, Tamura Y, Torikoshi K, Araki M, Kanamori H, Takahashi T, Tominaga T, Matsuura M, Iehara N, Fukatsu A, Kita T, Doi T. Urinary Smad1 is a novel marker to predict later onset of mesangial matrix expansion in diabetic nephropathy. *Diabetes.* 2008; 57(6): 1712-22.

78) Hirahashi J. Omega-3 Polyunsaturated Fatty Acids for the Treatment of IgA Nephropathy. *J. Clin. Med.* 2017; 6(7): 70.

79) Han E, Yun Y, Kim G, Lee YH, Wang HJ, Lee BW, Cha BS, Kim BS, Kang ES. Effects of Omega-3 Fatty Acid Supplementation on Diabetic Nephropathy Progression in Patients with Diabetes and Hypertriglyceridemia. *PLoS One.* 2016; 11(5): e0154683.

80) Kajikawa S, Harada T, Kawashima A, Imada K, Mizuguchi K. Highly purified eicosapentaenoic acid ethyl ester prevents development of steatosis and hepatic fibrosis in rats. *Dig. Dis. Sci.* 2010; 55(3): 631-41.

81) Kajikawa S, Imada K, Takeuchi T, Shimizu Y, Kawashima A, Harada T, Mizuguchi K. Eicosapentaenoic acid attenuates progression of hepatic fibrosis with inhibition

of reactive oxygen species production in rats fed methionine- and choline-deficient diet. *Dig. Dis. Sci.* 2011; 56(4): 1065-74.

82) Mima A, Hiraoka-Yamomoto J, Li Q, Kitada M, Li C, Geraldes P, Matsumoto M, Mizutani K, Park K, Cahill C, Nishikawa S, Rask-Madsen C, King GL. Protective effects of GLP-1 on glomerular endothelium and its inhibition by PKCbeta activation in diabetes. *Diabetes*. 2012; 61(11): 2967-79.

83) Huang H, Nakamura T, Yasuzawa T, Ueshima S. Effects of Coriandrum sativum on Migration and Invasion Abilities of Cancer Cells. *J. Nutr. Sci. Vitaminol.* 2020; 66(5): 468-77.

84) Mima A. Inflammation and oxidative stress in diabetic nephropathy: new insights on its inhibition as new therapeutic targets. *J. Diabetes. Res*. 2013; 2013: 248563.

85) Mima A. Incretin-Based Therapy for Prevention of Diabetic Vascular Complications. *J. Diabetes. Res.* 2016; 2016: 1379274.

86) Mima A. Sodium-Glucose Cotransporter 2 Inhibitors in Patients with Non-Diabetic Chronic Kidney Disease. *Adv. Ther*. 2021; 38(5): 2201-12.

87) Diez M, Musri MM, Ferrer E, Barberà JA, Peinado VI. Endothelial progenitor cells undergo an endothelial-to-mesenchymal transition-like process mediated by TGFbetaRI. *Cardiovasc. Res.* 2010; 88(3): 502-11.

88) Shang J, Zhang Y, Jiang Y, Li Z, Duan Y, Wang L, Xiao J, Zhao Z. NOD2 promotes endothelial-to-mesenchymal transition of glomerular endothelial cells via MEK/ERK signaling pathway in diabetic nephropathy. *Biochem. Biophys. Res. Commun.* 2017; 484(2): 435-41.

89) He Y, Huang C, Lin X, Li J. MicroRNA-29 family, a crucial therapeutic target for fibrosis diseases. *Biochimie*. 2013; 95(7): 1355-9.

90) Wang B, Jha JC, Hagiwara S, McClelland AD, Jandeleit-Dahm K, Thomas MC, Cooper ME, Kantharidis P. Transforming growth factor-beta1-mediated renal fibrosis is dependent on the regulation of transforming growth factor receptor 1 expression by let-7b. *Kidney. Int.* 2014; 85(2): 352-61.

91) Park JT, Kato M, Lanting L, Castro N, Nam BY, Wang M, Kang SW, Natarajan R. Repression of let-7 by transforming growth factor-beta1-induced Lin28 upregulates collagen expression in glomerular mesangial cells under diabetic conditions. *Am. J. Physiol. Renal. Physiol.* 2014; 307(12): F1390-403.

92) Matsubara T, Araki M, Abe H, Ueda O, Jishage K, Mima A, Goto C, Tominaga T, Kinosaki M, Kishi S, Nagai K, Iehara N, Fukushima N, Kita T, Arai H, Doi T. Bone Morphogenetic Protein 4 and Smad1 Mediate Extracellular Matrix Production in the Development of Diabetic Nephropathy. *Diabetes*. 2015; 64(8): 2978-90.

93) Bhatt DL, Steg PG, Miller M, Brinton EA, Jacobson TA, Ketchum SB, Doyle RT Jr, Juliano RA, Jiao L, Granowitz C, Tardif JC, Ballantyne CM; REDUCE-IT Investigators. Cardiovascular Risk Reduction with Icosapent Ethyl for Hypertriglyceridemia. *N. Engl. J. Med*. 2019; 380(1): 11-22.

94) Matsuzaki M, Yokoyama M, Saito Y, Origasa H, Ishikawa Y, Oikawa S, Sasaki J, Hishida H, Itakura H, Kita T, Kitabatake A, Nakaya N, Sakata T, Shimada K, Shirato K, Matsuzawa Y; JELIS Investigators. Incremental effects of eicosapentaenoic acid on cardiovascular events in statin-treated patients with coronary artery disease. *Circ. J*. 2009; 73(7): 1283-90.

95) Mori TA, Bao DQ, Burke V, Puddey IB, Beilin LJ. Docosahexaenoic acid but not eicosapentaenoic acid lowers ambulatory blood pressure and heart rate in humans. *Hypertension.* 1999; 34(2): 253-60.

96) Theobald HE, Goodall AH, Sattar N, Talbot DC, Chowienczyk PJ, Sanders TA. Low-dose docosahexaenoic acid lowers diastolic blood pressure in middle-aged men and women. *J. Nutr.* 2007; 137(4): 973-8.

97) Grimsgaard S, Bønaa KH, Hansen JB, Myhre ES. Effects of highly purified eicosapentaenoic acid and docosahexaenoic acid on hemodynamics in humans. *Am. J. Clin. Nutr.* 1998; 68(1): 52-9.

98) Stark KD, Holub BJ. Differential eicosapentaenoic acid elevations and altered cardiovascular disease risk factor responses after supplementation with docosahexaenoic acid in postmenopausal women receiving and not receiving hormone replacement therapy. *Am. J. Clin. Nutr.* 2004; 79(5): 765-73.

99) von Schacky C, Weber PC. Metabolism and effects on platelet function of the purified eicosapentaenoic and docosahexaenoic acids in humans. *J. Clin. Invest.* 1985; 76(6): 2446-50.

100) Woodman RJ, Mori TA, Burke V, Puddey IB, Barden A, Watts GF, Beilin LJ. Effects of purified eicosapentaenoic acid and docosahexaenoic acid on platelet, fibrinolytic and vascular function in hypertensive type 2 diabetic patients. *Atherosclerosis*. 2003; 166(1): 85-93.

101) Sherratt SCR, Mason RP. Eicosapentaenoic acid and docosahexaenoic acid have distinct membrane locations and lipid interactions as determined by X-ray diffraction. *Chem. Phys. Lipids.* 2018; 212: 73-9.

102) Mason RP, acob RF, Shrivastava S, Sherratt SCR, Chattopadhyay A. Eicosapentaenoic acid reduces membrane fluidity, inhibits cholesterol domain formation, and normalizes bilayer width in atherosclerotic-like model membranes. *Biochim. Biophys Acta.* 2016; 1858(12): 3131-40.

103) Shaikh SR. Biophysical and biochemical mechanisms by which dietary N-3 polyunsaturated fatty acids from fish oil disrupt membrane lipid rafts. *J. Nutr. Biochem.* 2012; 23(2): 101-5.

104) Ohshiro Y, Ma RC, Yasuda Y, Hiraoka-Yamamoto J, Clermont AC, Isshiki K, Yagi K, Arikawa E, Kern TS, King GL. Reduction of diabetes-induced oxidative stress, fibrotic cytokine expression, and renal dysfunction in protein kinase Cbeta-null mice. *Diabetes*. 2006; 55(11): 3112-20.

105) Cao Y, Feng B, Chen S, Chu Y, Chakrabarti S. Mechanisms of endothelial to mesenchymal transition in the retina in diabetes. *Invest. Ophthalmol. Vis. Sci.* 2014; 55(11): 7321-31.

106) Piera-Velazquez S, Jimenez SA. Endothelial to Mesenchymal Transition: Role in Physiology and in the Pathogenesis of Human Diseases. *Physiol. Rev.* 2019; 99(2): 1281-324.

107) Liu X, Mujahid H, Rong B, Lu QH, Zhang W, Li P, Li N, Liang ES, Wang Q, Tang DQ, Li NL, Ji XP, Chen YG, Zhao YX, Zhang MX. Irisin inhibits high glucose-induced endothelial-to-mesenchymal transition and exerts a dose-dependent bidirectional effect on diabetic cardiomyopathy. *J. Cell. Mol. Med.* 2018; 22(2): 808-22.

108) Medici D, Potenta S, Kalluri R. Transforming growth factor-beta2 promotes Snail-mediated endothelial-mesenchymal transition through convergence of Smad-dependent and Smad-independent signalling. *Biochem. J.* 2011; 437(3): 515-20.

109) Cheng JC, Chang HM, Leung PC. Transforming growth factor-beta1 inhibits trophoblast cell invasion by inducing Snail-mediated down-regulation of vascular endothelial-cadherin protein. *J. Biol. Chem.* 2013; 288(46): 33181-92.

110) Kokudo T, Suzuki Y, Yoshimatsu Y, Yamazaki T, Watabe T, Miyazono K. Snail is required for TGFbeta-induced endothelial-mesenchymal transition of embryonic stem cell-derived endothelial cells. *J. Cell. Sci*. 2008; 121(Pt 20): 3317-24.

111) Cifarelli V, Lashinger LM, Devlin KL, Dunlap SM, Huang J, Kaaks R, Pollak MN, Hursting SD. Metformin and Rapamycin Reduce Pancreatic Cancer Growth in Obese Prediabetic Mice by Distinct MicroRNA-Regulated Mechanisms. *Diabetes*. 2015; 64(5): 1632-42.

112) Tang Y, Tang Y, Cheng YS. miR-34a inhibits pancreatic cancer progression through Snail1-mediated epithelial-mesenchymal transition and the Notch signaling pathway. *Sci Rep*. 2017; 7: 38232.

113) Dankel SN, Grytten E, Bjune JI, Nielsen HJ, Dietrich A, Blüher M, Sagen JV, Mellgren G. COL6A3 expression in adipose tissue cells is associated with levels of the homeobox transcription factor PRRX1. *Sci. Rep.* 2020; 10(1): 20164.

114) Zhang X, Liu Q, Zhang X, Guo K, Zhang X, Zhou Z. FOXO3a regulates lipid accumulation and adipocyte inflammation in adipocytes through autophagy: Role of FOXO3a in obesity. *Inflamm. Res.* 2021; 70(5): 591-603.

115) Park K, Mima A, Li Q, Rask-Madsen C, He P, Mizutani K, Katagiri S, Maeda Y, Wu IH, Khamaisi M, Preil SR, Maddaloni E, Sørensen D, Rasmussen LM, Huang PL, King GL. Insulin decreases atherosclerosis by inducing endothelin receptor B expression. *JCI Insight*. 2016; 1(6): e86574.

116) Katagiri S, Park K, Maeda Y, Rao TN, Khamaisi M, Li Q, Yokomizo H, Mima A, Lancerotto L, Wagers A, Orgill DP, King GL. Overexpressing IRS1 in Endothelial Cells Enhances Angioblast Differentiation and Wound Healing in Diabetes and Insulin Resistance. *Diabetes*. 2016; 65(9): 2760-71.

117) Lopez D, Niu G, Huber P, Carter WB. Tumor-induced upregulation of Twist, Snail, and Slug represses the activity of the human VE-cadherin promoter. *Arch. Biochem. Biophys*. 2009; 482(1-2): 77-82.

118) Cucoranu I, Clempus R, Dikalova A, Phelan PJ, Ariyan S, Dikalov S, Sorescu D. NAD(P)H oxidase 4 mediates transforming growth factor-beta1-induced differentiation of cardiac fibroblasts into myofibroblasts. *Circ. Res*. 2005; 97(9): 900-7.

119) Shimizu H, Ohtani K, Tanaka Y, Sato N, Mori M, Shimomura Y. Long-term effect of eicosapentaenoic acid ethyl (EPA-E) on albuminuria of non-insulin dependent diabetic patients. *Diabetes Res. Clin. Pract*. 1995; 28(1): 35-40.

120) Hagiwara S, Makita Y, Gu L, Tanimoto M, Zhang M, Nakamura S, Kaneko S, Itoh T, Gohda T, Horikoshi S, Tomino Y. Eicosapentaenoic acid ameliorates diabetic nephropathy of type 2 diabetic KKAy/Ta mice: involvement of MCP-1 suppression and decreased ERK1/2 and p38 phosphorylation. *Nephrol. Dial. Transplant*. 2006; 21(3): 605-15.

121) Zhang M, Hagiwara S, Matsumoto M, Gu L, Tanimoto M, Nakamura S, Kaneko S, Gohda T, Qian J, Horikoshi S, Tomino Y. Effects of eicosapentaenoic acid on the early stage of type 2 diabetic nephropathy in KKA(y)/Ta mice: involvement of anti-inflammation and antioxidative stress. *Metabolism*. 2006; 55(12): 1590-8.

122) Jeong BY, Uddin MJ, Park JH, Lee JH, Lee HB, Miyata T, Ha H. Novel Plasminogen Activator Inhibitor-1 Inhibitors Prevent Diabetic Kidney Injury in a Mouse Model. *PLoS One*. 2016; 11(6): e0157012.

123) Brück K, Stel VS, Gambaro G, Hallan S, Völzke H, Ärnlöv J, Kastarinen M, Guessous I, Vinhas J, Stengel B, Brenner H, Chudek J, Romundstad S, Tomson C,

Gonzalez AO, Bello AK, Ferrieres J, Palmieri L, Browne G, Capuano V, Van Biesen W, Zoccali C, Gansevoort R, Navis G, Rothenbacher D, Ferraro PM, Nitsch D, Wanner C, Jager KJ; European CKD Burden Consortium. CKD Prevalence Varies across the European General Population. *J. Am. Soc. Nephrol*. 2016; 27(7): 2135-47.

124) Isogai C, Laug WE, Shimada H, Declerck PJ, Stins MF, Durden DL, Erdreich-Epstein A, DeClerck YA. Plasminogen activator inhibitor-1 promotes angiogenesis by stimulating endothelial cell migration toward fibronectin. *Cancer Res*. 2001; 61(14): 5587-94.

125) Ruiz MA, Chakrabarti S. MicroRNAs: the underlying mediators of pathogenetic processes in vascular complications of diabetes. *Can. J. Diabetes*. 2013; 37(5): 339-44.

126) Shah MY, Ferrajoli A, Sood AK, Lopez-Berestein G, Calin GA. microRNA Therapeutics in Cancer - An Emerging Concept. *EBioMedicine*. 2016; 12: 34-42.

127) Lorenzen JM, Haller H, Thum T. MicroRNAs as mediators and therapeutic targets in chronic kidney disease. *Nat. Rev. Nephrol*. 2011; 7(5): 286-94.

128) Schauerte C, Hübner A, Rong S, Wang S, Shushakova N, Mengel M, Dettling A, Bang C, Scherf K, Koelling M, Melk A, Haller H, Thum T, Lorenzen JM. Antagonism of profibrotic microRNA-21 improves outcome of murine chronic renal allograft dysfunction. *Kidney Int.* 2017; 92(3): 646-56.

129) Brennan EP, Nolan KA, Börgeson E, Gough OS, McEvoy CM, Docherty NG, Higgins DF, Murphy M, Sadlier DM, Ali-Shah ST, Guiry PJ, Savage DA, Maxwell AP, Martin F, Godson C; GENIE Consortium. Lipoxins attenuate renal fibrosis by

inducing let-7c and suppressing TGFbetaR1. *J. Am. Soc. Nephrol.* 2013; 24(4): 627-37.

130) Frost RJ, Olson EN. Control of glucose homeostasis and insulin sensitivity by the Let-7 family of microRNAs. *Proc. Natl. Acad. Sci. U. S. A.* 2011; 108(52): 21075-80.

131) Mima A, Yasuzawa T, Nakamura T, Ueshima S. Linagliptin affects IRS1/Akt signaling and prevents high glucose- induced apoptosis in podocytes. *Sci. Rep*. 2020; 10(1): 5775, 2020

132) Nathan DM, Genuth S, Lachin J, Cleary P, Crofford O, Davis M, Rand L, Siebert C, Diabetes Control and Complications Trial Research Group. The effect of intensive treatment of diabetes on the development and progression of long-term complications in insulin-dependent diabetes mellitus. *N. Engl. J. Med. 1993;* 329: 977–986.

133) Drapeau N, Lizotte F, Denhez B, Guay A, Kennedy CR, Geraldes P. Expression of SHP-1 induced by hyperglycemia prevents insulin actions in podocytes. *Am. J. Physiol. Endocrinol. Metab.* 2013; 304: E1188–1198.

134) Rosenstock J, Perkovic V, Johansen OE, Cooper ME, Kahn SE, Marx N, Alexander JH, Pencina M, Toto RD, Wanner C, Zinman B, Woerle HJ, Baanstra D, Pfarr E, Schnaidt S, Meinicke T, George JT, von Eynatten M, McGuire DK; CARMELINA Investigators. Effect of Linagliptin vs Placebo on Major Cardiovascular Events in Adults with Type 2 Diabetes and High Cardiovascular and Renal Risk: The CARMELINA Randomized Clinical Trial. *JAMA* 2019; 321: 69–79.

135) Zheng H, Whitman SA, Wu W, Wondrak GT, Wong PK, Fang D, Zhang DD. Therapeutic potential of Nrf2 activators in streptozotocin-induced diabetic nephropathy. *Diabetes* 2011; 60: 3055–3066.

136) Sireesh D, Dhamodharan U, Ezhilarasi K, Vijay V, Ramkumar KM. Association of NF-E2 Related Factor 2 (Nrf2) and inflammatory cytokines in recent onset Type 2 Diabetes Mellitus. *Sci. Rep.* 2018; 8: 5126.

137) Zhu X, Chen Y, Chen Q, Yang H, Xie X. Astaxanthin Promotes Nrf2/ARE Signaling to Alleviate Renal Fibronectin and Collagen IV Accumulation in Diabetic Rats. *J. Diabetes Res.* 2018; 6730315.

138) Kern M, Klöting N, Niessen HG, Thomas L, Stiller D, Mark M, Klein T, Blüher M. Linagliptin improves insulin sensitivity and hepatic steatosis in diet-induced obesity. *PLoS One.* 2012; 7: e38744.

139) Civantos E, Bosch E, Ramirez E, Zhenyukh O, Egido J, Lorenzo O, Mas S. Sitagliptin ameliorates oxidative stress in experimental diabetic nephropathy by diminishing the miR-200a/Keap- 1/Nrf2 antioxidant pathway. *Diabetes Metab. Syndr. Obes.* 2017; 10: 207–222.

140) Pagtalunan ME, Miller PL, Jumping-Eagle S, Nelson RG, Myers BD, Rennke HG, Coplon NS, Sun L, Meyer TW. Podocyte loss and progressive glomerular injury in type II diabetes. *J. Clin. Invest.* 1997; 99: 342–348.

141) Gubler MC. Podocyte differentiation and hereditary proteinuria/nephrotic syndromes. *J. Am. Soc. Nephrol.* 2003; 14(Suppl 1): S22–26.

142) Lizotte F, Denhez B, Guay A, Gévry N, Côté AM, Geraldes P. Persistent Insulin Resistance in Podocytes Caused by Epigenetic Changes of SHP-1 in Diabetes. *Diabetes* 2016; 65: 3705–3717.

143) Denhez B, Lizotte F, Guimond MO, Jones N, Takano T, Geraldes P. Increased SHP-1 protein expression by high glucose levels reduces nephrin phosphorylation in podocytes. *J. Biol. Chem.* 2015; 290: 350–358.

144) Tsuprykov O, Ando R, Reichetzeder C, von Websky K, Antonenko V, Sharkovska Y, Chaykovska L, Rahnenführer J, Hasan AA, Tammen H, Alter M, Klein T, Ueda S, Yamagishi SI, Okuda S, Hocher B. The dipeptidyl peptidase inhibitor linagliptin and the angiotensin II receptor blocker telmisartan show renal benefit by different pathways in rats with 5/6 nephrectomy. *Kidney Int.* 2016; 89: 1049–1061.

145) Yang J, Campitelli J, Hu G, Lin Y, Luo J, Xue C. Increase in DPP-IV in the intestine, liver and kidney of the rat treated with high fat diet and streptozotocin. *Life Sci.* 2007; 81: 272–279.

146) Wang Z, Grigo C, Steinbeck J, von Hörsten S, Amann K, Daniel C. Soluble DPP4 originates in part from bone marrow cells and not from the kidney. *Peptides.* 2014; 57: 109–117.

147) Nakashima S, Matsui T, Takeuchi M, Yamagishi SI. Linagliptin blocks renal damage in type 1 diabetic rats by suppressing advanced glycation end products-receptor axis. *Horm. Metab. Res.* 2014; 46: 717–721.

148) Ishibashi Y, Matsui T, Maeda S, Higashimoto Y, Yamagishi S. Advanced glycation end products evoke endothelial cell damage by stimulating soluble dipeptidyl peptidase-4 production and its interaction with mannose 6-phosphate/insulin-like growth factor II receptor. *Cardiovasc. Diabetol.* 2013; 12: 125.

149) Sharkovska Y, Reichetzeder C, Alter M, Tsuprykov O, Bachmann S, Secher T, Klein T, Hocher B. Blood pressure and glucose independent renoprotective effects of dipeptidyl peptidase-4 inhibition in a mouse model of type-2 diabetic nephropathy. *J. Hypertens.* 2014; 32: 2211–2223. discussion 2223.

150) Groop PH, Cooper ME, Perkovic V, Sharma K, Schernthaner G, Haneda M, Hocher B, Gordat M, Cescutti J, Woerle HJ, von Eynatten M. Dipeptidyl peptidase-4 inhibition with linagliptin and effects on hyperglycaemia and albuminuria in patients with type 2 diabetes and renal dysfunction: Rationale and design of the MARLINA-T2D trial. *Diab Vasc. Dis. Res.* 2015; 12: 455–462.

151) Zhou LL, Hou FF, Wang GB, Yang F, Xie D, Wang YP, Tian JW. Accumulation of advanced oxidation protein products induces podocyte apoptosis and deletion through NADPH- dependent mechanisms. *Kidney Int.* 2009; 76: 1148–1160.

152) Udell JA, Bhatt DL, Braunwald E, Cavender MA, Mosenzon O, Steg PG, Davidson JA, Nicolau JC, Corbalan R, Hirshberg B, Frederich R, Im K, Umez-Eronini AA, He P, McGuire DK, Leiter LA, Raz I, Scirica BM; SAVOR-TIMI 53 Steering Committee and Investigators. Saxagliptin and cardiovascular outcomes in patients with type 2 diabetes and moderate or severe renal impairment: observations from the SAVOR-TIMI 53 Trial. *Diabetes Care.* 2015; 38: 696–705.

153) Groop PH, Cooper ME, Perkovic V, Hocher B, Kanasaki K, Haneda M, Schernthaner G, Sharma K, Stanton RC, Toto R, Cescutti J, Gordat M, Meinicke T, Koitka-Weber A, Thiemann S, von Eynatten M. Linagliptin and its effects on hyperglycaemia and albuminuria in patients with type 2 diabetes and renal dysfunction: the randomized MARLINA-T2D trial. *Diabetes Obes. Metab.* 2017; 19: 1610–1619.

154) Fufaa GD, Weil EJ, Lemley KV, Knowler WC, Brosius FC 3rd, Yee B, Mauer M, Nelson RG. Structural Predictors of Loss of Renal Function in American Indians with Type 2 Diabetes. *Clin. J. Am. Soc. Nephrol.* 2016; 11: 254–261.

155) Li H, Zhang L, Wang F, Shi Y, Ren Y, Liu Q, Cao Y, Duan H. Attenuation of glomerular injury in diabetic mice with tert-butylhydroquinone through nuclear factor erythroid 2-related factor 2-dependent antioxidant gene activation. *Am. J. Nephrol.* 2011; 33: 289–297.

156) Palsamy P, Subramanian S. Resveratrol protects diabetic kidney by attenuating hyperglycemia-mediated oxidative stress and renal inflammatory cytokines via Nrf2-Keap1 signaling. *Biochim. Biophys. Acta.* 2011; 1812: 719–731.

157) Taguchi K, Hirano I, Itoh T, Tanaka M, Miyajima A, Suzuki A, Motohashi H, Yamamoto M. Nrf2 enhances cholangiocyte expansion in Pten-deficient livers. *Mol. Cell Biol.* 2014; 34: 900–913.

158) Senmaru T, Fukui M, Kobayashi K, Iwase H, Inada S, Okada H, Asano M, Yamazaki M, Hasegawa G, Nakamura N, Iwasaki M, Yabe D, Kurose T, Seino Y. Dipeptidyl-peptidase IV inhibitor is effective in patients with type 2 diabetes with high serum eicosapentaenoic acid oncentretions. *J Diabetes Investig*. 2012; 3: 498-502.

10. List of papers

Main publications

1. **Yasuzawa T**, Nakamura T, Ueshima S, Mima A. Protective Effects of Eicosapentaenoic Acid on the Glomerular Endothelium via Inhibition of EndMT in Diabetes. *J. Diabetes Res.* 2021; 2182225, DOI. 10.1155/2021/2182225.
2. *Mima A, ***Yasuzawa T**, Nakamura T, Ueshima S. Linagliptin affects IRS1/Akt signaling and prevents high glucose- induced apoptosis in podocytes. *Sci. Rep*. 2020; 10(1): 5775, DOI. 10.1038/s41598-020-62579-7. *Equal contribution
3. **Yasuzawa T**, Mima A, Ueshima S. Antithrombotic effect of oral administration of Mozuku (Cladosiphon okamuranus, Brown Seaweed) extract in rat. *J. Nutr. Sci. Vitaminol.* 2019; 65(2): 171-176, DOI. 10.3177/jnsv.65.171.
4. *Mima A, ***Yasuzawa T**, King GL, Ueshima S. Obesity-associated glomerular inflammation increases albuminuria without renal histological changes. *FEBS open Bio.* 2018; 8(4): 664-670, DOI. 10.1002/2211-5463.12400. *Equal contribution

Other publications

1. Huang H, Nakamura T, **Yasuzawa T**, Ueshima S. Effects of Coriandrum sativum on Migration and Invasion Abilities of Cancer Cells. *J. Nutr. Sci. Vitaminol.* 2020; 66(5): 468-477.
2. **安澤 俊紀**, 中村 友美, 黄 禾甯, 美馬 晶, 上嶋 繁. 脂肪細胞の内皮間葉移行(EndMT)誘導作用とエイコサペンタエン酸(EPA)の効果. *日本病態生理学会雑誌.* 2019; 28(3): 17-20.

3. Sakai O, **Yasuzawa T**, Sumikawa Y, Ueta T, Imai H, Sawabe A, Ueshima S. Role of GPx4 in human vascular endothelial cells, and the compensatory activity of brown rice on GPx4 ablation condition. *Pathophysiology.* 2017; 24(1): 9-15.
4. **Yasuzawa T**, Sato T, Tsuchiya K, Kobayashi Y, Kuwahata M, Izumi Y, Ueshima S, Kido Y. 5-Aminolevulinic acid reduces food intake. *近畿大学農学部紀要.* 2015; 48: 17-29.
5. Sato T, **Yasuzawa T**, Uesaka A, Izumi Y, Kamiya A, Tsuchiya K, Kobayashi Y, Kuwahata M, Kido Y. Type 2 diabetic conditions in Otsuka Long-Evans Tokushima Fatty rats are ameliorated by 5-aminolevulinic acid. *Nutr. Res*. 2014; 34(6): 544-551.